THERMAL MODEL AND ANALYSIS OF TWO ZONE PASSIVE SOLAR HOUSE

Issa Helou

A Thesis

in

The Department

of

Building, Civil and Environmental Engineering

Presented in Partial Fulfillment of the Requirements
for the Degree of Master of Applied Science at
Concordia University
Montreal, Quebec, Canada

September 2003

Your file Votre référence
ISBN: 0-612-83857-9
Our file Notre référence
ISBN: 0-612-83857-9

ABSTRACT

THERMAL MODEL AND ANALYSIS OF TWO ZONE PASSIVE SOLAR HOUSE

Issa Helou

This thesis presents a nonlinear transient finite difference two zone coupled thermal-air flow model for a solar house. The two zones may be adjacent to each other (Bungalow) or one above the other (Cottage). One zone is generally hotter than the other which can be used in summer for natural ventilation. The model developed includes floor heating and studies the effect of important design variables such as window area and thermal resistance as well as amount of thermal mass on energy consumption and room temperature swings. For natural ventilation, size of openings and shading strategy are considered.

Results are presented for winter and summer and optimal values for the design variables are discussed for a typical case. The model is validated by comparison with measured published data and simulations. The effect of modeling detail is also considered.

ACKNOWLEDGEMENTS

I would like to express my deepest gratitude and appreciation to my supervisor Dr. A. K. Athienitis for his unending support, expert guidance and continuous encouragement during my graduate studies.

Special thanks to my wife Kim, for her patience, understanding and moral support throughout my studies.

To my son Bernard Helou.

I would like to thank my parents, brothers and sister for their support throughout my studies.

TABLE OF CONTENTS

LIST OF FIGURES

LIST OF TABLES

NOMENCLATURE

A	Area (m^2)
Ad	Door area (m^2)
Aw	Window area (m^2)
C	Thermal capacitance (joule/°C)
Ci	conductivity specific heat for layer i (Joule/kg. °C)
Cpair	Specific heat of air (joule/kg.°C)
f f	Fraction of area (Framing)
g	Acceleration due to gravity (m/s^2)
G.ai	Radiation absorbed in inner glazing (W/m^2)
G.ao	Radiation absorbed in outer glazing (W/m^2)
Gb	Transmitted beam solar radiation (W/m^2)
Gd	Transmitted diffuse irradiation (W/m^2)
h	Height (m)
ha	Air film coefficient (Attic) ($W/m^2.°C$)
ha it	Hour angle
ha s	Sunset hour (hr)
hc	Convective heat transfer coefficient ($W/m^2.°C$)
hi	Film coefficient for surface i ($m^2.°C/W$)
ho	Exterior film coefficient ($W/m^2.°C$)
hr	Radiative heat transfer coefficient ($W/m^2.°C$)
i	Node number or time interval(-)
Ib	Beam solar radiation (W/m^2)

I_{dg}	Intensity of ground diffuse solar radiation (W/m^2)
I_{ds}	Intensity of sky diffuse solar radiation (W/m^2)
I.on	Extraterrestrial normal solar radiation
it	Time array
j	Node connected to node i
K	Thermal conductivity (W/m. k)
Kair	Thermal conductivity of air (W/m. k)
kb	Hourly beam clearness index(-)
kd	Hourly diffuse clearness index(-)
K_L	Extinction coefficient for glazing
K_p	Proportionality constant (W/°C)
K_T	Daily clearness index (-)
kt	Hourly clearness index(-)
L	Latitude (degree)
Li	Thickness of layer i (m)
nd	Day number
ng	Refractive index
p	The time step number in the thermal network model
q	Mass flow rate (kg/sec)
q_{aux}	Auxiliary heat (W)
Qh	Heating energy consumption (MJ)
Rd	Thermal resistance of the door (m^2.°C/W)
Rij	Thermal resistance between node I and j (m^2.°C/W)

Rins	Thermal resistance of insulation ($m^2.^\circ C/W$)
Rsid	Thermal resistance of siding and sheathing ($m^2.^\circ C/W$)
Rw	Window's thermal resistance ($m^2.^\circ C/W$)
S	Solar radiation (W)
t	Time (second)
Ti	Node temperature ($^\circ C$)
t_{it}	Solar time for solar radiation calculation.(hr)
To	Outside temperature ($^\circ C$)
ts	Sunset time (hr)
TS	Time step (second)
Tspg	Set point temperature for the ground floor ($^\circ C$)
Tsp1	Set point temperature for the first floor ($^\circ C$)
Tb	Basement temperature ($^\circ C$)
U	Conductance ($W/^\circ C$)
Uinf	Infiltration heat transfer coefficient ($watt/m^2.^\circ C$)
Vol	Volume (m^3)
w	Frequency (rad/sec)
Yg	Zone admittance for the ground floor ($W/^\circ C$)
Y1	Zone admittance for the first floor ($W/^\circ C$)

Greek symbols

α	Solar altitude (degree) or absorptance
β	Tilt angle (degree)
γ	Surface solar azimuth(degree)
δ	Declination angle (degree)
θ	Angle of incident (degree)
ρ_{air}	Density of air (kg/m^3)
ρ	Reflectance
τ	Transmittance
τ_b	Beam solar transmittance
τ_d	Diffuse solar transmittance
Φ	Solar azimuth (degree)
ψ	Surface azimuth (degree)

CHAPTER 1

INTRODUCTION

1.1 Background

For many years the impact of design decisions on the overall performance of buildings had not been adequately considered. Due to increased cost of energy and the prospect for future energy shortages building designers investigated ways to improve the performance of the building envelope in order to reduce heat losses and excess heat gains. Renewable sources of energy are also exploited in order to reduce the dependency on the use of fossil fuels. This is feasible since only a small amount of the solar energy reaching our planet, if properly utilized, could significantly reduce energy consumption in buildings [Carter and Villiers, 1985].

Solar radiation is the abundant renewable energy source, without which life on earth would be impossible. It is the driving energy of our ecosystem and of the precipitation cycle.

Passive solar design deals with utilization of solar energy in order to reduce heating and possibly cooling energy consumption based on natural energy flows-radiation, conduction and natural convection; forced convection based on mechanical means such as pumps and fans is not expected to play a major role in the heat transfer processes. The term passive building is often employed to emphasize utilization of passive energy flows both in heating and cooling.

Passive solar design techniques address the following basic requirements and principles:

- Transmission and /or absorption of the maximum possible quantity of solar radiation during Winter so as to minimize or reduce to zero the heating energy consumption
- Utilization of received solar gains to cover instantaneous heating load and storage of the remainder in embodied thermal mass or specially built thermal storage devices.
- Reduction of heat losses to the environment through use of the appropriate amount of insulation and windows with high solar heat gain factor.
- Shading control devices or strategically planted deciduous trees to exclude unwanted solar gains, which would create an additional cooling load.
- Utilization of natural ventilation to transfer heat from hot zones to cool in winter and for natural cooling in summer.

A key aspect of passive solar design is the choice of the following design parameters: Fenestration area, orientation and type.

1. Amount of insulation.
2. Shading devices –type, locations and areas.
3. Effective thermal storage.

It is very important in the design to predict the air flow rate with the use of natural ventilation for the calculation of the thermal response of the buildings, as well as for ensuring appropriate air renewal rates for a healthy building environment. Due to its importance, this issue has been given a lot of attention, and significant effort has been put

into the development of theoretical models and experimental techniques for the evaluation of the air flow rate in natural ventilation configurations.

1.2 Motivation

In recent years, passive solar design has been given a lot of attention to reduce the energy consumption due to the increase on energy cost. During the design stage of passive solar system the designer should consider the requirements of this system and preventing overheating that may occur. An appropriate control strategy for the system plays a major role in achieving the thermal comfort and preventing frequent overheating of the building.

Air movement in a building plays an important role in thermal comfort, energy saving, and indoor air quality because the distribution of temperature is directly depends on the airflow pattern. For the design of multizone buildings it is important to predict the air flow rate inside the building and couple it with the thermal model to study the thermal response of the building and achieve the thermal comfort. This issue has been given a lot of attention and a number of studies have been done for the coupled airflow thermal model but still there is a lot of work to be done regarding this issue especially for two zone model like the one that will be studied in this thesis.

Natural ventilation systems have long been employed in European residences to control indoor air quality and provide thermal comfort. European building designers have turned to natural ventilation to control air quality and cool buildings by using the night ventilation. These systems may be adapted to the North American context, but much work will need to be done to realize the full potential natural ventilation may offer to

North America. In this study a two zone model with natural ventilation in summer will be studied for Montreal weather.

This thesis develops a two zone model. The model consists of two zones one on top of the other (Cottage) or next to each other (Bungalow) which are a common type of houses in Canada. A zone is a region in which the air temperature can be assumed to be uniform. Although more than two zones can be often identified, a two zone model is practical for the analysis of most cases where part of the house receives higher solar gains than the rest. The model is a passive solar direct gain. The thermal performance of the model is studied into two seasons' winter and summer. In winter the model considered includes an integrated floor heating system, and in summer it is a naturally ventilated direct gain passive solar two zone model. Optimum parameters for achieving good thermal comfort inside the model are obtained.

1.3 Objectives

The main objectives of this thesis are the following:

- To develop a two zone model. Couple the air flow – heat transfer and study the thermal performance of the developed model in two seasons' winter and summer for Montreal weather.
- To develop a control strategy for the auxiliary heating to achieve the thermal comfort inside the two zone model and avoid overheating.
- To study the passive response of the developed model during summer season by the use of natural ventilation technique. The best opening area for natural ventilation will be determined. The study will be performed with and without shading.

1.4 Thesis orientation

Chapter 2 presents the review of the related literature.

Chapter 3 presents background regarding the solar radiation and the methods for calculating the solar radiation transmitted into the house and absorbed by the interior surfaces. It also presents background regarding modeling techniques and natural ventilation.

Chapter 4 presents the model developed in this thesis which is two zone model; it also presents the simulations performed and the results.

Chapter 5 presents validation of the model by comparison with measurements and simulations. It also presents the effect of changing the number of capacitances for the thermal mass floor in the thermal network.

Chapter 6 presents the conclusions of this study and also recommendations for future work.

CHAPTER 2

LITERATURE REVIEW

2.1 Introduction

Passive solar design deals with utilization of solar energy in order to reduce heating and possibly cooling energy consumption based on natural energy flows-radiation, conduction and natural convection, and prevents frequent room overheating.

This chapter presents the basics of the passive solar design and its methods, thermal modeling, natural ventilation, air flow modeling and reviews the related literature.

2.2 Passive solar building design

2.2.1 Introduction

Passive solar design concerns the determination of the most suitable passive system and components and the appropriate use of the climatic and environmental factors in order to minimize energy usage by effective utilization of solar energy. The main common characteristic of these systems is that thermal energy transfer into and out of buildings, into and out of thermal energy storage and around a conditioned space, occurs naturally through conduction, convection and radiation. The primary objective in the thermal design and analysis of a passive solar building is to achieve high saving in energy consumption through maximum utilization of solar gains, while at the same time preventing frequent room overheating.

During the thermal analysis and design of a passive solar building, it is necessary to evaluate heating or cooling loads and room temperature fluctuation with given weather data such as solar radiation and ambient temperature. Moreover, it is desirable to evaluate the building response under extreme weather conditions for many design options, each time changing only a few of the parameters, until an optimum response is obtained. Thus, it is desirable to have efficient simulation and design tools which can be used for routine passive solar analysis.

2.2.2 Passive systems

Various passive solar systems have been developed through many years of experiencing the building behavior in different climatic conditions which provide means for more effective utilization of solar energy. A passive solar heating or cooling system is one in which the thermal energy flow is by natural means. These natural energy flows are the most important, and controlled auxiliary heating becomes less significant than in thin-walled buildings, in which intermittent heating is required to respond to sudden changes in weather [Athienitis and Santamouris, 2002]. The three functions of any solar heating system are collection of the solar energy, storage of the energy as heat and distribution of the heat throughout the building when needed.

One of the basic decisions in building design concerns form and shape. Generally basic passive solar principles dictate a rectangular form with the longest side facing south or near-south. Another basic decision is the type of passive solar system to be selected for each zone of the building, type of fenestration, thermal storage and insulation. The main type of passive solar system are shown in the Figure 2.1 and discussed below:

2.2.3 Direct Gain System

Direct gain is the most popular passive solar design approach Figure 2.1, due to its simplicity, effectiveness and relatively low cost. This type of passive system is characterized by large south-facing glazing areas that allow solar radiation to enter the living space directly. These solar gains serve either to meet part of the current heating needs or are stored in the building mass to meet heating needs that arise later [Balcomb et al.1982].

The effectiveness of thermal storage mass in direct buildings depends on its thickness, surface area and thermal properties (volumetric heat capacity and thermal conductivity).The location of the thermal mass in a direct gain room is also very important and affects the amount of transmitted solar radiation absorbed by each room interior surface. The absorbed radiation is a function of the following parameters [Athienitis and Stylianou, 1991]

1- Mass location

2- Mass solar absorptance

3- Absorptance of the other surfaces

4- Room and window geometry

5- Latitude

6- Time of the year

The best materials for efficient thermal storage capabilities are those that can store large quantities of heat (high heat capacity) and that can readily transport heat from the mass surface to the mass interior for storage and back again to the surface to meet the building heat load (high thermal conductivity) [Balcomb et al., 1982].

Significant objectives in the design of a passive solar direct gain building is to select the area and characteristics of the direct gain windows, and the thermal mass properties and its distribution in order to prevent frequent overheating while at the same time achieving savings in energy consumption. As for all buildings, the amount of insulation is also an important parameter to be selected; in passive solar buildings thermal storage mass should be placed on the room-side of the insulation. In order to meet these objectives the designer should perform many cycles of synthesis and analysis to investigate through different design alternatives the possibilities of an optimum building response.

2.2.4 Indirect gain systems

Systems in which the thermal storage mass is separate from the main building envelope systems are known as indirect gain systems Figure 2.1. Of these, the most common is the collector-storage wall, also know as the mass of Trombe Wall [Athienitis and Santamouris, 2002].

•**Collector-storage wall (Trombe Wall) systems :** part of the south-facing wall is glazed and inside the glazing there is a thick layer of thermal mass such as concrete, brick or water tanks with a black surface to absorb and store the transmitted solar radiation. [Athienitis and Santamouris, 2002].

• **Transparent insulation systems:** The same principle as for the storage walls is employed but in this case the solar energy collection and storage is achieved in an exterior wall. Instead of having glazing in front of the thermal mass, in this case there is

transparent or translucent insulation such as a plastic honeycomb with relatively high thermal resistance.

•**Air Heating systems such as air-flow windows and air collectors:** in air-flow windows, a dark surface such as dark blinds between two glazings is employed to absorb the solar heat, which then rises by natural convection, and assisted by the fan to flow through hollow floors/ceiling mass or an isolated thermal storage device such as a rock bed. The principle is very similar to air flow solar collectors, installed in the past on the roof of a building. By integrating air flow collectors into the building envelope, the overall building cost is reduced [Athienitis and Santamouris, 2002].

•**Solar Chimneys:** they are often employed for natural cooling. In these systems, one wall of the chimney is heated by solar radiation, warming up the air, which rises by buoyancy to the outside, creating a negative pressure and drawing cooler outside air into the building.

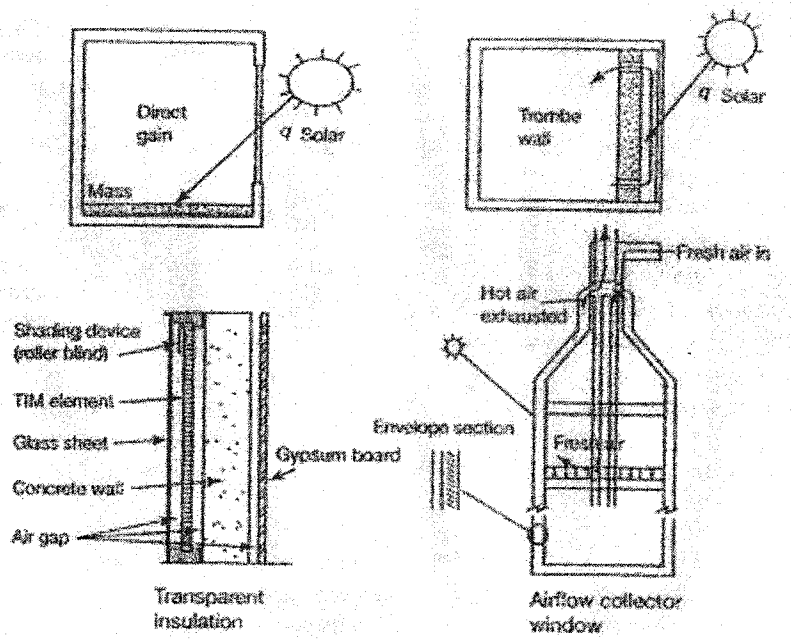

Figure 2.1 Passive solar systems [Athienitis & Santamouris, 2002]

2.3. Mathematical modeling of transient conduction

Two approaches dominate the mathematical treatment of transient heat conduction: The response function methods and the numerical methods [Haghighat and Liang, 1992]. Both techniques are widely used for passive solar analysis [Athienitis, 1985].

2.3.1 Response function methods

Response function methods are an analytical approach to solve the governing differential heat equation. [Carslaw and Jaeger, 1959], [Churchill, 1958], [Davies, 1978] described this method in detail.

2.3.2 Numerical methods

The use of numerical methods for solving heat transfer problems is a result of the complexity of the analytical solutions associated with practical engineering problems. Factors that bring about the use of numerical methods are complex geometry, non-uniform boundary conditions, time - dependent and temperature dependent properties. In some cases, analytical solutions are possible if many implications are made [Lien, 1981].

Although numerical methods must be regarded as representing approximate solutions, their accuracy can, by careful design, be made to satisfy even the most demanding criteria. In the field of building energy analysis, different numerical techniques have been used. The finite difference method is one of the most widely used [Minkowyez et al, 1988]. It is conceptually a simple method to implement and is appropriate for most of the problems encountered in building thermal analysis [Holman, 1986]. It can be used to handle problems of almost any degree of complexity such as transient heat conduction within multi-layered constructions under non-linear boundary conditions or where

thermal properties are considered to be temperature and time dependent [Patankar, 1980]. Numerical methods are called sometimes discretization methods since the numerical solution is obtained in the form of the values of the dependent variables at a number of discrete locations in the domain of interest. The discrete locations are often called nodes. The finite difference thermal network approach will be considered on this thesis, because it generally provides more accurate estimation of temperature and heat flows owing to the capability to model non-linear effects such as convection and radiation. In this approach, each layer is divided into a number of sub-layers (regions). Each region is represented by a node. Each node (i) has a thermal capacitance (Ci) associated with it and resistances connecting it to adjacent nodes.

2.3.2.1 Explicit versus implicit solution

The three dimensional transient conduction equation is expressed as:

$$k.\left[\frac{\partial^2 T}{\partial x^2}+\frac{\partial^2 T}{\partial y^2}+\frac{\partial^2 T}{\partial z^2}\right]=\rho.c_p.\frac{\partial T}{\partial t} \qquad (2.11)$$

where T is the temperature, k is the thermal conductivity, c_p is the specific heat, ρ is the density, it is time and x, y and z represent the direction of the heat flow. However, for the plane wall case, the effect of the second and third-space coordinate may be so small as to justify its neglect, and the multidimensional heat flow problem may be approximated with a one dimensional analysis [Schneider, 1955]. So the above equation may be reduced to a simpler expression. That is,

$$k.\frac{\partial^2 T}{\partial x^2} = \rho.c_p.\frac{\partial T}{\partial t} \tag{2.12}$$

This equation is substituted by finite difference expression. It may be represented in explicit (forward) or implicit (backward) formulation. As follows:

$$T(i,p+1) = \left(\frac{\Delta t}{C_i}\right)\cdot\left(q_i + \sum_j \frac{T(j,p) - T(i,p)}{R(i,j)}\right) + T(i,p) \tag{2.13}$$

$$T(i,p+1) = \left(\frac{\Delta t}{C_i}\right)\cdot\left(q_i + \sum_j \frac{T(j,p+1) - T(i,p+1)}{R(i,j)}\right) + T(i,p) \tag{2.14}$$

where *j* represent all nodes connected to node *i*, qi represents all heat sources at node (*i*) such as solar radiation or auxiliary heat , *p* is the time interval and Δt is the time step , C*i* is the thermal capacitance for node *i* and R*i,j* is the conductive, radiative or convective thermal resistance.

The explicit finite difference method is particularly suitable for modeling of non-linear heat diffusion problems such as the present case of heat transfer through the floor heating system and its control. The advantage of the explicit finite difference representation is that it gives the future temperature of a single node in term of current temperatures of that node and its neighbors. Thus, if at the end of a certain time period, all the nodal temperatures are known, then each of the nodal temperatures at the end of the next moment, Δt, may be explicitly found, node by node without a matrix inversion or

solution of simultaneous equations [Dusinbere, 1961]. However, the implicit finite difference form expresses a future nodal temperature in terms of its current value and the future values of its neighbors' temperature. Thus, to progress from one time step to the next, a system of equations of the form of equation (2.14) must be solved. For this reason, using the direct explicit formulation is preferred, also because non-linearities can be modeled more easily. However, the time increment should be carefully selected in relation to the spatial increment to avoid any numerical instability errors.

2.3.2.2 Errors involved in finite differences

Two types of errors are associated with the finite difference approximation: rounding off and discretization [Flower, 1945]. The former occurs at each time step of the calculation. However, this error may be reduced significantly by carrying out the numerical calculation in double precision.

Discretization or stability error results from the replacement of the differential equation by the explicit finite difference expression. This could be avoided by reducing the space and time increment. That is, the time step must be chosen as [Holman 1986]:

$$\Delta t_{critical} = \min\left(\frac{C_i}{\sum_j \frac{1}{R_{i,j}}}\right) \qquad (2.15)$$

for all nodes i

2.4 Natural Ventilation

Natural ventilation is the flow of outdoor air due to wind and thermal pressure through intentional openings in the building's shell. Under some circumstances, it can effectively control both temperature and contaminants in mild climates, but it is not considered practical in hot and humid climates or in cold climates. Temperature control by natural ventilation is often the only means of providing cooling when mechanical air conditioning is not available. The arrangement, location, and control of ventilation openings should combine the driving forces of wind and temperature to achieve a desired ventilation rate and good distribution of ventilation air through the building. However, intentional openings cannot always guarantee adequate temperature and humidity control or indoor air quality because of the dependence on natural (wind and stack) effects to drive the flow [Wilson and Walker, 1992].

There are two major natural ventilation types, namely: single-sided and cross natural ventilation. Single-sided natural ventilation occurs when the building communicates with the outdoor environment through one or more openings located on the same exterior wall; cross ventilation occurs when there are openings on opposite building walls.

2.4.1 Driving Mechanisms for ventilation

Utilization of natural ventilation requires an appropriate understanding of principles of building pressurization. Two pressure-driving mechanisms must be considered for the natural ventilation to perform properly: the temperature difference across the opening (buoyancy or stack effect) and the wind. The interaction of these parameters creates pressure difference across the openings driving the air inside/outside the ventilated space.

The indoor-outdoor pressure difference at a location depends on the magnitude of each of the driving mechanisms as well as on the characteristics of the openings in the building envelope i.e. their locations and the relationship between pressure difference and air flow for each opening.

2.4.1.1. Wind pressure

When wind impinges on a building, it creates a distribution of static pressures on the building's exterior surface that depends on the wind direction, wind speed, air density, surface orientation, and surrounding conditions. Wind pressures are generally positive with respect to the static in the undisturbed air stream on the windward side of a building and negative on the leeward sides. However, pressures on these sides can be negative or positive, depending on wind angle and building shape. Static pressures over building surfaces are almost proportional to the velocity pressure are given by the Bernoulli equation, assuming no height change or pressure losses:

$$P_w = \frac{1}{2}.\rho.C_p.V^2 \qquad (2.16)$$

where:

Pw = the wind surface pressure relative to outdoor static pressure in undisturbed flow (Pa)

ρ = the outside air density (Kg/m^3)

V = the wind speed (m /sec)

Cp = wind surface pressure coefficient, dimensionless

2.4.1.2 Stack pressure

The pressure due to buoyancy (stack effect) arises from the difference in temperature, hence density, between the air inside and outside of an opening. The variation of air density with temperature produces pressure gradients both within the internal and external zones. During the heating season, the warmer inside air rises and flows out of the building near its top and it is replaced by colder outside air that enters the building near its base. During the cooling season the flow directions are reversed.

The height at which transition between inflow and outflow occurs is the neutral plane where the pressures inside and outside are equal. In practice, the position of the neutral plane level (NPL) at zero wind speed is a structure-dependent parameter that depends only on the vertical distribution of openings in the envelope, the resistance of the openings to air flow, and the resistance to vertical air flow within the building . If the openings are uniformly distributed vertically, they have the same resistance to air flow, and there is no internal resistance, the NPL is at the mid-height of the building. The NPL in tall building varies from 0.3 to 0.7 of the total building height. For the same buildings and especially buildings with chimneys, the NPL is usually above mid-height.

Internal partitions, stairwells, elevator shafts, utility duct, chimneys and mechanical supply and exhaust systems complicate the analysis of NPL location [ASHRAE, Fundamentals, ch.26, 2001]. In general, exhaust systems increase the height of the NPL and outdoor air supply systems lower it [Etheridge and Sandberg, 1996]. The pressure difference due to buoyancy (Pa) is given by:

$$\Delta P_s = \rho.g.(H_{NPL} - h).\left[\frac{Ti - To}{Ti}\right] \qquad (2.17)$$

where ρ = the air density (kg/m³)

g = the gravitational acceleration (m/s³)

H_{NPL} = the height of the neutral pressure level (m)

Ti = the internal temperature (K)

To = the outside temperature (K)

h = the height from ground level (m)

The above equation provides a maximum stack pressure difference, given no internal resistance. In a building with airtight separations at each floor, each floor acts independently, with its own stack effect being unaffected by that of any other floor. Real multi-story buildings are neither open inside not airtight between stories. Vertical air passages, stairwells, elevator shafts, etc, allow air flow between floors. In that case the total effect of the building remains the same as that with no internal flow resistance, but some of the total pressure difference maintains flow through openings in the floors and vertical shafts. As a result, the pressure difference across the exterior wall at any level is less than it would be with no internal flow resistance [ASHRAE, Fundamentals, ch.26, 2001].

2.5. Air flow

2.5.1 Introduction to Airflow and Temperature Distribution

Airflow and thermal distribution within buildings has attracted international attention, either at a research level or industry level. There are several international conferences

regarding this issue, such as the Air Infiltration and Ventilation Centre (AIVC) conference, the International Conference on Air Distribution in Rooms (ROOMVENT).

2.5.1.1 Air flow through openings

At present most standards are descriptive and there is no direct specification of the required air quality, only indirectly by specifying the required flow rates. The primary requirement of a ventilation system is to realize an acceptable indoor air quality or, if the air flow rates are specified, to meet the specified air flow rates [Wouters et al. 1999].
In general, the air flow through an opening is dependent on: 1- the size of the opening. 2-the leakage characteristics of the opening and 3- the pressure difference across it. For the evaluation of the air flow through an opening it is essential that all these three influential factors be know.

Prediction of air flow rate in naturally-ventilated buildings is very important for the calculation of the thermal response of the building, as well as for ensuring appropriate air renewal rates for a healthy building environment. Due to its importance, this issue has been given a lot of attention and significant effort has been put onto the development of theoretical models and experimental techniques for the evaluation of the air flow rate in natural ventilation configurations.

2.5.2 Mathematical models

2.5.2.1 Basic equations

The most common equation describing the air flow through an opening is the orifice equation, which is based on the Bernoulli's equation with steady incompressible flow.

This equation can be used for a relatively large opening area (typical dimension larger than 10mm), such as vent or large crack. In that case, the flow tends to be turbulent under normal pressures and the flow rate Q (m^3/sec), is proportional to the square root of the pressure difference and equal to:

$$Q = C_d.A.\sqrt{\frac{2.\Delta P}{\rho}} \qquad (2.18)$$

where C_d = the discharge coefficient of the opening, dimensionless

A = the effective opening area of a building (m^2)

ΔP = the pressure difference across the opening (Pa)

ρ = the air density (kg/m^3)

The discharge coefficient C_d is a dimensionless number that depends on the geometry of the opening and the Reynolds number of the flow, and includes the influence of contraction and friction. For turbulent flow, C_d is constant at a fixed Reynolds number and therefore, the flow is proportional to square root of ΔP. For a sharp-edge orifice flow the discharge coefficient is almost independent of the Reynolds number and has a value between 0.6 and 0.65. However, in most of the cases C_d appears to be variable because of the geometry of the openings and the variation in pressure difference with the environmental conditions inside and outside the building [Awbi, 1991].

For extremely narrow openings (cracks) the flow within the opening is essentially laminar. In such cases the flow rate (m^3/sec) is given by the Couette flow equation:

$$Q = \frac{b \cdot h^3}{12 \cdot \mu \cdot L} \cdot \Delta P \qquad (2.19)$$

where b is the length of crack(m), h the height of crack(m), L the depth of crack in flow direction(m) and μ the dynamic viscosity of air (Pa.s).

For wider cracks the flow is usually neither laminar nor fully turbulent but in the transition region. The flow (m^3/sec) is given by a power-law equation of the form:

$$Q = C.(\Delta P)^n \qquad (2.20)$$

where C is the flow coefficient ($m^3/s/Pa^n$), ΔP the pressure difference across the opening (Pa) and *n* a dimensionless flow exponent. The flow coefficient is dependent on the opening geometry. The flow exponent is dependent on the flow regime and acquires a value of 0.5 for fully turbulent flow and 1 for laminar flow .However, in practice the value of n for several types of openings tends to be between 0.5 and 1.

2.5.2.2 Network model

Network modeling is based on the solution of the mass balance equation for the calculation of the pressure at discrete nodes representing the simulated zones. Two basic types have been developed: single-zone and multi-zone models. In the single-zone modeling approach, the interior of the building is considered as one zone and it is represented by a single node; in the multi-zone approach, the building is subdivided into a number of zones represented by an equivalent number of nodes. Models of this

category can be used for simulations of naturally-ventilated buildings to provide information on the individual air flows in each simulated zone, as well as through each opening. In a multi-zone model, the mass balance equation assuming *(j)* flow paths may be written as follows:

$$\sum_{i=1}^{j} \rho_i . Q_i = 0 \qquad (2.21)$$

where Q_i (m^3/sec) is the volumetric flow rate through *i*th path , and ρ_i (kg/m^3) the density of air flowing through *i*th path.

Many models of this type have recently been developed because they are easy to use and require simple input data. Some of them are: NatVent [Svensson and Aggreholm, 1998], COMIS [Feustel et al. 1990], AIRNET [Walton, 1988], BREEZE [BRE, 1992], ESP [Clark, 1993], NORMA [Santamouris, 1994], PASPRT-AIR [Dascalaki and Santamouris, 1995], CONTAM [Walton, 1993 & 1996], Doe-2 [Lawrence Berkeley Laboratory, 1993].

Kronvall et al. (1998) using the NatVent program determined the parameters that have the largest influence on the performance of natural ventilation. The interaction between different parameters is also discussed. An air flow and thermal model are coupled together in this model, which can be used in the early design process, to determine possible restriction in the use of natural ventilation in an office building.

Haghighat and Mergi, (1996) carried out a comprehensive validation of two models: COMIS and CONTAM. The validation processes was carried out at three different levels: inter-program comparison, validation with experimental data, which was collected in a

controlled environment, and finally, validation with field measurement data. At the inter program level, the fir flow rates and pressure values predicted by COMIS and CONTAM for a four-zone paper building were compared with the air flow rates and pressures predicted by CBSAIR, AIRNET and BUS. The results showed good agreement between these software programs. Fan depressurization, smoke and tracer gas tests were conducted to estimate the permeability of building envelope components, to locate the cracks, and to determine the inter zonal air flow rates between rooms. The results confirm that there is a good agreement between predictions made by COMIS and CONTAM; there are, however, some differences between these models' predictions and the measured data. The predictions made by these models were also compared with the results of a tracer gas measurement carried out in a residential building and the predicted and measured values were in good agreement.

Chen (1990) studied energy consumption and thermal comfort in a ventilated office equipped with a radiant panel, radiator heating, and a warm-air heating system, respectively. The thermal boundary condition used in his computation through walls. Although radiative heat transfer between walls was studied in his work, the heat sources in the room were assumed to be convective.

Ajiboye (1998a and 1998b) using NatVent, developed a design tool to suggest suitable air inlets for buildings in polluted urban areas, in order to reduce the impact of external pollution on air quality within buildings, several types of openings, like inlets with noise and particle attenuation, and inlets that can be closed during peak traffic periods were considered.

Linden et al. (1990) investigated displacement natural ventilation in single-zone building with two-level openings. Theoretical expressions were obtained for the airflow rate through the openings and the stratification interfacial position induced by a single point source and a single line source, respectively. It was found that while the airflow rate does depend on the source strength, the location of the stratification is exclusively determined by the geometrical parameters of the building and independent of the source strength. The theoretical predictions were confirmed by their experimental results by using salt-bath modeling system as well as in recent work by Chen et al. using a fine-bubble modeling technique.

Cooper and Linden (1996) extended the work by Linden et al.1995, to cover two and multiple buoyancy sources for a building enclosure with two-level openings. It was shown that for natural ventilation flows induced by two or multiple buoyancy sources, a multi-layer stratification is established with each plume terminating in a given layer.

Li 2000, developed two new "emptying air-filling box" models for a single-zone building with buoyancy-driven ventilation. And shown that the fully mixed model and the emptying water-filling box model are special cases of the more general emptying air-filling box model. Also found that the fully mixed model over predicts the clean zone height and the ventilation airflow rate, while the emptying water-filling box model under predicts the two ventilation parameters. One major finding by Li is that when the surface thermal radiation effect is considered, the airflow rate as well as the stratification interface level are both affected by the strength of the buoyancy source.

Li et al. 2000, used pressure-based formulation for natural ventilation of single-zone and multi-zone building with multiple opening and made it easier to implement by

introducing an auxiliary concept of external pressure, which allows all the formulas to be presented in an integrated form. Multi-zone situations considered include vertically interconnected zones, and horizontally interconnected zones with same heights and different heights. The formulation includes the combined effect of wind, thermal buoyancy and mechanical ventilation, and it can be used for internal and external large openings.

A simple and easy implementation method was then presented. Single-zone and multi-zone analytical solutions were developed by the pressure-based formulations and used for validation of the implementation method. A CFD method is also used to cross-check the implementation methods in a single-zone building with very large external openings. A reasonable agreement had been found between the results predicted by the pressure-based formulation and those predicted by the analytical solutions and CFD methods.

For a two-zone system which is similar to this thesis as shown in the figure below:

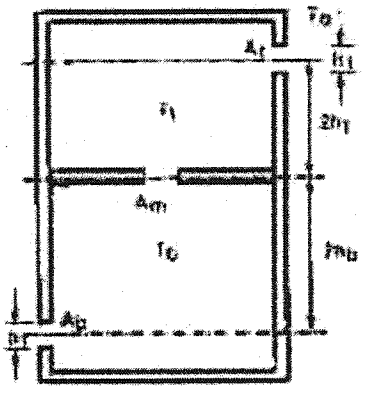

Figure 2.2 Two zone airflow [Li et al. 2000]

Assuming Tb is the temperature in the bottom zone and Tt is the temperature in the top zone, the flow rates were found to be:

$$q_b = C_d \cdot A_b \cdot \sqrt{\frac{2 \cdot \Delta P_b}{\rho}} \tag{2.22}$$

$$q_m = C_d \cdot A_m \cdot \sqrt{\frac{2 \cdot \Delta P_m}{\rho}} \tag{2.23}$$

$$q_t = C_d \cdot A_t \cdot \sqrt{\frac{2 \cdot \Delta P_t}{\rho}} \tag{2.24}$$

and the pressure difference across each opening is equal to :

$$\Delta P_b = \frac{2 \cdot A_m^2 \cdot A_t^2}{A_{tmb}^2} \cdot \left| \left[(\rho_o - \rho_b) g \cdot h_b + (\rho_o - \rho_t) g \cdot h_t \right] \right| \tag{2.25}$$

$$\Delta P_m = \frac{2 \cdot A_b^2 \cdot A_t^2}{A_{tmb}^2} \cdot \left| \left[(\rho_o - \rho_b) g \cdot h_b + (\rho_o - \rho_t) g \cdot h_t \right] \right| \tag{2.26}$$

$$\Delta P_t = \frac{2 \cdot A_b^2 \cdot A_m^2}{A_{tmb}^2} \cdot \left| \left[(\rho_o - \rho_b) g \cdot h_b + (\rho_o - \rho_t) g \cdot h_t \right] \right| \tag{2.27}$$

where: Ab (m^2) is the bottom opening area

At (m^2) is the top opening area

g (m/sec^2)is the gravity acceleration

A_m (m^2) is the opening area between the two floors.

A_{tmb} (m^2) is equal to:

$$A_{tmb}^2 = A_m^2 \cdot A_b^2 + A_m^2 \cdot A_t^2 + A_t^2 \cdot A_b^2 \qquad (2.28)$$

C_d is the discharge coefficient

h_b (m) $2h_b$ is equal to the height between the middle of the bottom opening and the level between the two floors.

h_t (m) $2h_t$ is equal to the height between the middle of the top opening and the level between the two floors.

ρ_i is the air density for zone *i*

2.5.2.3. Computational fluid dynamics (CFD) models

CFD can provide users with the detailed knowledge of airflow pattern, temperature and contaminant distributions within a room. This method has been highly recognized in air movement analysis. Nielsen has shown that the predictions of CFD models agree with the measurements in the simulation of rooms with different ventilation systems. The CFD was also demonstrated to be a potential tool to predict and model time dependent distribution in enclosed spaces [Nielsen, 1989].

In a CFD approach to predict the airflow pattern in a single room, the room is divided into a large number of cells about 10,000 [Schalin, 1992]. For each cell transport equations for mass, momentum, energy, turbulence quantities and concentrations of

contaminants are solved. Variables solved for this application are pressure, air velocity, temperature and contaminant concentration.

CFD results are very rich in terms of detailed information regarding the flow and temperature field within a room, nevertheless, it is too complicated to be used by non-specialists and it takes a long time for the user to feel comfortable with the software.

2.6 Coupled airflow -thermal

In building energy prediction it is still common practice to separate the thermal analysis from the estimation of air infiltration and ventilation. Although this might be a reasonable assumption for many practical problems, this simplification is not valid for cases involving relatively strong couplings between heat and fluid flow. Passive cooling by increasing natural ventilation to reduce summertime overheating is a typical example.

There are various approaches for integrating heat and air flow calculations, each having specific consequences in terms of computing resources and accuracy. One way to actually quantify this, is to use a simulation environment which supports these various approaches, and to compare the results of the approaches for a typical case study.

Walton (1982) integrated a simple network airflow analysis technique with the conduction transfer function approach to multi-zone building thermal analysis to solve the coupled airflow-thermal problem. He provided two options. In the first option, at each step in time, the nonlinear flow problem was formed and solved, given the current estimate of system temperatures, then the thermal problem was formed and solved. In the second option the sequential solution of the flow and thermal problems were repeated, in an iterative manner, until convergence was realized.

Clarke(1985), described an airflow analysis technique and briefly outlined a computational solution strategy for the coupled problem that has been implemented as part of the ESP building thermal simulation program. His approach is equivalent to Walton's first option. In both studies [Walton & Clarke] the nonlinear flow problem was simply inserted into the time-stepping scheme used to solve the dynamic thermal analysis problem.

Axley and Grot (1989), presented an approach to modeling the coupled problem that involves integrating element-assembly formulations of both airflow analysis and thermal analysis techniques to form a coupled set of equations that accounts both for the nonlinearity of the airflow analysis problem and the thermal analysis problem.

Hensen and Clarke (1991) have described a "modular-simultaneous" technique for the simulation of combined heat and fluid flow in a building/ plant context. The performance of the model indicates that it is practical to solve the building/ plant heat and mass flow network in detail.

Hensen (1995) studied two methods (ping-pong and onion method) of linking heat and airflow models using two different time step lengths.. The "ping-pong" method in which the thermal and flow model run in sequence (ie each uses the results of the other model in the previous time step), and the "onion" method in which the thermal and flow model iterate within one time step until satisfactory small error estimates are achieved. It was found that the differences in air flow are larger than the differences in air temperatures. The temperature differences between the various methods grow with the number of stacked zones. The results indicate that when properly used, each method will give satisfactory results.

Okuyama (1999) has developed a simulation program for thermal and airflow systems in buildings using thermal and airflow network models called NETS. The program has high degrees of freedom and generality, and provides a tool for designers and developers of building facilities and designs to investigate new concepts by flexible simulations. The main part of the program named NETS, which has been developed using Fortran language, originally aimed at simulating passive solar houses. In some passive solar houses, heat flow is controlled by varying airflow paths and opening of heat insulating panels according to the time zones, seasons, and ambient temperature.

Srebric et al. (2000) have developed a coupled airflow and energy simulation program to calculate simultaneously the distributions of indoor air, heating/cooling load, and thermal comfort in a space. The coupled program can take the non uniform distributions of indoor airflow and heating/cooling load into account. It can also provide thermal and fluid boundary conditions normally needed for room airflow calculation. They demonstrated the program's capacity by applying the program to study the thermal environment in a house and an atrium. The results show that indoor air distribution in mixing ventilation may not be uniform. The impact of the nonuniform distribution of indoor air can be considered in the calculation of heating /cooling load by the coupled program.

Li (2002) discussed the qualitative features of the iterative solution processes of the Newton-Raphson method when used for coupled thermal and ventilation analyses of a simple one-zone building with two openings. Chaotic solutions were found in a very simple coupled air flow and thermal analysis problem using the standard Newton-Raphson method.

Axley et al. (2002) described a modeling study of a representative naturally ventilated building constructed in the Netherlands, and investigated the performance of this building in two challenging North American climates using a multi zone coupled thermal/airflow simulation tool CONTAM97R.

This thesis will study a passive solar two zone model (house) for two seasons- winter and summer. For winter the model is direct gain passive solar two zone house, and for summer the model is naturally ventilated passive solar house. The solar radiation transmitted into the house and absorbed by the interior surfaces will be calculated and the thermal network will be drawn for the house in using the explicit finite difference method.

In winter the air flow inside the house will be coupled with the thermal network and study the thermal performance of the house, an appropriate control strategy of the set point will be developed to avoid overheating that might happened and achieve the thermal comfort in the house while at the same time achieve energy saving.

In summer the thermal performance of the house will be studied with the use of natural ventilation at night to cool the house. The effect of using shading devices in summer will be investigated.

CHAPTER 3

THEORY BACKGROUND

3.1. Introduction

This chapter presents some theory background regarding the solar radiation due to its importance in the design of passive solar building. The explicit finite difference thermal network method is employed in this study, so this chapter presents a theory background regarding the model, and the natural ventilation in building.

3.2 Solar radiation theory background

Solar radiation transmitted into a room consists of three components: the direct beam radiation, diffused sky radiation and the solar radiation reflected by the ground. Two models have been developed for calculating these components, these models are explained in this section in additional to the solar angles and the angle of incidence as it is the most important angle in the calculation of solar radiation.

3.2.1 Solar angles

The position of the sun and the geometric relationships between a plane and the beam solar radiation incident on it may be described in terms of the following angles:

• L Latitude, equal to the angle of the location relative to the equator; north is positive.

• δ declination, equal to the angular position of the sun at solar noon with respect to the equatorial plane (Varies from -23.45° to 23.45°)

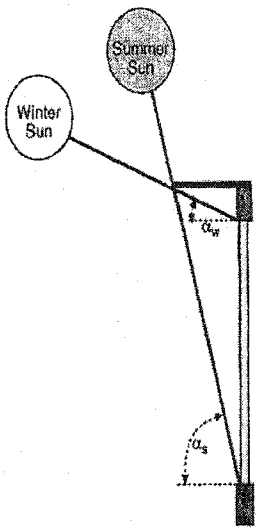

Figure3.1 Sun Position

• α solar altitude, equal to the angle between the sun's rays and the horizontal (between 0-90°) .

• z zenith angle , equal to the angle between the sun's rays and the vertical .

• φ solar azimuth , equal to the angle between the sun's rays and the vertical rays from due south (positive in the afternoon).

• γ surface solar azimuth , equal to the angle between the projections of the sun's rays and of the normal to the surface on the horizontal plane .

• ψ surface azimuth, equal to the angle between the projection of the normal to the surface on a horizontal plane and due south (east is negative).

• β tilt angle between the surface and the horizontal (0 - 90°).

• θ the angle of incidence is the angle between the solar rays and a line normal to the surface.

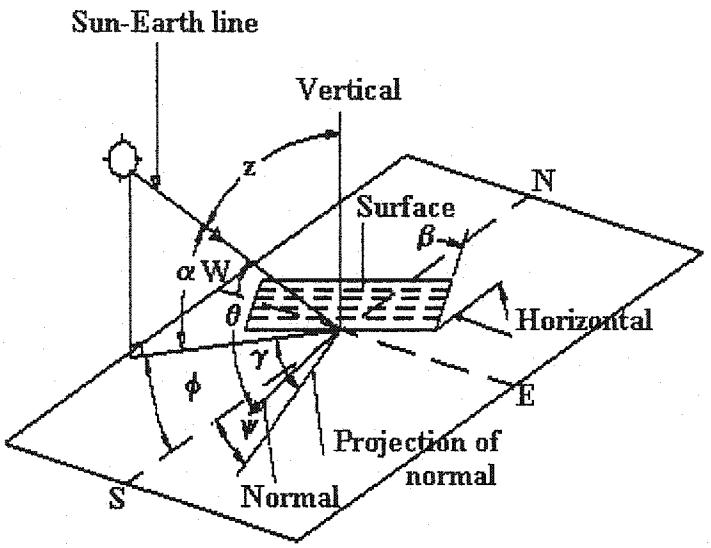

Figure 3.2 Solar angles (Athienitis ,1994)

3.2.2 The angle of incidence (θ)

The evaluation of the angle of incident has a significant importance. This angle determines the percentage of the direct sunshine intercepted by any surface. It is calculated as [Duffie and Beckman, 1991]:

$$\theta = \text{acos}\,[\cos(\alpha).\cos(\gamma).\sin(\beta) + \sin(\alpha).\cos(\beta)] \qquad (3.1)$$

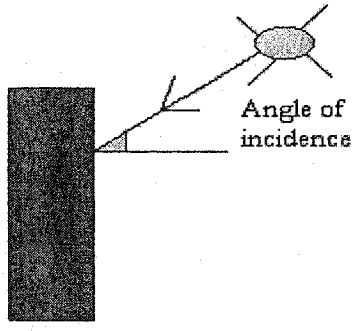

Figure 3.3 Angle of incidence

the declination angle can be determined from [Cooper, 1969] . That is ,

$$\delta = 23.45\text{deg} \cdot \sin \{ 360\ [(284+n)/365]\text{deg} \} \qquad (3.2)$$

where n is the day number.

3.2.3 Intensity of solar radiation

The solar radiation intensity reaches the earth varies from 75% of the solar constant to zero [Angstrom, 1924]. The solar radiation from the sun interacts with the atmosphere causing some of it to be reflected by clouds, scattered by dust and absorbed by ozone, carbon dioxide, water vapor and other gases in the earth's atmosphere. The solar radiation reaching the earth is characterized as direct and diffuse. Direct radiation is that solar radiation which reaches us directly from the sun without being scattered or reflected. The diffuse radiation is solar radiation which is scattered or reflected at least once [Duffie and Veckman, 1991].

The intensity of the solar radiation, I_o, on a plane normal to the sun's rays outside the earth's atmosphere caries from 1398 W/m² on December 21 when the earth is closest to the sun to 1310 W/m² on June 21. The value at the mean earth-sun distance is known as the solar constant I_{sc}, and has the value 1353 W/m².

3.2.4 Transmitted solar radiation into a room

The solar radiation incident on the window and transmitted into a room is consists of three components: the direct beam radiation, diffused sky radiation and the solar radiation reflected by the ground.

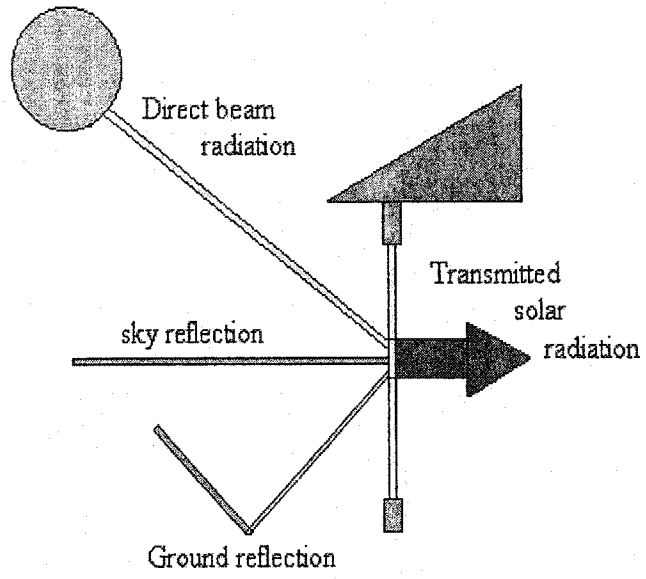

Figure 3.4 Solar Radiation Components

Two models have been developed for calculating the solar radiation incident on the window and transmitted into a building: Hottel's clear sky model [Hottel, 1976], and the hourly clearness index Kt model. In this thesis both models were considered in the calculation, the first model used to determine the transmitted solar radiation in summer and the second model used to determine the transmitted solar radiation in winter.

3.2.4.1 Daily clear index model

It uses the minimum possible amount of solar radiation data as input, namely the daily clearness index KT, which is the ratio of daily total solar radiation incident on a horizontal surface to the extraterrestrial horizontal radiation for that day .Thus, the need for hourly data which is often not available is eliminated. The hourly clearness index Kt is evaluated from the daily value.

The instantaneous solar irradiance transmitted is given as the sum of the beam component G_b and the diffuse component G_d. The beam component is given as

$$G_b = G_{sc} \cdot e_n \cdot (\tau_b \cdot K_b \cdot \cos(\theta)) \qquad (3.3)$$

where k_b is the hourly beam atmospheric transmittance and τ_b is the window beam transmittance for incidence angle θ. Also, e_n is the earth's orbit eccentricity factor on day number n_d and G_{sc} is the solar constant (1353 W/m²). The diffuse component is given by:

$$G_d = G_{sc} \cdot e_n \cdot \tau_d \cdot \cos(\theta_z) \cdot [\, k_d ((1 + \cos(\beta)) / 2) + \rho_g \cdot k_t \cdot ((1 - \cos(\beta)) / 2)\,] \qquad (3.4)$$

where β and θ_z are the inclination and zenith angles respectively, while ρ_g the ground reflectance, and τ_d is the diffuse window transmittance . The hourly clearness index is approximated as [Collares and Rabl, 1979]

$$k_t = (a + b \cos(wt))\, K_T \qquad (3.5)$$

where

$$a = 0.4090 + 0.5016 \sin(\omega_s - 1.047 \text{ rad}) \qquad (3.6)$$

$$b = 0.6609 - 0.4767 \sin(\omega_s - 1.047 \text{ rad}) \qquad (3.7)$$

(ω is the earth's spin rate $2\pi / 86400$ rad/sec , and ω_s is the sunset hour angle – radians).

The above relation has been developed for mean values k_t and K_T, but it is not expected to introduce significant error when used on a single day basis for relatively clear

days, since on these days the variance of KT is small. The hourly diffuse clearness index kd is calculated from kt using the Orgill-Hollands correlation (1977):

$kd / kt = 1.0 - 0.249\ kt$ for $kt < 0.35$ (3.8)

$kd / kt = 1.557 - 1.84\ kt$ for $0.35 < kt < 0.75$ (3.9)

$kd / kt = 0.177$ for $kt > 0.75$ (3.10)

The hourly beam clearness index kb is equal to kt - kd .

3.2.4.2 Hottel clear sky model

Hottel (1976) has presented a convenient method for estimating the beam radiation transmitted through clear atmosphere. The atmosphere transmittance for beam radiation is given in the form

$$\tau_b = a_o + a_1 . \exp\left(\frac{-k}{\cos(z)}\right) \qquad (3.11)$$

where the constants a and k depend on climate and altitude A (km).

$$a0 = ro\,[\,0.4327 - 0.00821\,(\,6 - A\,)^2\,] \qquad (3.12)$$

$$a1 = r1\,[\,0.5055 - 0.00595\,(\,6.5 - A\,)^2\,] \qquad (3.13)$$

$$k = rk\,[\,0.2711 - 0.01858\,(\,2.5 - A\,)^2\,] \qquad (3.14)$$

The correction constants for climate types are given in the table below.

Table 3.1 Correction factors for Hottel's clear sky model

Climate type	r_o	r_1	r_k
Tropical	0.95	0.98	1.02
Midlatitude summer	0.97	0.99	1.02
Subarctic summer	0.99	0.99	1.01
Midlatitude winter	1.03	1.01	1.00

From ASHRAE 1993 the intensity of extraterrestrial normal solar radiation is defined as:

$$Ion = Isc \ . \ [1 + 0.033 \cos [360 .(n / 365)deg] \qquad (3.15)$$

where Isc is the solar constant = 1353 W/m²

n = day of year (1-365)

Consequently, the intensity of beam on an inclined surface is calculated as follows :

$$Ib = Ion \ . \ \tau_b \ . \ \cos(\theta) \qquad (3.16)$$

where θ is the angle of incidence

Liu and Jordan (1963) correlated the beam atmospheric transmittance to the diffuse atmospheric transmittance for clear sky. Assuming isotropic distribution of diffuse radiation [Liu and Jordan 1963], considered the diffuse radiation made up of two components; sky and ground diffuse solar radiation. The intensity is expressed as:

$$I_{d-sky} = I_{on} . \tau_d . \sin(\alpha) . \left(\frac{1 + \cos(\beta)}{2} \right) \qquad (3.17)$$

$$I_{d-ground} = I_{on} . (\tau_d + \tau_b) . \rho_g . \sin(\alpha) . \left(\frac{1 - \cos(\beta)}{2} \right) \qquad (3.18)$$

where τ_d is the diffused transmittance which can be determined after determining the beam transmittance τ_b as follows [Liu and Jordan 1960]:

$$\tau_d = 0.271 - 0.294\,\tau_b \qquad (3.19)$$

and [(1 + cos(β)) / 2] is the view factor from window to sky

[(1 - cos(β)) / 2] is the view factor from window to ground

β is the tilt angle between the surface and the horizontal (0 - 90°)

α is the solar altitude (0-90°)

ρg is the ground reflectance = 0.2

The total solar radiation It incident on a surface is given by the sum of the direct (beam) component Ib, the diffused sky component Ids and the diffuse solar radiation reflected from the ground Idg.

$$I_t = I_b + I_{ds} + I_{dg} \qquad (3.20)$$

As mentioned above the transmitted solar radiation consists of two components: Transmitted beam solar radiation and transmitted diffused solar radiation. The transmitted beam radiation is equal to the incident beam radiation multiplied by the effective transmittance of the window.

$$G_b = I_b . \tau_{ew} \qquad (3.21)$$

where τ_{ew} is the effective transmittance of double glazing window and equal to

$$\tau_{ew} = \frac{\tau_i . \tau_o}{1 - \rho_2 . \rho_3} \qquad (3.22)$$

where τ_i is the inner window transmittance.

τ_o is the outer window transmittance.

ρ_2 & ρ_3 is the reflectance of the inner side of the two glazing (Figure 3.5).

Transmitted diffused solar radiation is equal to the total diffused solar radiation from sky and ground multiplied by the effective transmittance of the window.

$$Gd = (Ids + Idg) . \tau ew \qquad (3.23)$$

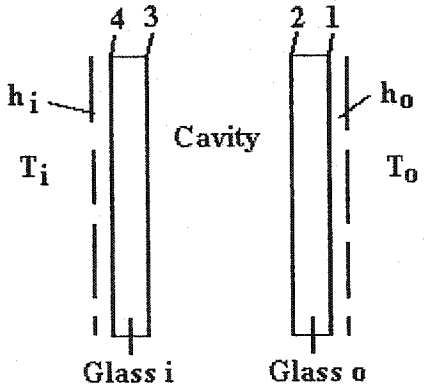

Figure 3.5 Double glazing window

The total solar radiation transmitted is given:

$$Gt = Gb + Gd \qquad (3.24)$$

3.3 Numerical methods

The use of numerical methods for solving heat transfer problems is a result of the complexity of the analytical solutions associated with practical engineering problems.

The finite difference method is one of the most widely used because it generally provides more accurate estimation of temperature and heat flows owing to the capability to model non-linear effects such as convection and radiation. In this approach, each layer is divided into a number of sub-layers (regions). Each region is represented by a node. Each node (*i*) has a thermal capacitance (*Ci)* associated with it and resistances connecting it to adjacent nodes.

3.3.1 The explicit finite difference model

The explicit finite difference method was used because it is particularly suitable for modeling of non-linear heat diffusion problems. The advantage of the explicit finite difference representation is that it gives the future temperature of a single node in term of current temperatures of that node and its neighbors. Thus, if at the end of a certain time period, all the nodal temperatures are known, then each of nodal temperatures at the end of the next moment, Δt, may be explicitly found, node by node without a matrix inversion or solution of simultaneous equations [Dusinbere, 1961].

The general form of the explicit finite difference formulation corresponding to node *i* and time interval *p* is:

$$T(i,p+1) = \left(\frac{\Delta t}{C_i}\right)\cdot\left(q_i + \sum_j \frac{T(j,p) - T(i,p)}{R(i,j)}\right) + T(i,p) \qquad (3.25)$$

where *j* represent all nodes connected to node *i*, q*i* represents all heat sources at node *i* such as solar radiation, *p* is the time interval and Δt is the time step , Ci is the thermal capacitance for node *i* and R*(i,j)* is the conductive, radiative or convective thermal resistance.

The time step selected based on the following condition for numerical stability:

$$\Delta t_{critical} = \min\left(\frac{C_i}{\sum_j \frac{1}{R_{i,j}}}\right) \tag{3.26}$$

for all nodes *i*.

3.4. Natural ventilation

Transfer of air between the building and the surrounding environment plays a very important role in the overall thermal balance of buildings, which also affects the levels of thermal comfort and indoor air quality. Exchange of air can be achieved either by mechanical means (mechanical ventilation or through large openings of the building's envelope (natural ventilation). The air flow rate (Q) through large opening is given by the common orifice flow equation:

$$Q = Cd.A.\left(\sqrt{\frac{2.\Delta p}{\rho}}\right) \tag{3.27}$$

where C_d is the discharge coefficient of the opening, A is the opening area(m^2), ΔP is the pressure difference across the opening in Pa and ρ is the density of air (1.2 kg/m^3).

Based on the above equation, Li et al. 2000, have developed equations for calculating the air flow in a two-zone system (Figure 2.6). Which can be written in the following form after substituting ΔP from equations (2.25, 2.26, 2.27) in equations (2.22, 2.23, 2.24):

$$q = \rho_{air} \cdot Cd \cdot A \cdot \sqrt{\left(\frac{T_b - To}{To + 273} \cdot g \cdot hb\right) + \left(\frac{T_t - To}{To + 273} \cdot g \cdot ht\right)} \qquad (3.28)$$

where A is the effective area and equal to:

$$A = \frac{2 \cdot Am \cdot At \cdot Ab}{Atmb \cdot m^2} \qquad (3.29)$$

Ab (m^2) is the bottom opening area, At (m^2) is the top opening area, g (m/sec^2) is the gravity acceleration, Am (m^2) is the opening area between the two floors. Cd is the discharge coefficient, h_b (m) $2h_b$ is equal to the height between the middle of the bottom opening and the level between the two floors, h_t (m) $2h_t$ is equal to the height between the middle of the top opening and the level between the two floors and ρ_i is the air density for zone *i*

CHAPTER 4

MODEL FOR TWO ZONE HOUSE

4.1 Introduction

In this chapter the two zone model is developed. The model is studied for two seasons winter and summer. In winter the model is that of an integrated radiant floor heating – direct gain passive solar house. The solar radiation transmitted into the house through windows is calculated. An explicit finite difference model is employed to study the performance of the house, and the air flow inside the house is coupled with the thermal model.

In summer the model is a naturally ventilated direct gain passive solar house. The solar radiation transmitted into the house is calculated. An explicit finite difference model is also employed to study the performance of the house. Two-sided natural ventilation especially at night is used to cool the house and achieve the thermal comfort without the use of mechanical systems. The model is also studied with shading device to reduce the transmitted solar radiation into the house when necessary.

4.2 Description of the two zone model

The two-zone models are divided into two types, first type is two zones next to each other (bungalow) shown in Figure 4.1, and the second type is two zone on top of each

other (Cottage) shown in Figure 4.2. Both types of houses are common type of houses in Canada.

In two zone model the two zones are linked by air flow paths- doors, doorway, ventilation fan, small openings, etc. Air movement through these paths affects the room air temperature, so for studying the thermal performance of each room the air flow should be calculated and coupled with the thermal network of the two zones. In a direct gain passive solar building, for first type, the south facing room is connected by a door to the north facing room to allow the heat to be transferred by natural ventilation. In the second type the two zones are connected by a doorway and the air flow between the two floors is a bidirectional flow. The second type is considered in this study and the thermal performance of the house is studied in two seasons - winter and summer.

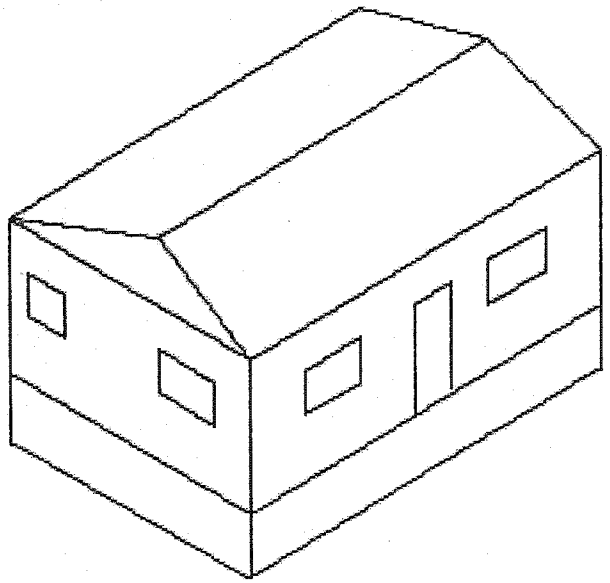

Figure 4.1 Two zones next to each other (bungalow).

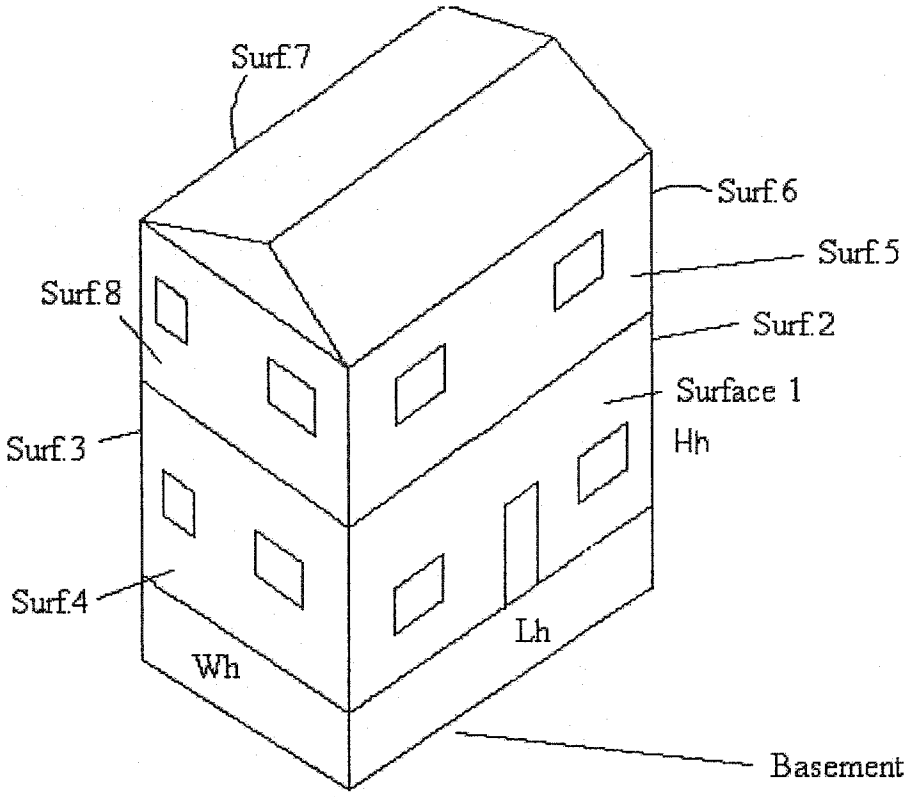

Figure 4.2 Two zones on top of each other

4.3 Case study

The studied two zone model is presented graphically in Figure 4.2. It consists of a basement and two floors (ground floor and first floor) located in Montreal (Latitude = 45°). The thermal performance of the house is studied in winter and summer. Walls are assumed to be made up of gypsum board with a thickness equal to 13mm and outdoor insulation with R-value equal to $R_{ins} = 5 \frac{m^2.°C}{watt}$, siding and sheathing with R-value

equal to $R_{sid} = 0.37 \frac{m^2.°C}{watt}$. The floor in each floor is made up of concrete thermal mass and insulation. The main parameters of the house are shown in Table 4.1.

Table 4.1 Main parameters for the studied house.

Floor area for each floor, m^2	100
Wall area, m^2	30
Internal height of each floor, m	3
South-facing glazing area, m^2	5 (5% of the floor area)
Door area, m^2	1.8
Windows area in north, west and east , m^2	3 (each)
Total glazing area, m^2	14
R-value for the walls , $m^2.°C / W$	3.854
R-value for the floor, $m^2.°C / W$	5.303
R-value for the ceiling in the 1^{st} floor, $m^2.°C / W$	3.754
R-value for the windows, m^2.degC /W	0.34
R-value for the door, m^2.degC /W	2

The house is assumed to be a direct gain. The south facing façade (surf. 1&5) assumed to have the maximum window area to allow more solar radiation to enter the house and to be stored in the thermal mass. The other surfaces (2,3,4,6,7,&8) were assumed to have equal window area smaller than the south facing window's area. The window assumed to be double glazing with R-values equal to $R = 0.34 \frac{m^2.°C}{watt}$.

The program for the calculation is developed in MathCAD 2001*i* professional and it is presented in Appendices A&B. The input parameters to the program are: house dimensions, internal height of each floor, location of the house (Montreal, L = 45°), windows and doors area, orientation, the thermal resistance of the windows and doors, wall absorptance (90%), interior film coefficient, day number, ground reflectance = 20% (no snow), the constructions of the walls, floors and ceiling, basement temperature which is assumed to be constant and equal to 16°C in winter and equal to 20°C in summer.

The program calculates the solar radiation on each face of the house. The distribution of the incoming solar radiation through the window to the interior surfaces of the house is approximated to be as 70% absorbed by the floor and 30% absorbed by the other surfaces in proportional to their area.

The outside temperature for a day is modeled by a Fourier series based on *NTo+1* values that are an input to the array below.

$$Ton_n = \sum_{it} To_{it} \cdot \frac{\exp(-j.w_n.t_{it})}{NTo+1} \qquad (4.1)$$

where $j = \sqrt{-1}$, n is the harmonic number (0,1..3), *it* is the time index (0,1..*NTo*), t_{it} is the time and equal to (it.3.hr) and w = 2.π.n/86400 (rad / sec).

Figure 4.3, shows the thermal network for the house. This thermal network is for winter with floor heating system. Summer thermal network is the same as winter but without the auxiliary heat. The thermal network for each floor consists of two thermal capacitances for the floor capacity interconnecting thermal resistances, and another

thermal capacitance for walls in the ground floor and for the walls and roof in the first floor. Two thermal capacitances for the floor surface were chosen because increasing the number to three or four or more has no effect on the result as it will be shown in the next chapter.

Node 1 represents the room air for the ground floor, node 2 represents the surface of the floor surface in the ground floor, node 3 represents the interior layer of the concrete, node 4 represents the interior layer of the concrete, node 5 represents the interior layer of the wall in the ground floor, node 6 represents the surface of the walls, node 7 represent the ceiling of the first floor, node 8 represents the interior layer of the concrete, node 9 represents the interior layer of the concrete, node 10 represents the surface of the floor surface in the first floor, node 11 represents the room air for the first floor, node 12 represents the unheated surfaces in the first floor which are the walls and roof, node 13 represents the interior layer of the unheated surfaces in the first floor. The network also contains two heat sources the solar radiation and the auxiliary heat, S2 is the solar radiation transmitted through the windows and absorbed by the storage mass, S6 is the solar radiation transmitted through the windows and absorbed by the wall, q_{aux} is the auxiliary heat, S10 is the solar radiation transmitted through the windows and absorbed at the floor surface in the first floor, S12 is the solar radiation transmitted through the windows and absorbed by unheated surfaces in the first floor. The thermal resistances in the thermal network are identified in Table 4.2. The two thermal networks for the ground floor and the first floor are coupled by a thermal resistance by convection between the room air in the ground floor and the room air in the first floor which is R111.

The explicit finite difference method is employed to calculate the temperature

variation of each node due to its suitability in modeling non linear heat diffusion problems. The energy balance equation (eqn.4.2) is applied at each node and solved repeatedly at each time step for the period of simulation.

$$T(i,p+1) = \left(\frac{\Delta t}{C_i}\right)\cdot\left(q_i + \sum_j \frac{T(j,p) - T(i,p)}{R(i,j)}\right) + T(i,p) \qquad (4.2)$$

where i is the node for which the energy balance is written, j represent all nodes connected to node i, qi represents all heat sources at node i such as solar radiation, p is the time interval and Δt is the time step, Ci is the thermal capacitance for node i and R(i,j) is the conductive, radiative or convective thermal resistance.

The time step is selected based on the following condition for numerical stability [Holman, 1986]:

$$\Delta t_{critical} \leq \min\left(\frac{C_i}{\sum_j \frac{1}{R_{i,j}}}\right) \qquad (4.3)$$

for node i . For the studied model the time step for the nodes with capacitances is calculated and the results are shown in Table 4.2.

Table 4.2 Calculated time step.

Node #	3	4	5	8	9	13
Time step (second)	862.7	2573.0	313.6	2573.0	862.7	313.6

To ensure stability Δt should be equal to or less than the minimum time step calculated before. So the time step selected is 300sec.

The thermal resistances by conduction, convection and radiation are calculated from the following equations:

$$R = \frac{L}{k.A} \qquad \text{for conduction} \qquad (4.4)$$

$$R = \frac{1}{h.A} \qquad \text{for convection and radiation} \qquad (4.5)$$

where A is the area (m^2)

h is the heat transfer coefficient by radiation or convection $\left(\frac{W}{m^2.°C}\right)$

k is the thermal conductivity $\left(\frac{W}{m.°C}\right)$

The thermal capacitances are calculated from the following equation:

$$C = c.\rho.A.L \qquad (4.6)$$

where c is the specific heat $\left(\frac{Joule}{kg.°C}\right)$

ρ is the density $\left(\frac{kg}{m^3}\right)$

A is the area (m^2)

L is the thickness (m)

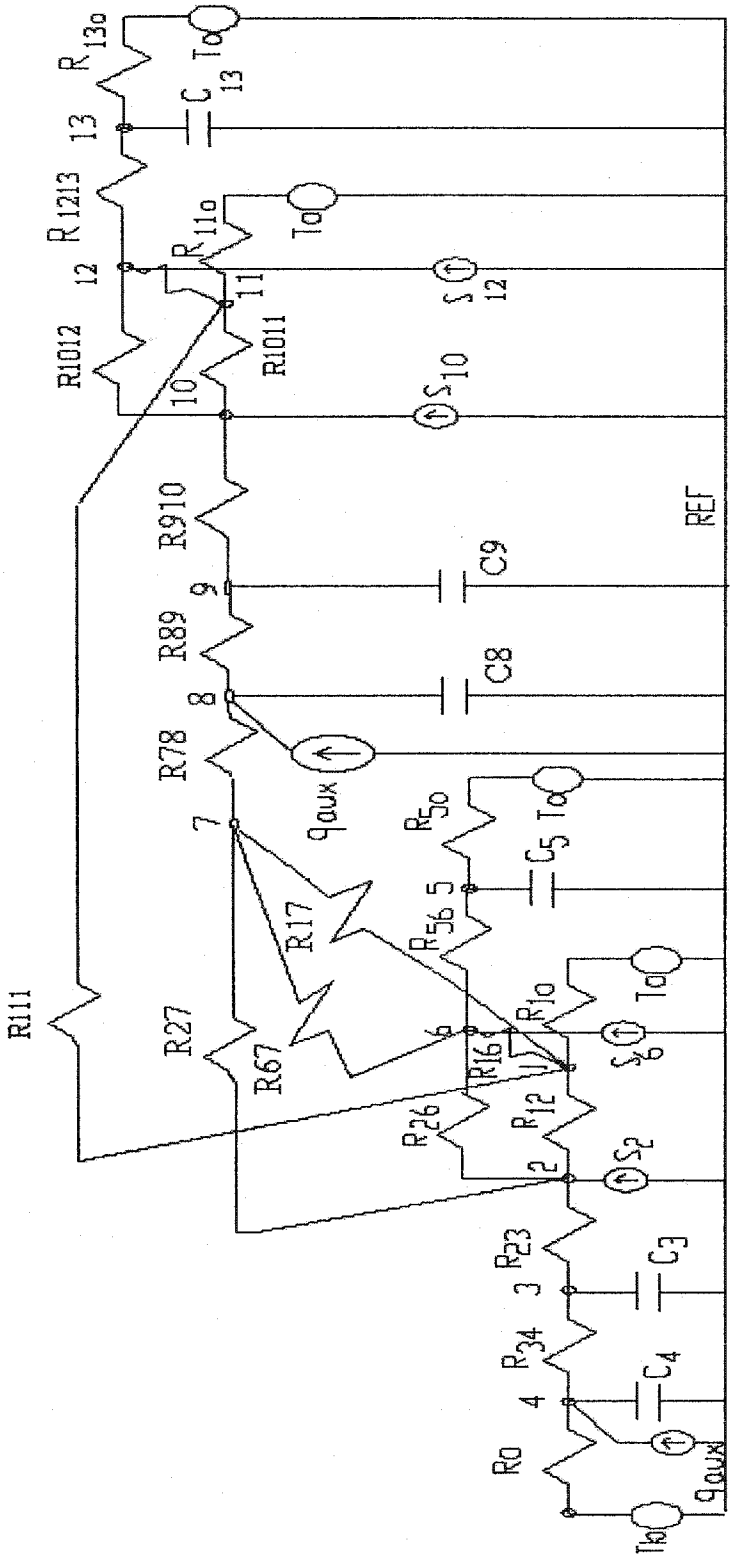

Figure 4.3 Thermal network of the two zone model

Table 4.3 Thermal resistances of the house

R_{4o}	Thermal resistance between the basement and ¼ of the floor in the GF
R_{34}	Thermal resistance for half of the floor surface for the ground floor.
R_{23}	Thermal resistance for the second half of the floor surface for the ground floor.
R_{12}	Thermal resistance by convection between the floor surface and the room air for the G.F.
R_{26}	Thermal resistance by radiation between the floor surface and the walls for the G.F.
R_{27}	Thermal resistance by radiation between the floor surface and the ceiling for the G.F.
R_{17}	Thermal resistance by convection between the room air and the ceiling for the G.F.
R_{16}	Thermal resistance by convection between the room air and the walls for the G.F.
R_{67}	Thermal resistance by radiation between the walls and ceiling for the G.F.
R_{1o}	Thermal resistance between the room air and outside due to windows, doors and infiltration
R_{56}	Thermal resistance for the interior layers of the walls for the G.F.
R_{5o}	Thermal resistance between the interior layer of the walls and outside for the G.F.
R_{78}	Thermal resistance between the basement and ¼ of the floor in the GF
R_{89}	Thermal resistance for half of the floor surface for the 1^{st}.F.
R_{910}	Thermal resistance for the second half of the floor surface for the 1^{st}.F.
R_{1011}	Thermal resistance by convection between the floor surface and the room air for the 1^{st}.F.
R_{1012}	Thermal resistance by radiation between the floor surface and unheated surfaces for the 1^{st}.F.
R_{1112}	Thermal resistance by convection between the room air and unheated surfaces for the 1^{st}.F.
R_{11o}	Thermal resistance between the room air and outside due to windows, doors and infiltration for the 1^{st}.F.
R_{1213}	Thermal resistance for the interior layers of the walls for the 1^{st}.F.
R_{13o}	Thermal resistance between the interior layer of unheated surfaces and outside for the 1^{st}.F.

The thermal capacitance for each layer of the floor is equal to half of the total thermal capacitance of the floor ($C3 = C4 = C8 = C9 = \frac{C_{floor}}{2}$). And the thermal capacitance of the interior layer of the walls in the ground floor is equal to the sum of the thermal capacitances of the interior layer of each wall and for the first floor is equal to the sum of the thermal capacitance of the interior layer of the walls and the ceiling.

The simulations start after setting the initial conditions and the house details. Each temperature is then updated at each time step together with the different heat transfer coefficients, taking into account the instantaneous changes of solar radiation and ambient temperature which are simulated. The results can be obtained from the program for any period of simulation.

4.4 Winter case

The model for winter is an integrated radiant floor heating – direct gain passive solar house (two zone house) shown in Figure (4.2). The floor heating is used because it is more comfortable, the thermal mass in this case stores both heat produced by the under floor electric panels as well as solar gains transmitted through the windows. The solar gains are absorbed at the top surface of the floor mass, while the auxiliary heat is supplied at the bottom of the slab. The thermal network for the model in winter is shown in Figure 4.3 and explained above.

4.4.1 Auxiliary heating model

The auxiliary heat q_{aux} is proportional to the error between the set point T_{sp} and actual room air temperature T_R:

$$q_{aux} = K_p.(T_{sp} - T_R) \tag{4.7}$$

where K_p is the proportional control constant assumed 6155 watt/°C for the first floor and 5355 watt/°C for the ground floor and the maximum capacity of the heating system is equal to 12310 watt and it is equal to 10710 watt for the ground floor. *Tsp* is the set point and T_R is the room air temperature.

4.4.2 Control strategy of the auxiliary heat

Two major things should be given attention in the design for passive solar building with floor heating system which are overheating and energy consumption, overheating might happened when a significant amount of solar radiation is incident on the floor and its thermal storage mass is already warm from the auxiliary heating. Achieving high saving in the energy consumption is the main objective of the passive solar design. These two problems could by controlled by employing an appropriate control strategy for the indoor set point to maintain the thermal comfort inside the house and prevent the floor surface temperature from exceeding about 29°C [ASHRAE, 1989] while at the same achieve high saving in the auxiliary heat energy consumption.

For the studied model the control strategy is to lower the set point at night to reduce the possible overheating during the daytime for the ground floor, and lower the set point during the daytime for the first floor and increase it during night. The set point for the ground floor was set to 18°C from 9pm to 6am, and set to 22°C from 6am to 9pm. And for the first floor the set point was set to 19°C during the daytime from 7am to 2pm then

set it to 22°C during the night from 2pm to 7am. Figure 4.4 shows the control strategy for the studied model.

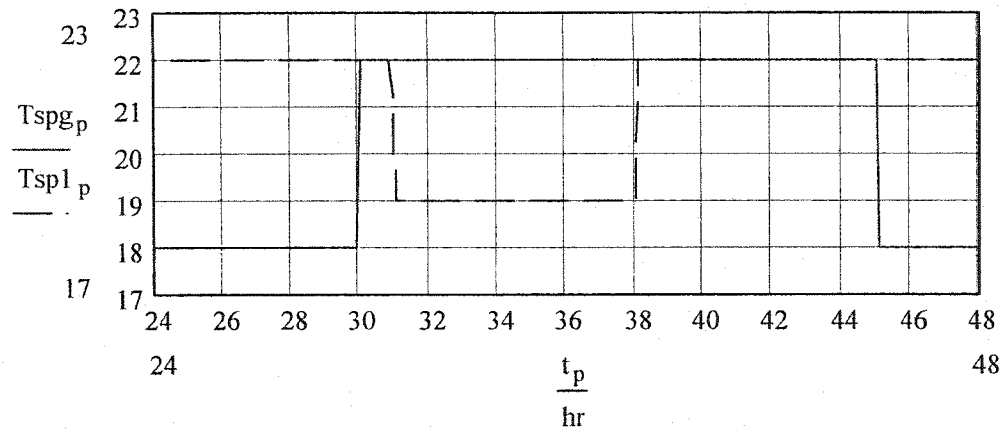

Figure 4.4 Control strategy for the set point. Tspg is the set point for the ground floor, and Tsp1 is the set point for the first floor.

4.4.3 Solar radiation calculation

As explained in chapter 3, the solar radiation incident on the window consists of three components: the direct beam radiation, diffused sky radiation and the solar radiation reflected by the ground. Also the two developed models for calculating the transmitted solar radiation into a building were explained. The hourly clearness index model is employed in winter. The design is performed for January 15 (day # 15). Daily clearness index for January equal to 0.45 (K_T= 0.45). Latitude = 45° (Montreal).

Figure 4.5, shows the solar radiation incident on the windows on both floors. And Figure 4.6 shows the solar radiation transmitted into the house, which is modeled as 70% absorbed at the floor surface and the remainder by the other surfaces in proportion to their areas.

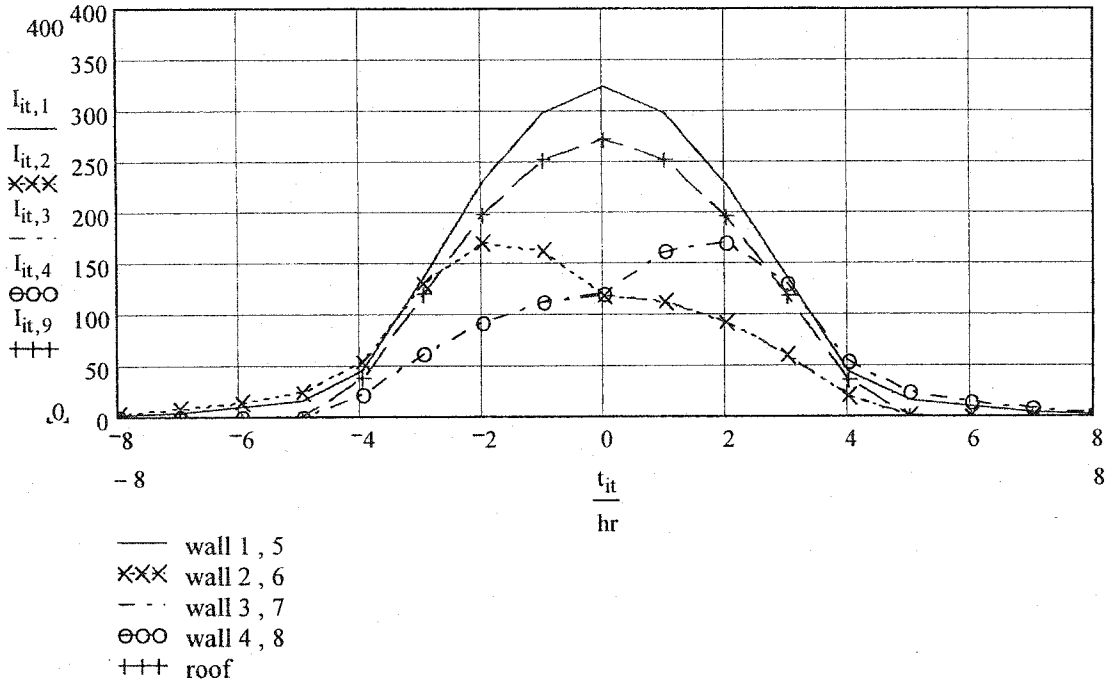

Figure (4.5) Solar radiation incident on windows (W/m²)

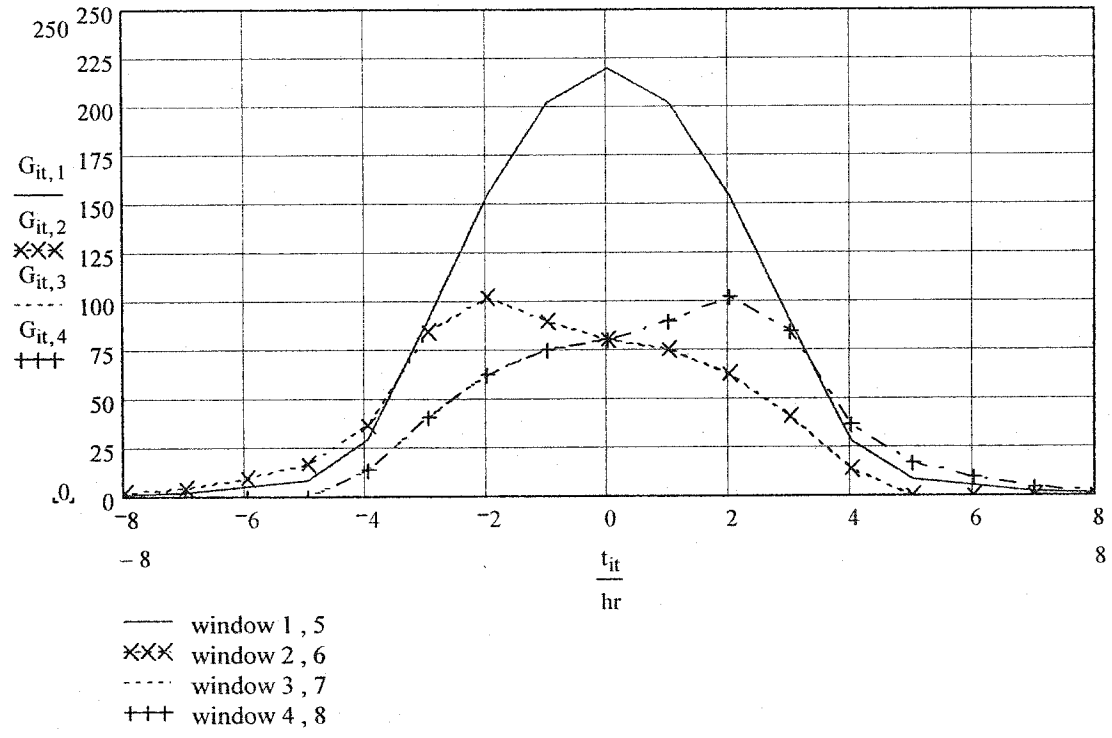

Figure (4.6) Solar radiation transmitted through the windows (W/m²)

4.4.4 Air flow inside the house

Air movement in buildings plays an important role in energy savings, thermal comfort, and indoor air quality because the distributions of temperature and contaminant concentration are directly dependent on the airflow pattern.

In this study the house was assumed to be tight, so there is no air movement from outside to inside or from inside to outside. There is only air movement between the two floor (bidirectional flow). The mass flow rate between the two floors can be found by determining the velocity of air moving between the two floor, for the studied model in this thesis the air velocity was calculated using CFD technique and the average velocity for the air flow between the two floors was found to be equal to 0.04m/sec. The calculation of air velocity using CFD model was done by Dr. A. Athienitis using the CFD program Fluent.

The mass flow rate between the two floors is equal to:

$$q = \rho_{air}.\upsilon.A \qquad (4.8)$$

where q is the mass flow rate (kg/sec), ρ_{air} is the air density (kg/m^3) and A is the opening area between the two floors (2m^2).

4.4.5 Coupled air flow - thermal

There are various approaches for integrating heat and air flow calculations, each having specific consequences in terms of computing resources and accuracy. One way to actually quantify this, is to use a simulation environment which supports these various approaches, and to compare the results of the approaches for a typical case study.

Coupling of building heat and mass flow in a mathematical / numerical sense, effectively means combining the energy and flow balance matrix equations for the building [Clark, 1985].

In this study the air flows inside the house in both directions (bidirectional flow) due to the natural convection, and the average air velocity was calculated before. This air flow is modeled in the thermal network by a convection thermal resistance *R111* connect the room air temperature is both floors. This thermal resistance is calculated as follows:

$$R_{111} = \frac{1}{q.c_{pair}} \qquad (4.9)$$

where q (kg/sec) is the mass flow rate between the two floors and calculated from equation (4.8), c_{pair} is the specific heat of air $\left(\frac{1000.Joule}{kg.°C}\right)$.

4.4.6 Simulations and results

Window area, the thermal mass thickness as well as window R-value are the main three parameters in the design for passive solar house. The window transmits the solar radiation into the house and the thermal mass absorbs the transmitted solar radiation through windows, stores and release it to the room air when it is needed. Different window area and thermal mass thickness were investigated to achieve the main objectives of the passive solar design in achieving the thermal comfort and high saving in the energy consumption.

The simulations are performed for two days (periodic). Thus, weather data have to be generated for *NT* times as follows:

$$NT = \frac{86400.\text{sec}}{\Delta t} x2 \qquad (4.10)$$

NT (number of time step) is equal to 576 based on the time step selected. The time at which simulation to be performed is equal to:

$$t_p = p.\Delta t \qquad (4.11)$$

where p is the number of time steps for two days ($p = 0,1..NT$), and Δt is the time step (300sec).

The figures below show the results of the room air temperature swing for both floors with the set point profile for each floor with different thermal mass thickness and different window area.

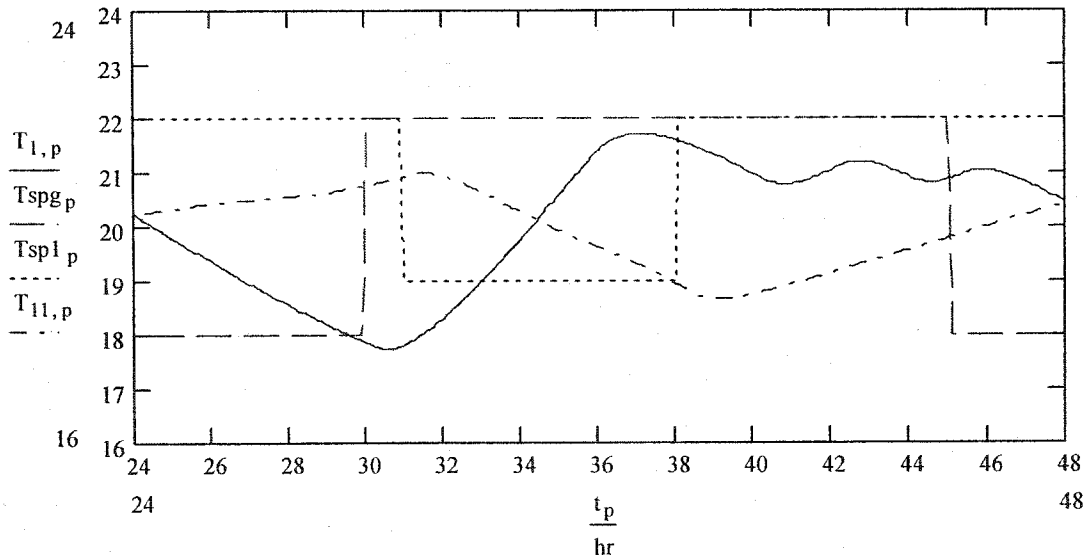

Figure 4.7 Room air temperature variation in both floors (thermal mass thickness 10cm and south facing window area 5% of the floor area). T1 is the room air temperature for the ground floor, and T11 is for the first floor. Tspg is the set point for the ground floor, and Tsp1 for the first floor.

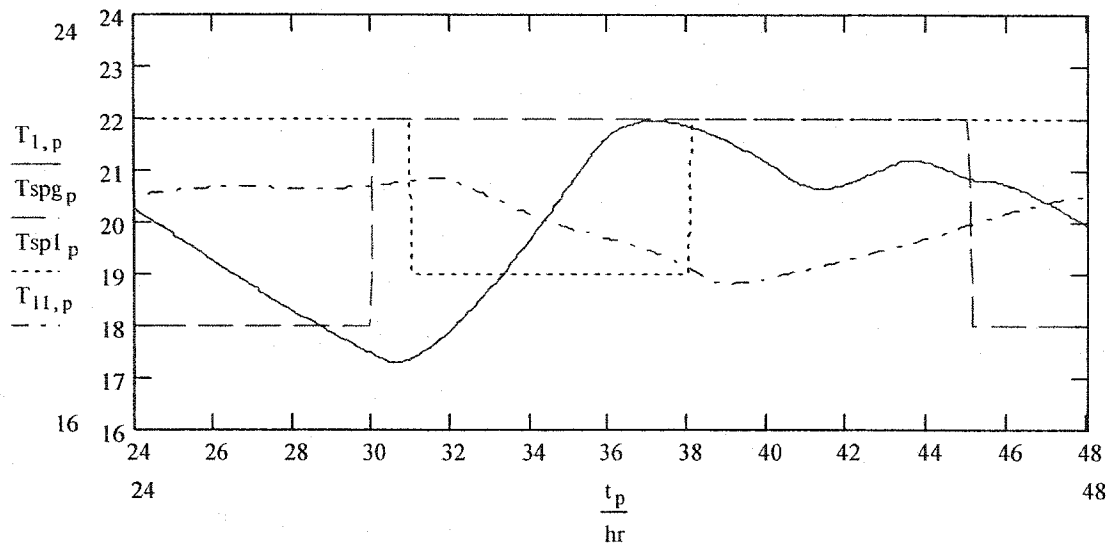

Figure 4.8 Room air temperature variation in both floors (thermal mass thickness 10cm and south facing window area 10% of the floor area). T1 is the room air temperature for the ground floor, and T11 is for the first floor. Tspg is the set point for the ground floor, and Tsp1 for the first floor.

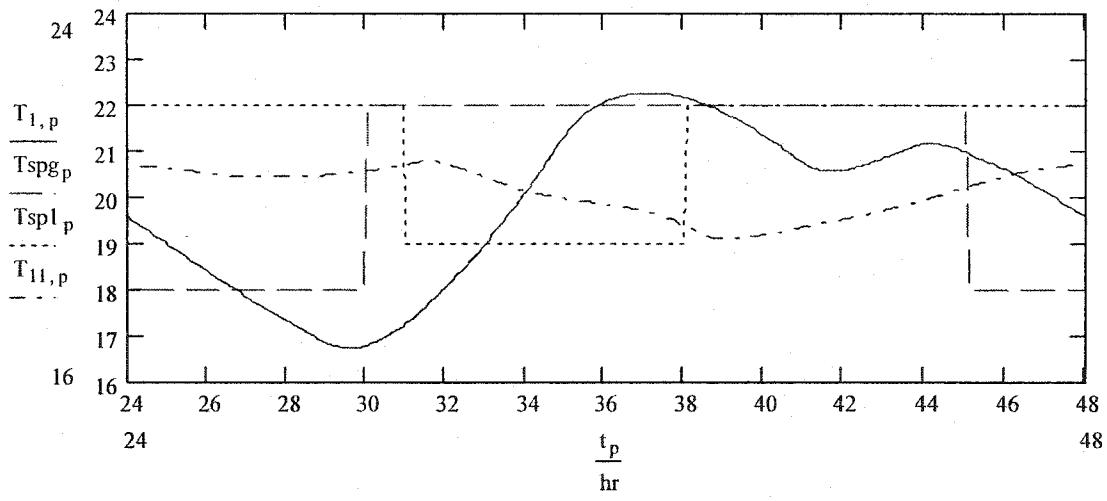

Figure 4.9 Room air temperature variation in both floors (thermal mass thickness 10cm and south facing window area 15% of the floor area). T1 is the room air temperature for the ground floor, and T11 is for the first floor. Tspg is the set point for the ground floor, and Tsp1 for the first floor.

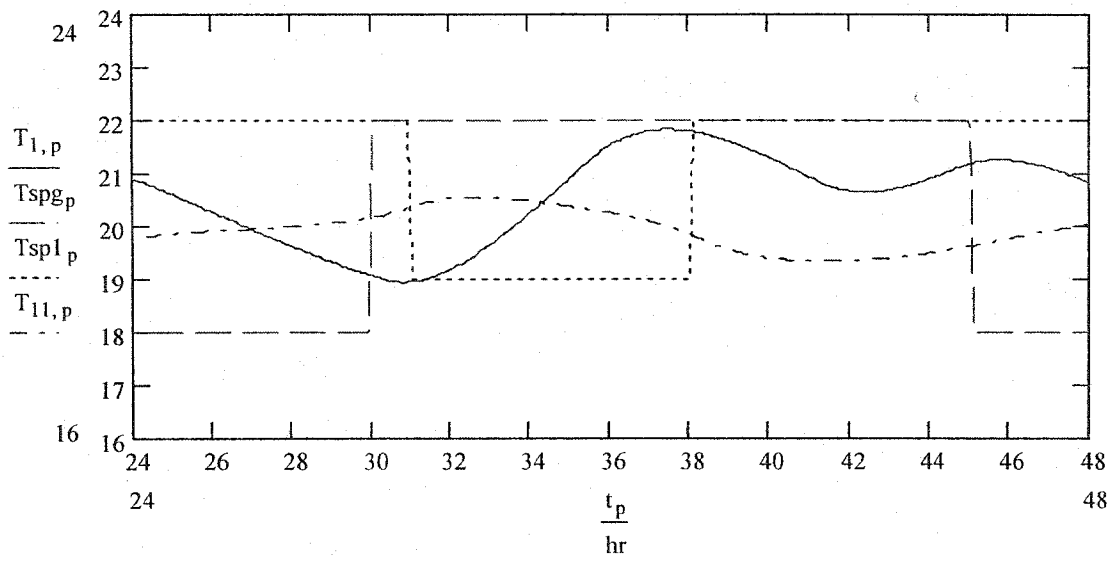

Figure 4.10 Room air temperature variation in both floors (thermal mass thickness 15cm and south facing window area 5% of the floor area). T1 is the room air temperature for the ground floor, and T11 is for the first floor. Tspg is the set point for the ground floor, and Tsp1 for the first floor.

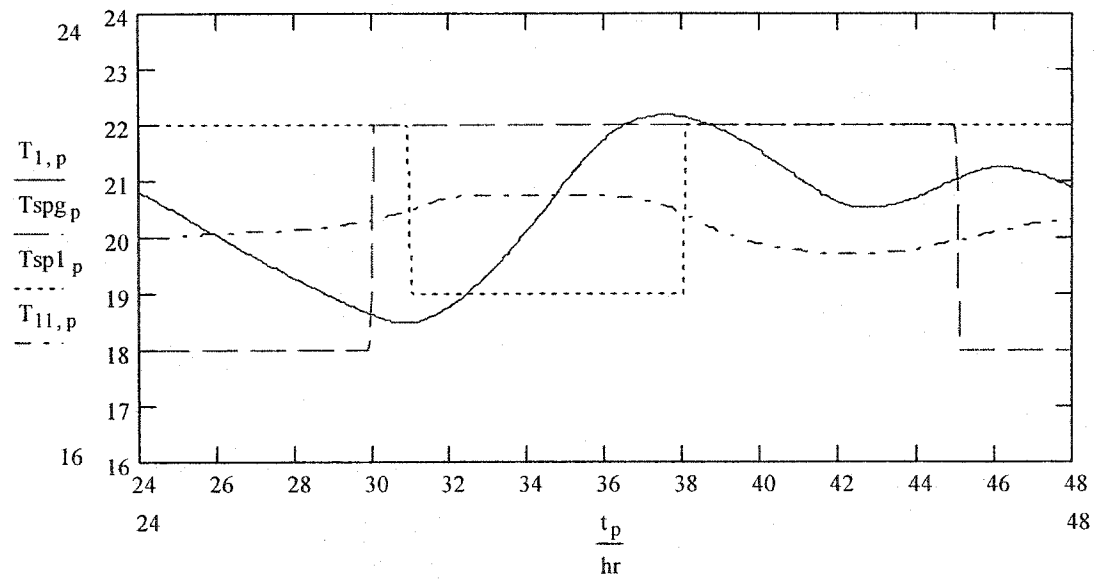

Figure 4.11 Room air temperature variation in both floors (thermal mass thickness 15cm and south facing window area 10% of the floor area). T1 is the room air temperature for the ground floor, and T11 is for the first floor. Tspg is the set point for the ground floor, and Tsp1 for the first floor.

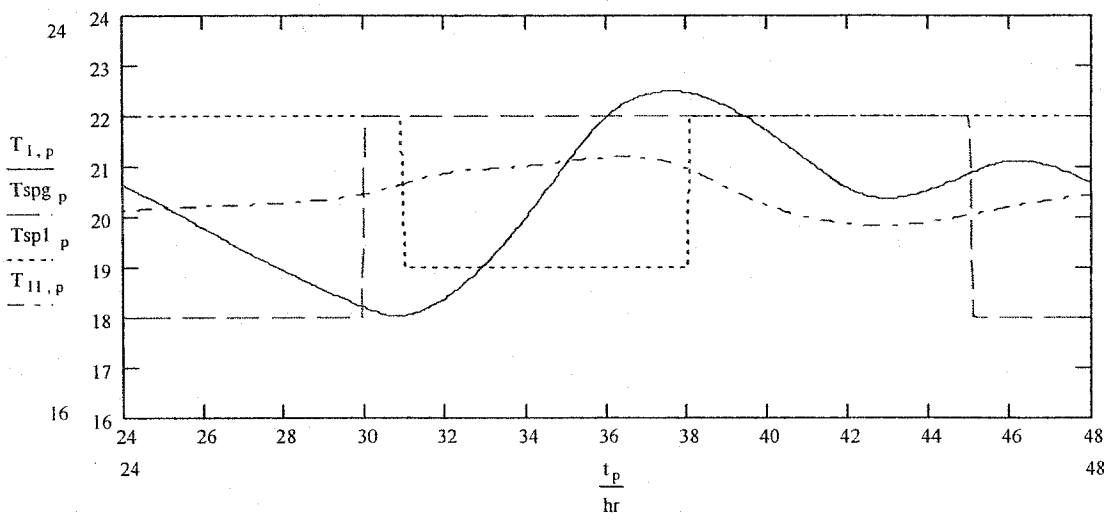

Figure 4.12 Room air temperature variation in both floors (thermal mass thickness 15cm and south facing window area 15% of the floor area). T1 is the room air temperature for the ground floor, and T11 is for the first floor. Tspg is the set point for the ground floor, and Tsp1 for the first floor.

Table 4.4 shows the auxiliary heat energy consumption for the above cases.

Table 4.4 The auxiliary heat energy consumption for average day in January [window R-value equal to 0.34(m^2.K / W)].

South Facing Window area	Thermal mass thickness	Tmax °C		Tmin °C		Auxiliary heat energy consumption for the G.F (MJ)	Auxiliary heat energy consumption for 1st.F (MJ)
		G.F	1st. F	G.F	1st.F		
5% of the floor area (1/6 of the façade area)	10cm	21.7	21	17.7	18.7	209.9	487.8
	15cm	21.8	20.2	18.9	19	207.3	490.2
10% of the floor area (1/3 of the façade area)	10cm	21.9	20.8	17.3	18.8	217.3	531.1
	15cm	22.2	20.8	18.5	19.7	234.4	547.8
15% of the floor area(1/2 of the façade area)	10cm	22.3	20.8	16.8	19.1	248.2	575.5
	15cm	22.5	21.2	18.1	19.8	254.1	594.1

As may be observed, the minimum temperature swing in both floors in the case is when the thermal mass thickness is equal to 15cm and the south facing window area equal to 5% of the floor area which is equal to 1/6 of the façade area (Figure 4.10). In this case the room air temperature for the ground floor reaches its minimum (18.9°C) in the early morning and starts going up when the auxiliary heat is set on till it reaches the maximum of 21.8°C in the afternoon, so the temperature swing during the day is equal to 2.85°C. While the room air temperature for the first floor reaches the maximum 20.2°C at night when the heat is on and starts going down to the minimum 19°C during the day time when the heat is off, so the temperature swing during the day is equal to 1.2°C. The auxiliary heat energy consumption in this case is the minimum for the ground floor, and it is very close to the minimum for the first floor.

Window R-value is very important parameter in the design of passive solar house. The above simulations are for a double glazed window with R-value equal to 0.34(m^2.K/ W). More simulations are performed for a double glazed window with R-value equal to 0.52(m^2.K / W) (low-e coating) for the same day (Jan, 15). Table 4.5 shows the maximum and minimum temperature as well as the energy consumption for both floors.

By comparing the two tables 4.4 & 4.5, it can be seen that when low-e coated window is used the temperature swing in both floors is reduced as well as the energy consumption. When higher amounts of mass are used on an average January day the energy consumption is higher but thermal comfort is improved due to the lower temperature swing.

Table 4.5 Max & min room air temperature and energy consumption in both floors for average day in January, window R-value equal to 0.52(m^2.K / watt).

South Facing Window area	Thermal mass thickness	Tmax °C		Tmin °C		Auxiliary heat energy consumption for the G.F (MJ)	Auxiliary heat energy consumption for 1^{st}.F (MJ)
		G.F	1^{st}. F	G.F	1^{st}.F		
5% of the floor area (1/6 of the façade area)	10cm	21.8	21.1	18.7	19.4	144.5	410.5
	15cm	21.9	21.1	19.5	20.2	155.1	428.8
10% of the floor area (1/3 of the façade area)	10cm	22.1	21.1	17.8	19.7	158.1	423.9
	15cm	22.4	21.2	19.2	20.4	165.3	437.0
15% of the floor area (1/2 of the façade area)	10cm	22.3	20.8	16.7	19.1	167.0	445.5
	15cm	22.8	21.8	18.9	19.8	170.5	431.2

The thermal performance of the house was further studied for a clear cold day in February. Days from mid February to March have higher solar gains which are useful given the cold weather at this time, so they are appropriate for system optimization. The day number taken was 50. The daily clearness index value used was equal to 0.75 (clear day).

The simulations were performed for double glazed window with two different R-values 0.34 & 0.52 (m^2.K/watt). Table 4.6 shows the maximum and minimum room air temperature as well as the energy consumption for both floors.

Table 4.6 Max & Min room air temperature and energy consumption for both floors on a clear cold day (day # 50).

Window R-Value (m^2.K/watt)	South Facing Window area (% of the floor area)	Thermal mass thickness	T(max) °C		T(min) °C		Auxiliary heat energy consumption (MJ)	
			G.F	1st.F	G.F	1st.F	G.F	1st.F
0.34	5%	10cm	22.7	21.2	18.2	20.6	131.5	409.9
		15cm	22.8	22.1	18.7	19.7	137.2	406.1
	10%	10cm	24.3	20.6	17.2	20.0	108.1	413.3
		15cm	24.2	23.4	17.8	19.5	120.5	412.5
	15%	10cm	26.2	24.4	17.3	19.9	104.3	410.3
		15cm	26.1	25.2	18.3	19.5	99.1	410.8
0.52	5%	10cm	22.9	21.1	18.4	20.8	82.3	319.7
		15cm	23.2	20.5	19.6	19.9	64.7	326.3
	10%	10cm	25.1	23.2	18.9	20.2	68.6	295.1
		15cm	25.3	24.4	19.9	20.1	54.8	298.5
	15%	10cm	27.5	25.3	19.8	20.3	51.3	263.9
		15cm	27.3	26.5	20.3	20.1	44.6	268.5

As can be observed, the room air temperature swing was reduced when low-e coated window was used as well as the energy consumption. R-value equal to 0.52 (m^2.K/watt) with window area equal to 10% of the floor area (1/3 of the south façade area) and with thermal mass thickness equal to 15cm is the optimal. This case is chosen because the maximum temperature is 25.3°C which is acceptable in the design for thermal comfort, and the energy consumption is the lowest comparing to the cases where the maximum temperature does not exceed 25°C. Although the temperature swing in this case is a little bit higher than other cases but it is still in the comfort zone.

4.5 Summer case

The model for summer is two-zone naturally ventilated direct gain passive solar house shown in Figure (4.2). Natural ventilation is used to allow the fresh air to enter the house through openings in the building envelope to cool the house especially at night. These openings are windows (other types of opening could be useful such as trickle vents or louvers). Cross natural ventilation type is used, in this type one-way air flow exists through the opening. The air enters from the ground floor and exits from the upper floor exploiting the stack effect.

The thermal network of the house in summer is the same as winter but without the auxiliary heat. The thermal network is shown in Figure 4.3 and explained above. The thermal resistances and capacitances are calculated from equations 4.4, 4.5, & 4.6.

The outside temperature for a day was modeled by a Fourier series as explained before (equation 4.1). The outside temperature assumed to varies from 15°C at night to 30°C at noon.

4.5.1 Solar radiation calculation

Solar radiation transmitted through the windows and absorbed by the interior surfaces was calculated using Hottel's clear sky model, this model was described in Chapter 3 section 3.2.4.2. The calculation of solar radiation is made for July 15 (day number 196). Figures 4.13 and 4.14 show the solar radiation incident on the walls and the transmitted solar radiation into the house in both floors.

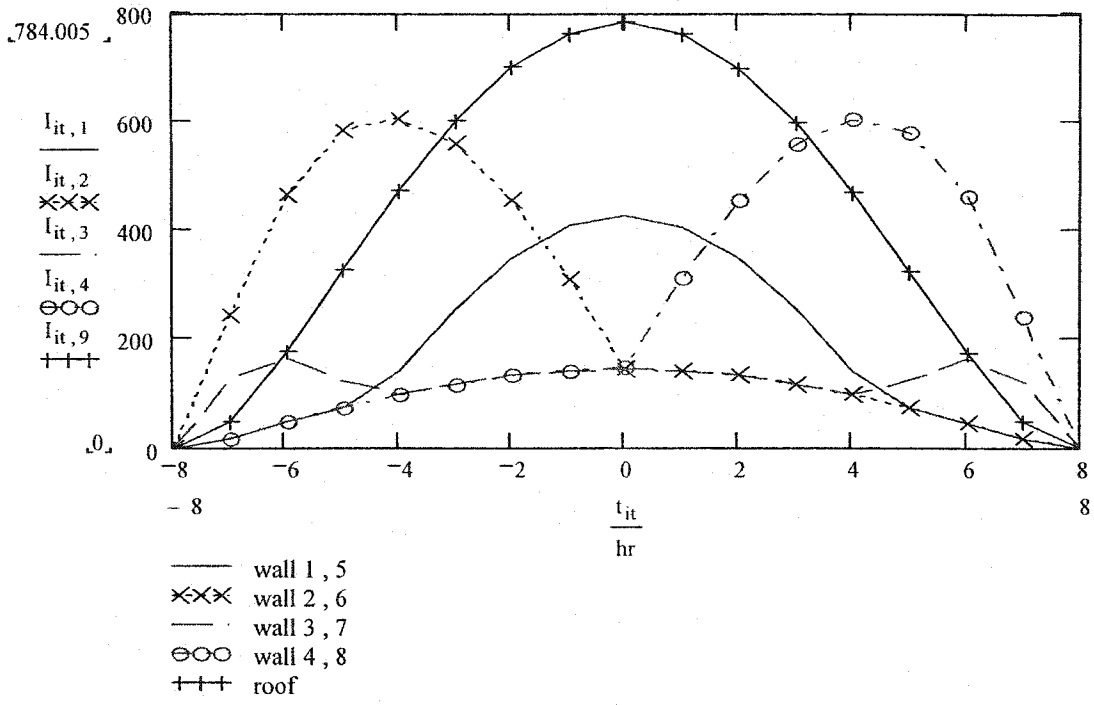

Figure (4.13) The incident solar radiation (W/m²)

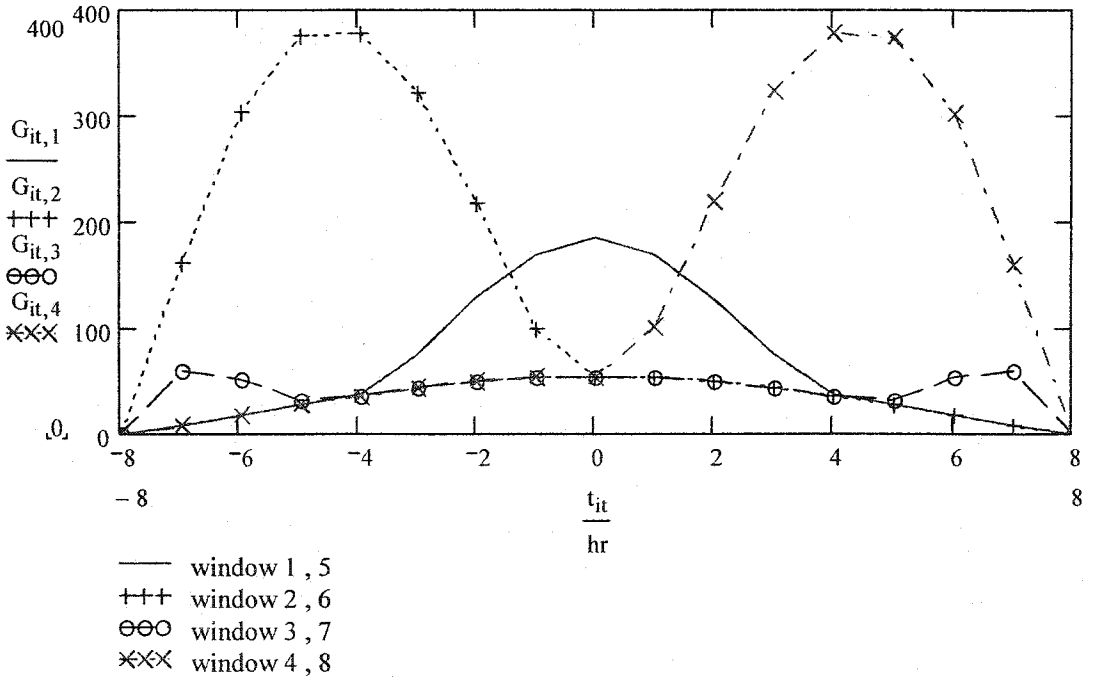

Figure 4.14 The transmitted solar radiation through windows (W/m²)

4.5.2 Natural ventilation calculation

Cross natural ventilation type, which means having openings located on opposite building walls is used in summer case to cool the house and avoid overheating during the day when the solar radiation enters the house and heats it. The strategy used is to have the windows open at night to allow fresh air to enter the house and cool it, and close the windows during the day time when the outside temperature goes above 24°C to prevent the heat from coming into the house. In this case the air enters the house from the ground floor and exits from the upper floor. The mass flow rate was calculated using equation 3.28.

4.5.3 Coupled airflow and heat transfer

In summer, calculating the air flow inside the house is divided into two cases. The first one is when the windows are open and the second one is when the windows are closed. In the first case there is a one way air flow, which means the air enters from the bottom and leaves from the top. The mass flow rate entering the house is equal to mass flow rate goes from ground floor, and equal to the mass flow rate exits from the first floor. The mass flow rate in this case is calculated using equation 3.28. In the second case the air flows between the two floors only which is bidirectional flow. The mass flow rate is calculated in this case using the same technique used in winter and the same average air velocity which is equal to 0.04 m/s.

The air flow is coupled with the thermal network by three resistances. First one is $R1o$ which is the thermal resistance between the room air for the ground floor and the outside due to windows, doors and infiltration. Second one is $R11o$ which is the thermal resistance

between the room air in the first floor and the outside due to windows. And the third one is *R111* which is the thermal resistance by convection between the two floors. These three resistances are calculated from the following equation:

$$R_q = \frac{1}{q.c_{pair}} \tag{4.12}$$

where q is the mass flow rate(kg/sec) and *Cpair* is the specific heat of air $\left(\frac{Joule}{kg.°C}\right)$.

The thermal resistances *R1o* & *R11o* are modeled as equal to the window's resistance *Rw* and the infiltration when the windows are closed; thus we have two resistances in parallel (window's resistance and the one calculated from equation 4.12) when the windows are open.

4.5.4 Simulations and results

The explicit finite difference method is employed to calculate the temperature variation in both floors. The energy balance equation (equ.4.2) is applied at each node and solved repeatedly at each time step for the period of simulation. The time step selected is 300sec (same as winter and for the same reason). Equations (4.4), (4.5) & (4.6) are used to calculate the thermal resistances and the thermal capacitances.

The simulations were performed for two days (periodic). Thus, weather data have to be generated for *NT* times as follows:

$$NT = \frac{86400.\text{sec}}{\Delta t} x2 \tag{4.13}$$

NT (number of time step) is equal to 576 based on the time step selected. And the time at which simulation to be performed is equal to:

$$t_p = p.\Delta t \tag{4.14}$$

where p is the number of time steps for two days ($p = 0,1..NT$), and Δt is the time step (300sec).

Window area, thermal mass thickness and the opening area are the most important parameters in achieving the thermal comfort in the house, at the same time avoid overheating might occur. The figures below show the result for summer with different window areas, thermal mass thicknesses and opening areas.

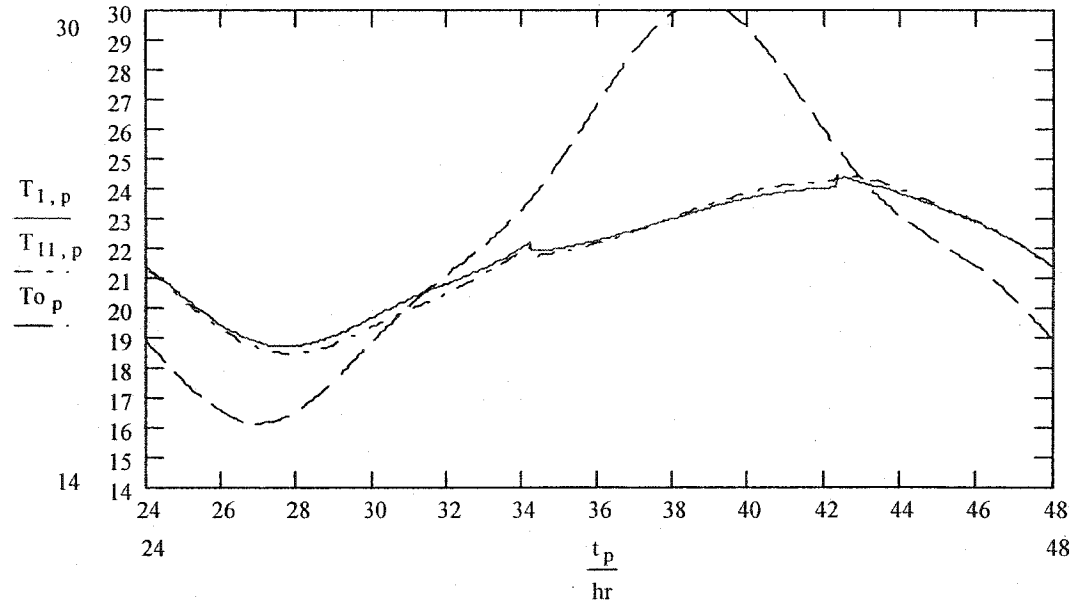

Figure 4.15 Room air temperature swing for ground and first floor. Thermal mass thickness = 10cm, south window area =5% of the floor area, opening area = 50% of the windows area. T1 is the room air temperature for the ground floor, T11 is the room air temperature for the first floor, and To is the outside temperature.

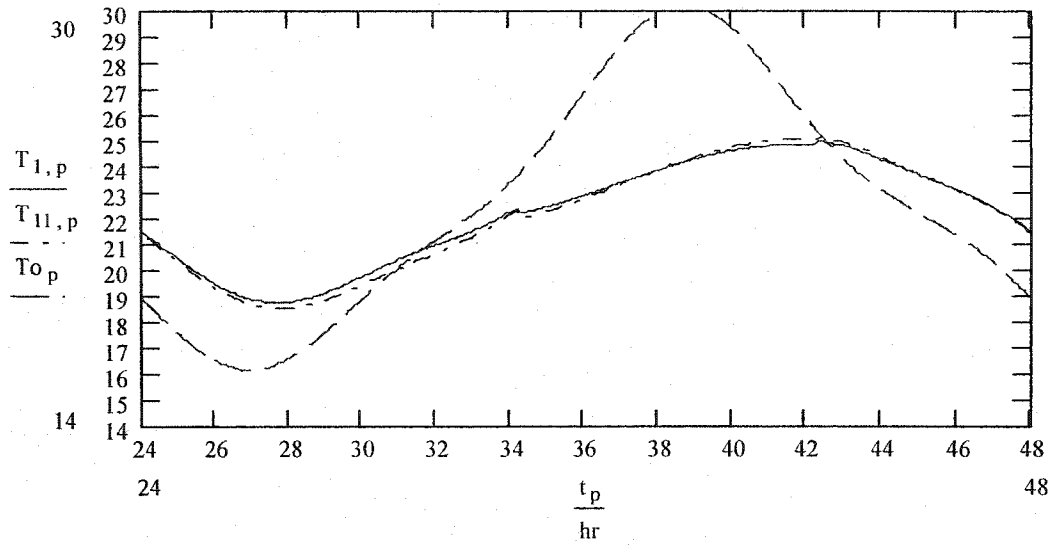

Figure 4.16 Room air temperature swing for ground and first floor. Thermal mass thickness = 10cm, south facing windows area =10% of the floor area, opening area = 50% of the windows area. T1 is the room air temperature for the ground floor, T11 is the room air temperature for the first floor, and To is the outside temperature.

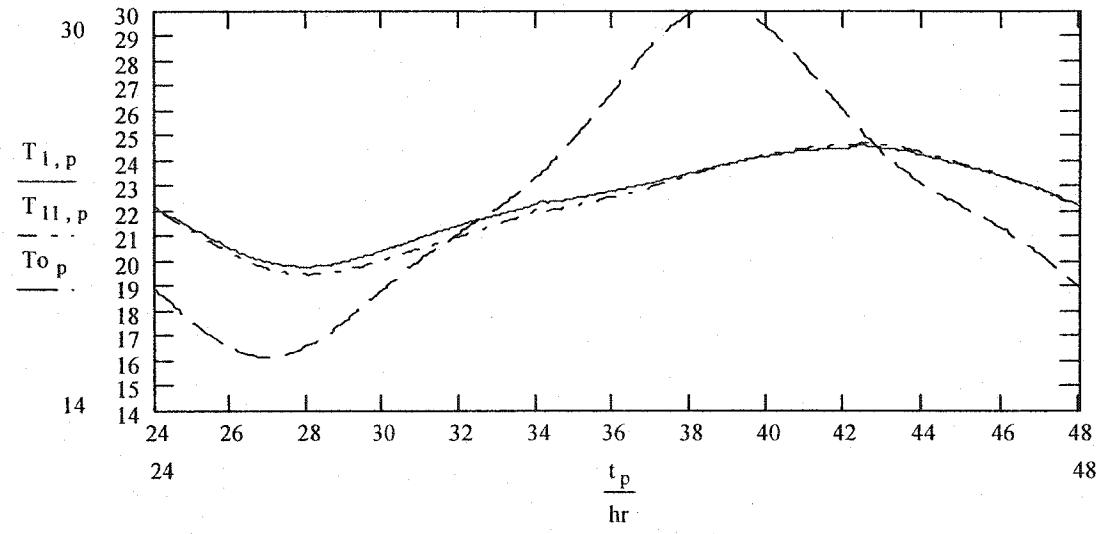

Figure 4.17 Room air temperature swing for ground and first floor. Thermal mass thickness = 10cm, south facing window area =5% of the floor area, opening area = 10% of the windows area. T1 is the room air temperature for the ground floor, T11 is the room air temperature for the first floor, and To is the outside temperature.

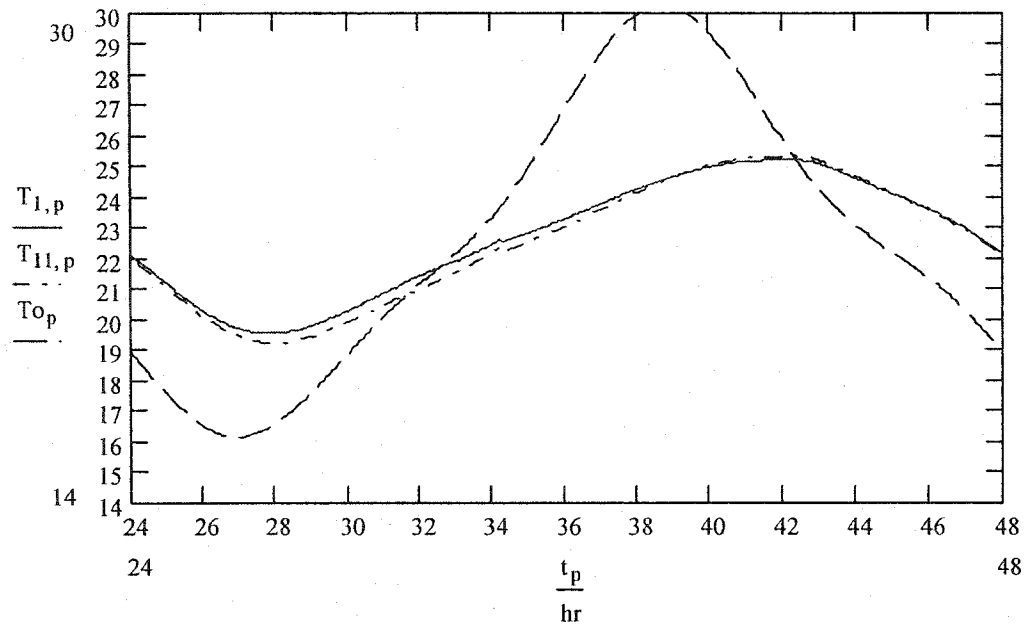

Figure 4.18 Room air temperature swing for ground and first floor. Thermal mass thickness = 10cm, south facing window area = 10% of the floor area, opening area = 10% of the windows area. T1 is the room air temperature for the ground floor, T11 is the room air temperature for the first floor, and To is the outside temperature.

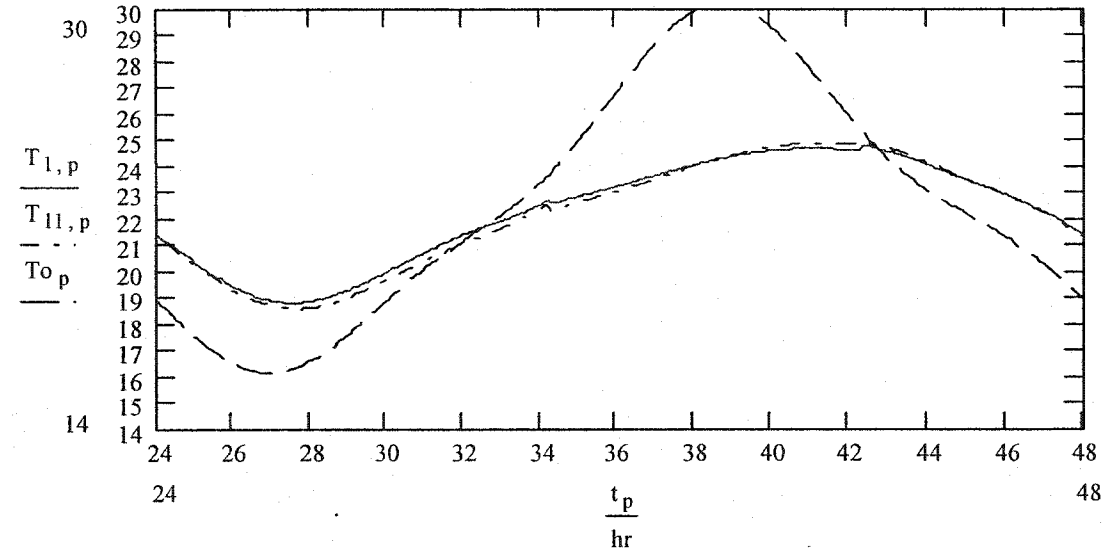

Figure 4.19 Room air temperature swing for ground and first floor. Thermal mass thickness = 15cm, south facing window area = 10% of the floor area, opening area = 50% of the windows area. T1 is the room air temperature for the ground floor, T11 is the room air temperature for the first floor, and To is the outside temperature.

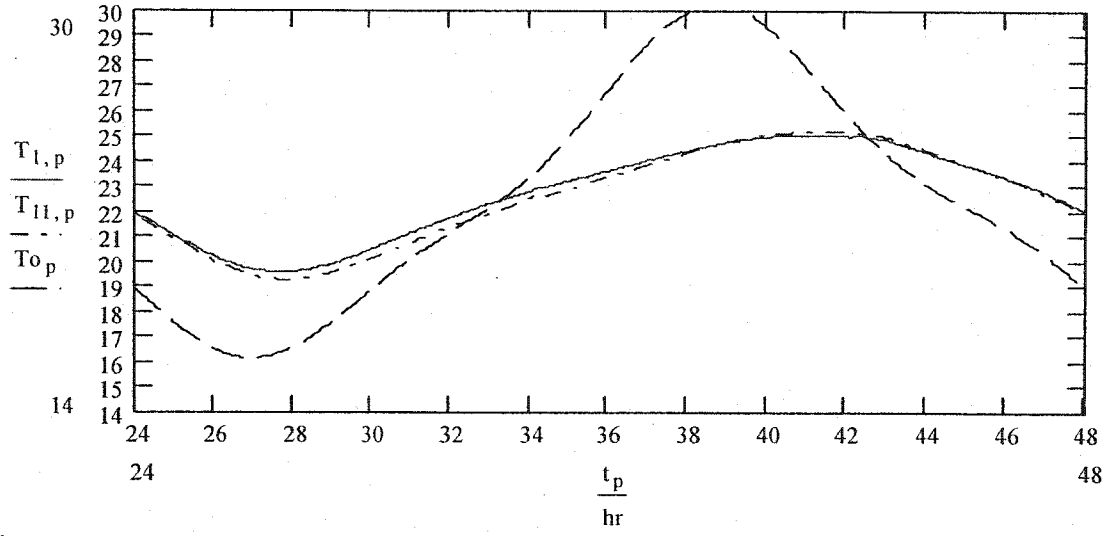

Figure 4.20 Room air temperature swing for ground and first floor. Thermal mass thickness = 15cm, south facing window area = 10% of the floor area, opening area = 10% of the windows area. T1 is the room air temperature for the ground floor, T11 is the room air temperature for the first floor, and To is the outside temperature.

The results show that, for the same window area and thermal mass thickness, the difference in room air temperature swing for opening area equal to 50% of the window area and opening area equal to 10% of the window area does not exceed 0.5°C which is very small. In both cases the maximum room air temperature dose not exceeds the thermal comfort level. So increasing the opening area more than 10% of the window area has a very little effect in the room air temperature.

Other simulations were performed with openings area smaller than 10%. Table 4.7 shows the max room air temperature for thermal mass thickness equal to 10cm, window area equal to 10% of the floor area and opening area equal to 10, 3 and 1% of the windows area.

Table 4.7 Max & Min room air temperature for window area equal to 10% of the floor area, thermal mass thickness equal to 10cm and opening area equal to 10, 3 and 1% of the window area

Window area % of the floor area	Thermal mass thickness	Opening area % of the window's area	Tmax °C	Tmin °C
10%	10cm	10%	19.5	25.2
10%	10cm	3%	21.4	26.2
10%	10cm	1%	23	27.3

The results show that when the opening area is decreased the room air temperature is increased. The max room air temperature is 25.2°C for an opening area equal to 10% of the window area while it is 27.3°C for opening area equal to 1%. Although the temperature swing for opening area equal to 10% is more but it is still in the thermal comfort.

As a result form the above an opening area equal to 10% of the window area is the best case in term of thermal comfort.

During the summer the outside temperature might reach a maximum of 35°C. In this case, a controlled shading device is required to reduce the amount of solar radiation transmitted into the house. The thermal performance of the house was studied in this case with and without the use of shading device. Figure 4.31 shows the shading profile which is allowing 30% of the total incident solar radiation to enter the house from 10am to 6pm; this 30% consist of two components first one is the transmitted solar radiation through windows which is equal to 10% and the second one is the heat absorbed by the shading

device and released to the room air temperature which is equal to 20% of the total incident solar radiation.

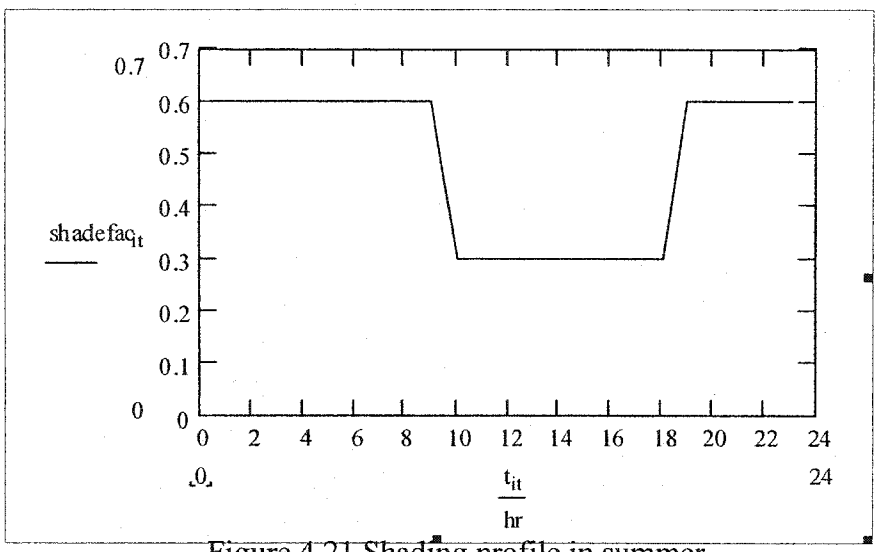

Figure 4.21 Shading profile in summer.

The strategy for cooling the house is to open the windows and allow fresh air enters the house at night and close it during the daytime when the outside temperature goes higher than 24°C which means closing it form 8am to 8pm based on the outside temperature profile assumed in this case.

The two figures below show the results for the room air temperature swing in both floors with and without shading.

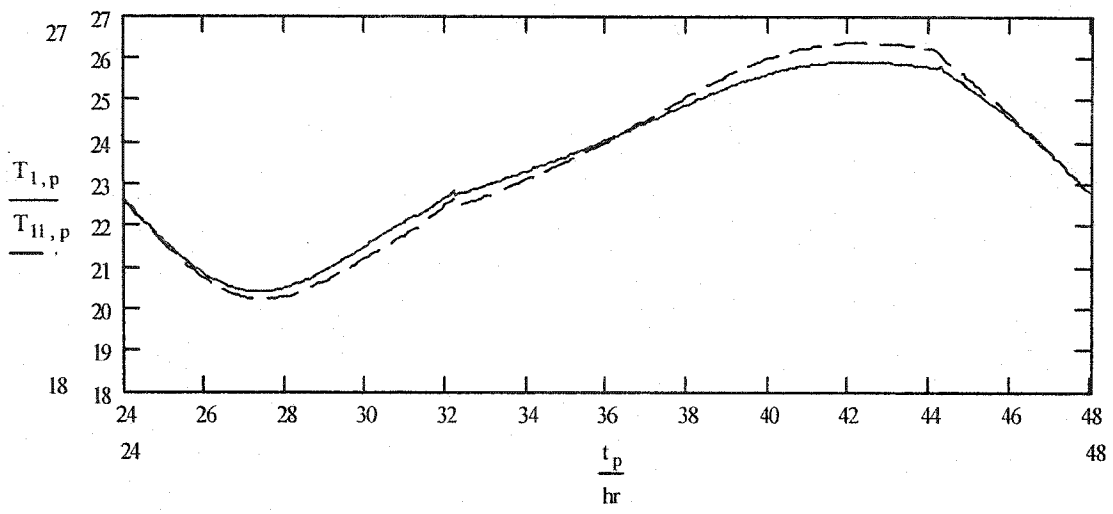

Figure 4.22 Room air temperature swing for both floors when the outside temperature reaches 35degC without shading. T1 is the room air temperature for the ground floor, T11 is the room air temperature for the first floor, and To is the outside temperature.

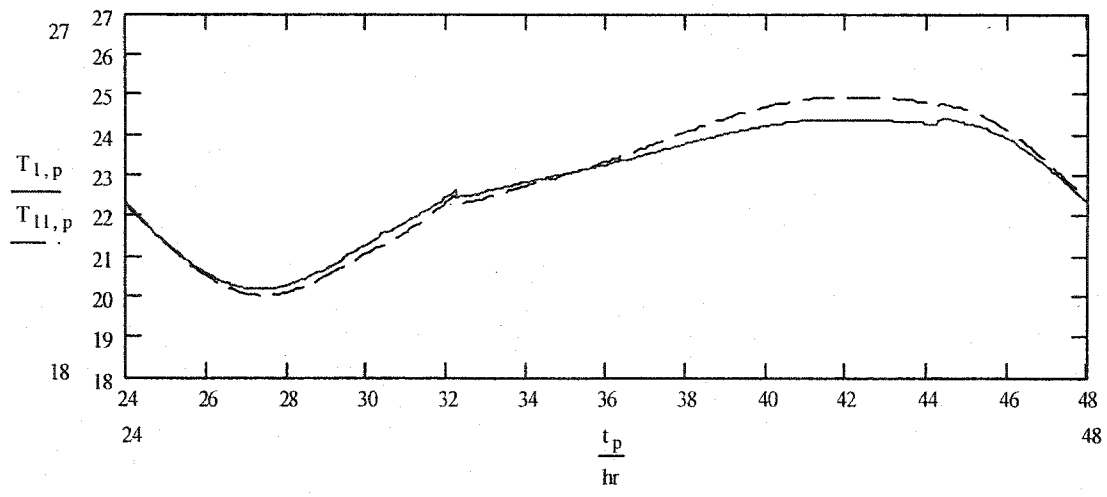

Figure 4.23 Room air temperature swing for both floors when the outside temperature reaches 35degC with shading. T1 is the room air temperature for the ground floor, T11 is the room air temperature for the first floor, and To is the outside temperature.

The above figures show that the maximum room air temperature in the ground floor is equal to 24°C with shading while it is equal to 26°C without shading. The minimum temperature is equal to 20°C with shading while it is equal to 20.5°C without shading. The maximum room air temperature in the first floor is 24.75°C with shading while it is equal to 26.35°C without shading. The minimum temperature is equal to 20°C with shading while it is equal to 20.25°C without shading.

CHAPTER 5

VALIDATION BY COMPARISON WITH MEASUREMENTS AND SIMULATIONS

5.1 Introduction

This chapter provides experimental validation for the two zone model developed. The simulations are performed for two-room unit which is part of the NRC passive solar test facility [Barakat, 1982]. The direct gain unit is briefly described below, followed by comparison of measured and predicted temperature swing for the room air.

It also presents the effect of changing the number of capacitances for the thermal mass in the thermal network, a form of numerical validation.

5.2 Th e DBR direct gain two-zone unit

The DBR passive solar test facility is located in Ottawa (latitude 45.32N). The facility is made up of three huts (Figure 5.1) which include the unit of interest. The details of the unit are shown in Figure 5.2.

The unit is consist of a south and a north room, each room having double glazed windows with areas 2.6m^2 and 1m^2 respectively. All floors are carpeted. The wall construction details are shown in Figure 5.3 and their effective thermal resistance values are given in Table 5.1.

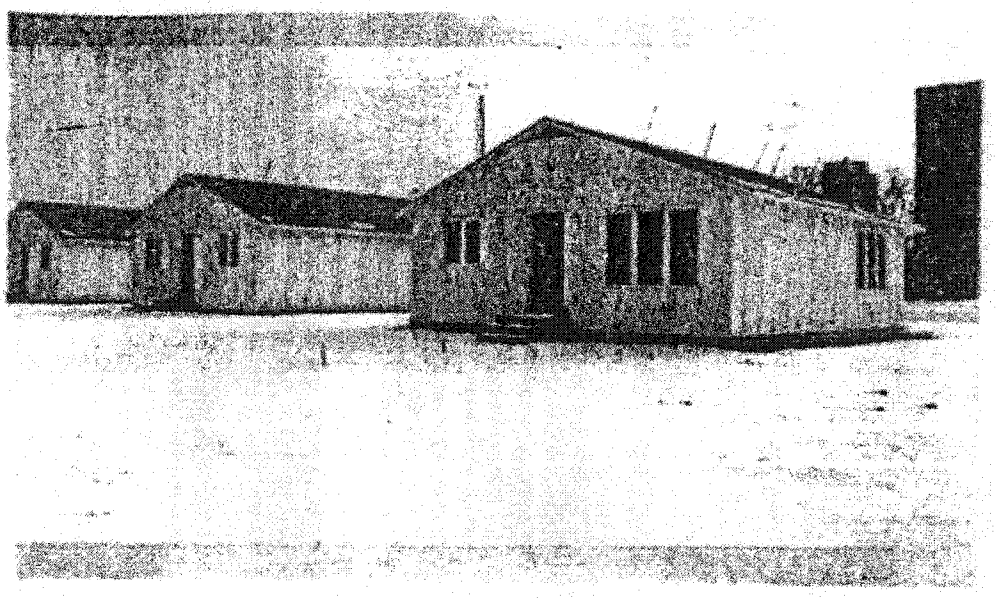

(a) NORTH FAÇADE

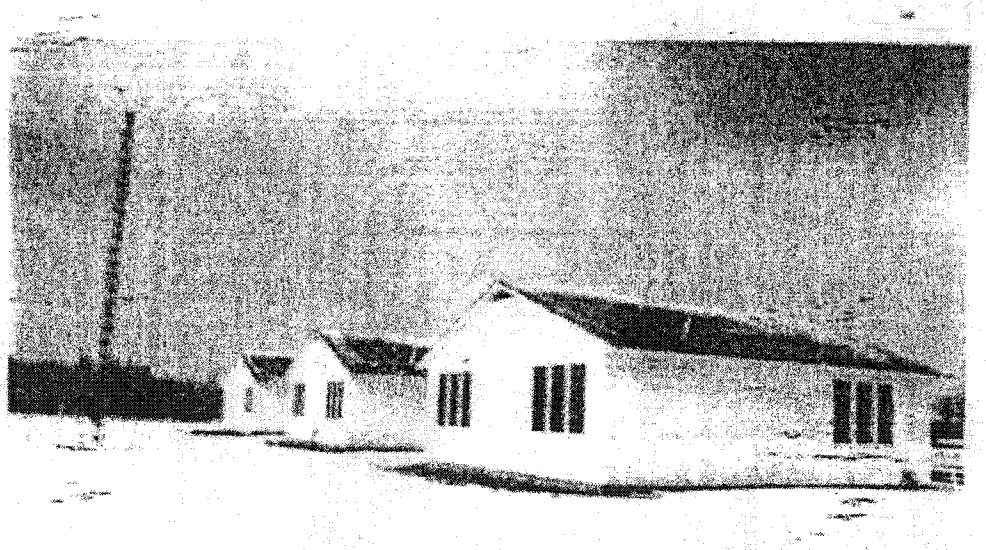

(b) SOUTH FAÇADE

Figure 5.1 View of the test facility [from Barakat, 1982]

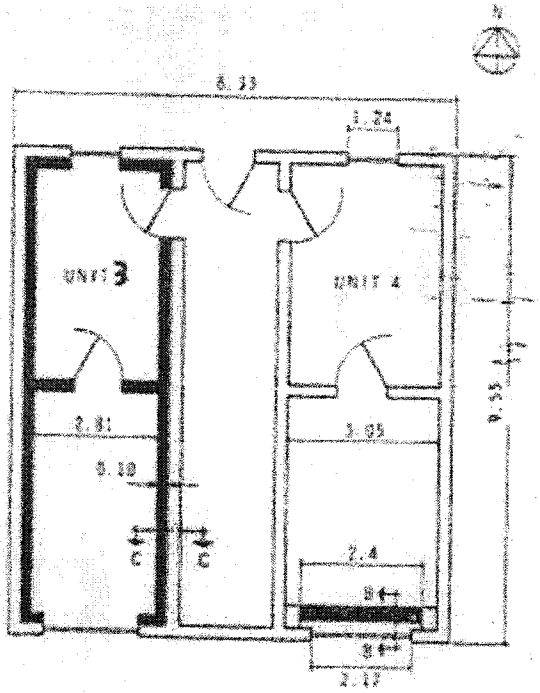

Figure 5.2 Details of the test unite [from Barakat, 1982]

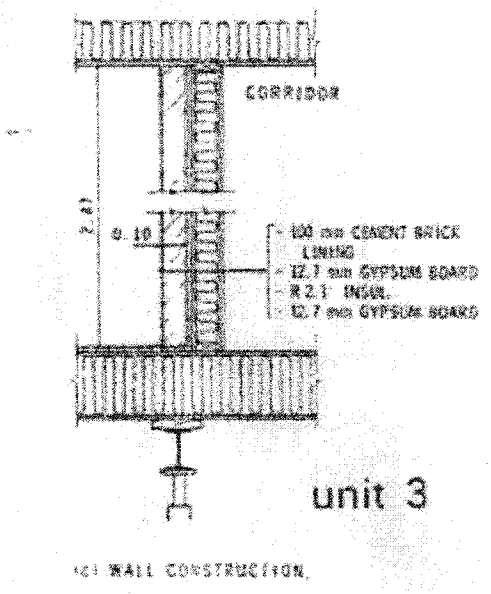

Figure 5.3 The wall construction of the test unit [from Barakat, 1982]

Table 5.1 Wall resistance values.

Element type	Construction	Thermal resistance ($m^2.K$ / watt)
Wall, Heavy.	Cement bricks, gypsum board, Insulation, particle board.	2.04
Internal Partition	10cm Brick	0.06
Windows, double glazed	Glass, Air space, Glass	0.2
Metal insulated door		1.03
Wooden partition door		0.2
Ceiling	Gypsum board, insulation	3.33
Floor	Carpet and underlay, wood, insulation, gypsum board	7.34
Outdoor air film, walls		0.03
Outdoor air film, ceiling/Attic		0.09

The unit consists of a single layer of 100mm thick cement bricks on the vertical walls.

The pertinent storage mass physical properties are shown in Table 5.2.

Table 5.2 Storage mass properties.

Property	Gypsum board	Cement Bricks	Carpet and underpad
Density kg/m^3	800	2114	650
Specific heat J/(kg.K)	837	937	1380
Thermal conductivity $W/(m^2.K)$	0.16	1.5	0.06
Solar absorptance (measured)	0.26	0.66	0.92
Normal emittance (measured)	0.88	0.91	0.84

The operation of the unit will now be briefly described.

1. The unit is pressurized with corridor air to eliminate infiltration.
2. Basement is heated and kept at 21°C.
3. The corridor temperature is kept constant at approximately 20°C.

Each room is heated to 20°C with an electric baseboard heater and the south room is equipped with an exhaust fan to cool the room with outside air when the room air temperature exceeds 27°C. The unit is operated in two modes: mode 1 where the door between the two rooms is closed and mode 2 where the door is open and air is circulated between the two rooms. The comparison was made for mode 2.

5.3 The simulation procedure

The simulation is performed for a time period of 1days (Jan 1st). The mean weather data for the time period is given in Table 5.3.

Table 5.3 Mean weather data for the time period.

Day #1	Ambient temp. (°C)	Attic temp.(°C)	Daily clearness index
January 1st	-17.6	-15	0.605

The two most important inputs are the solar irradiation transmitted into the direct gain room and the ambient temperature. The complex Fourier coefficients were determined numerically. The solar irradiation harmonics were multiplied by the window area and then room effective absorptance (equal to 0.96) and were also increased by the appropriate factor to account for the amount absorbed in the glazing. The resulting values are the harmonics for the total solar radiation absorbed in the room. These were then

divided among the room interior surfaces in proportion to the total radiation absorbed by each surface on the relatively clear day. The harmonics of solar radiation absorbed on exterior surfaces have a negligible effect because of the very low ambient temperature and the high exterior heat loss coefficient (33.3 W/m²/K). Thus, the solar component of each sol-air source was represented by its mean term.

The attic temperature closely followed the ambient but with a higher mean (Table 5.3). The maximum auxiliary heating power was set to 1701watt (the measured value), and the proportional control constant is assumed to be equal to $q_{max/2}$, which is equal to 850.5 watts.

5.4 Results and comparison with measured data

The north room temperature was kept approximately constant at 20°C while the south room temperature floated. The average measured swing during the test period is 2.7°C while the predicted one is 3°C. Figure 5.4 shows the predicted room air temperature swing for the south room. The predicted energy consumption is compared with the measured one. The measured energy consumption is equal to 82.68MJ for one day while the predicted one is equal to 83.09MJ. The difference is 0.5% which is very close.

In conclusion, although comparison with a one day period of time may provide only partial experimental validation, the satisfactory agreement between the measured and predicted results provided confidence in use of the model for practical passive solar analysis.

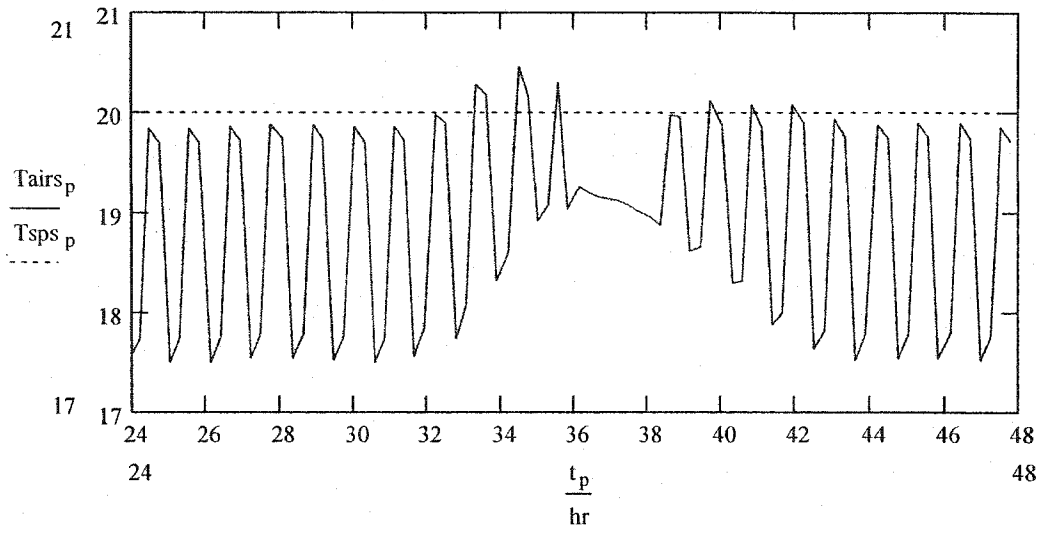

Figure 5.4 Predicted room air temperature variation for the south facing room. Tairs is the room air temperature for the south facing room, Tsps is the set point for the south facing room.

5.5 Changing the n umber of capacitances in the thermal network

This section is intended to show the effect of modeling detail - changing the number of capacitances for the thermal mass in the thermal network. The thermal network for the model was divided into two capacitances for the floor capacity interconnecting thermal resistances. Another simulation was performed dividing the floor into four capacitances. Figures 5.5 and 5.6 show the room air temperature swing for ground and first floor with two and four capacitances for the thermal mass floor.

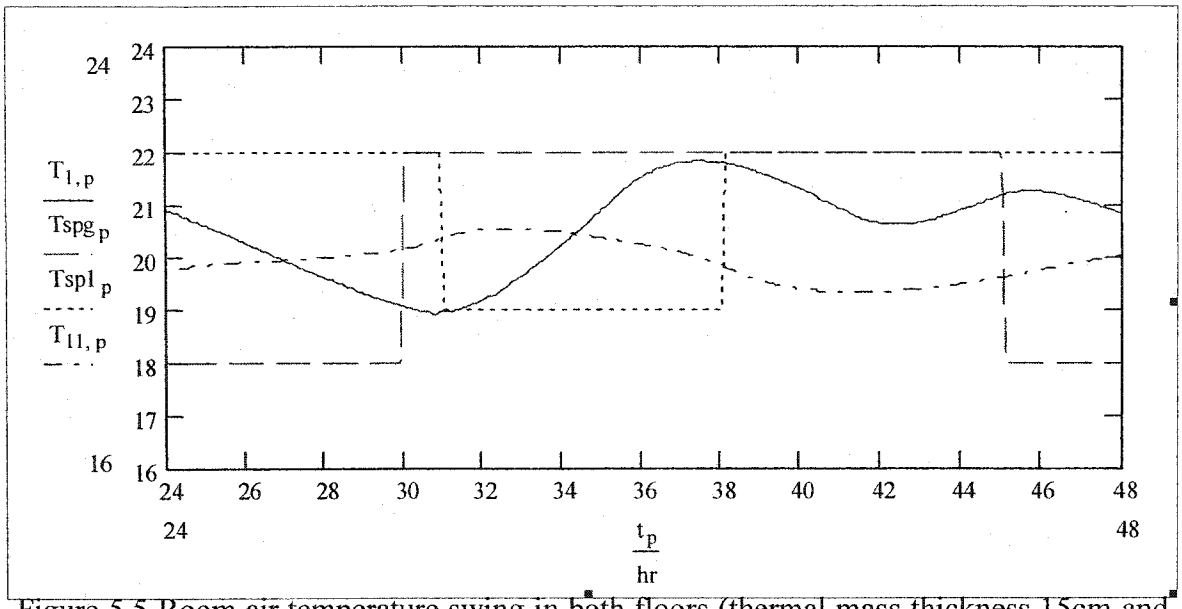

Figure 5.5 Room air temperature swing in both floors (thermal mass thickness 15cm and south facing window area 5% of the floor area) with two thermal capacitances in the floor.T1 is the room air temperature for the ground floor and T11 is the room air temperature for first floor. Tspg is the set point for the ground floor and Tsp1 is the set point for the first floor.

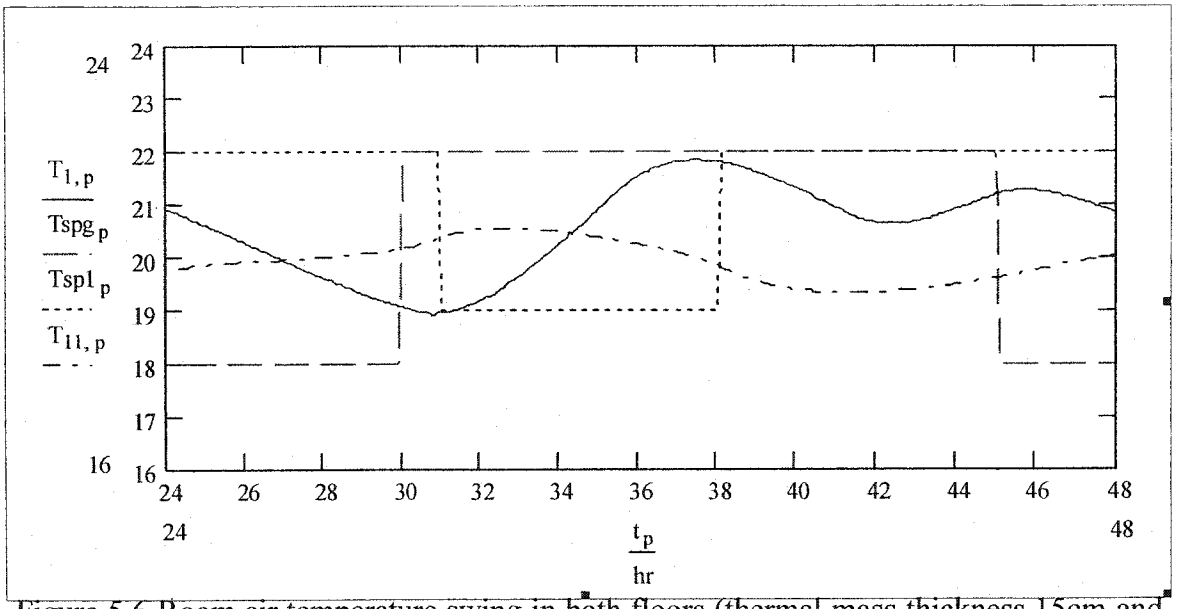

Figure 5.6 Room air temperature swing in both floors (thermal mass thickness 15cm and south facing window area 5% of the floor area) with four thermal capacitances in the floor. T1 is the room air temperature for the ground floor and T11 is the room air temperature for the first floor. Tspg is the set point for the ground floor and Tsp1 is the set point for the first floor.

As can be seen from the above figures, changing the number of capacitances from two to four has negligible effect on the results for the thermal mass thickness assumed. In another words increasing the number of capacitances for the thermal mass floor has no effect on the results, and therefore the model was studied dividing the floor into two thermal capacitances.

Number of capacitances might have an effect on the results for thermal mass thicker than 15cm, but in this case overheating may occur. In the developed model only two thermal mass thicknesses were considered (10 and 15cm) as more than 15 cm mass was considered unnecessary.

CHAPTER 6

CONCLUSION AND RECOMMENDATIONS FOR FUTURE WORK

This thesis presented a non-linear transient finite difference two-zone coupled thermal-airflow model for a solar house. The two zones are either on top of each other (Cottage) or next to each other (Bungalow). The model was studied for winter and summer seasons. In winter the model considered includes an integrated floor heating system. The solar radiation transmitted into the house was calculated using the daily clearness method. The explicit finite difference method was employed to investigate the thermal performance of the house in terms of thermal comfort and energy consumption. The air flow between the two floors (bidirectional flow) was coupled with the thermal network by modeling it as a convective thermal resistance. This thermal resistance was determined by determining the mass flow rate between the two floors, which was calculated from the air flow velocity. Simulations were performed for different window areas and thermal mass thicknesses as well as window R-values. The best design parameters were found and discussed. Energy savings were also achieved by developing an appropriate control strategy for the set point.

As a result of the simulations, the following conclusions can be drawn:

- The temperature swings as well as the heating energy consumption are reduced when low-e coated window is used. When higher amounts of mass are used on an

average January day the energy consumption is higher but the thermal comfort is improved due to lower temperature swing.

- The best values of the parameters for the model were found for a clear cold day in February because the days from February till mid of March have higher solar gains while at the same time they are cold days. A window area equal to 10% of the floor area which is equal to 1/3 of the south facing façade area with low-e coated window [R-value equal to 0.52 (m^2.K/watt)] and with thermal mass thickness equal to 15cm was found to be the best for the studied house. In this case the maximum temperature does not exceed the thermal comfort level while the heating energy consumption is the lowest comparing to the cases where the maximum temperature does not exceed 25°C. Although the temperature swing in this case is a little bit higher it is still inside the comfort level. Window area equal to 10% of the floor area which is equal to 1/3 of the south facing façade area allows more day lighting to enter the house so it can be utilized to minimize the use of artificial light.
- Thermal mass was employed for storage the solar radiation incident on it and also for storage of auxiliary heat. Increasing the thickness of the thermal mass might cause overheating inside the house as well as exceeding the floor surface temperature limit (29°C).
- Predicting the air flow between the two zone in both directions and coupling it with the thermal network of the house is very important in studying the thermal performance of the house.

- Energy savings can be achieved by developing an appropriate control strategy for the set point. The control strategy in this study was to lower the set point at night for the ground floor and increase it during the day time (assuming this floor is occupied during the day time), while it is lowering the set point for the first floor during the daytime and increase it at night (assuming this floor is occupied at night). This strategy reduces the possible overheating (which is the main problem in the design of passive solar building) which may happen if the auxiliary heat works continuously day and night at a high level.

In summer the model is two-zone naturally ventilated direct gain passive solar house. The transmitted solar radiation was calculated using Hottel's clear sky model. The explicit finite difference method was employed to investigate the thermal performance of the house in term of thermal comfort. Cross natural ventilation type was used to cool the house at night and avoid possible overheating during the day time when the transmitted solar radiation starts heating the house. In this type of ventilation one-way air flow exists through the opening. The air enters from the ground floor and exits from the upper floor. The air flow due to the natural ventilation was calculated and coupled with the thermal network of the house to study the thermal performance of the house. Simulations were performed for different thermal mass thickness, window area and opening area to reach the best case which can achieve the thermal comfort inside the house without overheating it. Shading devices were used in the case when the ambient temperature reaches 30°C or more. The passive response of the house was studied with and without shading. It was shown that a shading devise is required in summer especially when the outside

temperature reaches 35°C and more to reduce the amount of solar radiation entering the house and avoid overheating.

The MathCad 2000*i* professional software was used as a programming tool. It is simple to manipulate and able to handle complicated mathematical modeling. The developed model was validated by comparison with measurements from a two zone unit which is a part of the NRC passive solar test facility. A comparison between the predicted and measured room air temperature swing in the south facing room was made. The energy consumption is compared. The results were very close which provide confidence in use of the model for a passive solar analysis.

The following are recommended for future work:

1. Modeling the air flow inside the house in both directions using the CFD method in two cases when the upper floors temperature is higher than the lower floor and in the other way around.
2. Develop a correlation for calculating the mass flow rate between the two floors as a function of temperature difference and couple it with the thermal network.

REFERENCES

Ajiboye P. J. 28-30, September"A simple interactive design tool for sizing, locating and determining pollution attenuation features, of Urban Air Inlets suitable for office buildings", 19th annual AIVC conference, Oslo, Norway. 1998.

Angstom A.K., "Solar and Terrestrial radiation", Quart. J. Toy. Meterol. Soc. Vol.50, pp: 121-125.

ASHRAE fundamentals Handbook, 2001, ch.16: "Airflow around buildings", American Society of Heating Refrigeration and Air-conditioning Engineers , Atlanta, GA.

ASHRAE Fundamentals Handbook, 2001, ch. 26: "Ventilation and infiltration", American Society of Heating Refrigeration and Air-conditioning Engineers, Atlanta, GA.

ASHRAE, 1998. American Society of Heating Refrigeration and Air-Conditioning Engineers.

ASHRAE Fundamentals Handbook, 1989, American Society of Heating Refrigeration and Air-conditioning Engineers, Atlanta, GA.

ASHRAE Fundamentals Handbook, ch.22: "Ventilation and infiltration", American Society of Heating Refrigeration and Air-conditioning Engineers, Atlanta, GA, 1985.

Athienitis A.K., Santamouris M., "Thermal analysis and design of passive solar building ", James & James Pub, London, UK. 2002.

Athienitis A.K., Yang Chen, "Comparison of Control Strategies for Floor Heating ", ASHRAE Transaction, 2002, Vol.108, Pt.2, pp: 1005-1013, 2002.

Athienitis A. K., Tingyao Chen, "Numerical Study of Thermostat Set point Profiles for Floor Radiant Heating and the Effect of thermal Mass", ASHRAE Transaction, Vol.103, n1, pp: 939-948, 1997.

Athienitis A.K., "Theoretical Investigation of Thermal Performance of a Passive Solar Building with Floor Radiant Heating ", Solar Energy, 61:5, pp: 337-345, 1997.

Athienitis A.K., Building Thermal Analysis, an Electronic MathCad Book, 1994.

Athienitis, A.K., "Numerical model for a floor heating system", ASHRAE Transactions, Vol. 100, Pt. 1, pp. 1024-1030, 1994.

Athientitis A.K., Stylianou,M., "Method and Global Relationship for Estimation of Transmitted Solar Energy Distribution in Passive Solar Room", Energy Sources, Vol.13,pp:319-335,1991.

Athienitis A.K., Sullivan H.F., Hollands K. G. T., "Analytical Model, Sensitivity Analysis and Algorithm for Temperature Swings in Direct Gain Rooms", Solar Energy, Vol.36, No.4, pp: 303-312, 1986.

Awbi H. B., "Ventilation of Buildings", E.& F. N. Spon, London, UK, 1991.

Axley J. and R.A. Grot ''The coupled airflow and thermal analysis problem in building airflow system simulation,'' in *ASHRAE Transactions*, vol. 95:2, pp. 621-628, Atlanta, GA. 1989.

Axley J., Steven Emmerich and George Walton, " Modeling the performance of a naturally ventilated commercial building with a multi zone coupled thermal / airflow simulation tool" in ASHRAE Transactions, vol. 108, pt.2, pp. 1260-1275, 2002.

Balcomb, J.D. et al., "Passive Solar Design Handbook", Los Alamos Scientific Laboratory, Vol.3, 1982.

Barakat S. A, "NRCC Passive Solar Test Facility: Passive solar Studies at the Division of Building Research", Building Research note 188, Div. of Build. Research, NRCC, Ottawa, May, 1982.

Barakat S.A, "NRCC Passive Solar Test Facility: Performance of direct gain units", Building research note 215, Div. of Build. Research, NRCC, Ottawa, May, 1984.

Chen ZD, Li Y, Mahoney J. Experimental modeling of buoyancy-driven flows in buildings using a fine-bubble techniques. Building and Environment, 36, pp: 447- 455, 2001.

Chen Q., J. Srebric, and L. Glicksman, "A coupled airflow and energy simulation program for indoor thermal environmental studies" in ASHRAE Transactions, vol. 106, pp. 465 - 475, 2000.

Clark J., "Energy simulation in building design". Bristol and Boston: Adam Hilger Ltd. 1985.

Cooper P., Linden PF, Natural ventilation of an enclosure containing two buoyancy sources. Journal of Fluid Mechanics, Vol. 311, pp: 153-176, 1996.

Duffie J. A., Bechman W.A., Solar Engineering of Thermal Process, A Wiley-Interscience Publication, 1991.

Etheridge D., sandberg M "Building Ventilation: Theory and Measurement", John Willey & Sons, London, 1996.

Haghighat F., Megri A. C., "A comprehensive validation of two air flow models-COMIS and CONTAM "Indoor Air, Vol.6, pp: 278-288, 1996.

Hensen J., "Modeling coupled heat and air flow: Ping-Pong VS Onions". AIVC Conf. 1995.

Hensen J. and Clarke, J.A. ''An approach to the simulation of coupled heat and mass flow in buildings,'' in.Proc. 11th AIVC Conf. Ventilation System Performance held at Belgirate (I) 1990, vol. 2, pp. 339-354, IEA Air Infiltration and Ventilation Centre, Coventry (UK). 1991.

Hiroyasu Okuyama,. "Thermal and Airflow Network Simulation Program NETS", Proceedings of the 6th International IBPSA Conference (Building Simulation '99), Kyoto, September 1999, pp1237- 1244, 1999.

Holman J.P., Heat Transfer, McGraw-Hill Inc., New York. 1986 & 2002.

Hottel H.C. "A simple model of transmittance of direct solar radiation through clear atmospheres", Solar Energy. 1976.

Kronvall J., Svensson C., Adalberth K., "Practical guidelines for integral natural ventilation design", NATVENT Project, CD Rom. 1998.

Linden PF, Lane-Serff GF., Smeed DA. Empting filling boxes: the fluid mechanics of natural ventilation. Journal of Fluid Mechanics, 212, pp: 309-335, 1990.

Liu B. and Jordan R., "The interrelationship and characteristic distribution of direct, diffuse and total solar radiation", Solar Energy, Vol. 4, pp.1-19, 1960.

Neil B. Hutcheon, Gustav O.P. Handegord, "Building Science For A Cold Climate", John Wiley & Sons.

Nielsen, P.V. "Airflow simulation techniques-progress and trends". Proceeding of 10th AIVC conference, Dipoli, Finland, Paper10, pp: 203-223, 1989.

Schalin, A., Dorer, A., Ean der Mass, J. and Moser, A. " A new method for linking results of detailed airflow pattern calculation with multi-zone models", 13th AIVC Conference, Nice, France. 1992.

Walton, G. N. "Airflow and multi room thermal analysis", ASHRAE Transaction, Vol.88, Part 2, pp78-91, 1982.

Walton G. N., "Airflow Network Models for Element-Based Building Airflow Modeling", ASHRAE Transaction, Vol.95, Pt.2, pp: 611-620, 1998.

Walton G. N., "CONTAM96 User Manual ", National Institute of Standards and Technology, Gaithersburg, MD, USA. 1996.

Wilson, D.J. and I.S.Walker, Feasibility of passive ventilation by constant area vents to maintain indoor air quality in houses, 1992.

Woulters P., Heijmans N., Delmotte C., Vandaele L., " Classification of hybrid ventilation concepts" IEA-ECBBCS Annex 35 Hybvent, 1999.

Yuguo Li, "Buoyancy-driven natural ventilation in a thermally stratified one-zone building ", Building and Environment, Vol.35, pp: 207-214, 2000.

Yuguo Li, Angelo Delsante, Jeff Symons, "Prediction of natural ventilation in buildings with large openings ", Building and Environment, Vol.35, pp: 191-206, 2000.

Yuguo Li, Angelo Delsante, L. Chen, "Consideration of Thermal Stratification in Multi-Zone Models of Natural Ventilation ". International Energy Agency, 2002.

APPENDICES A & B

APPENDIX A
Two zone model (Winter)

This thesis presents a model for a two zones heated with a floor heating system. It is assumed that the heat delivered by the system is q_{aux}.

The auxiliary heating q_{aux} is proportional to the error between the setpoint Tsp and the actual room air temperature T1:

$$q_{aux} = K_p \cdot (Tsp - T_1) \qquad K_p \text{ ..proportional control constant}$$

1. Weather inputs:

(a) Outside temperature.

(b) Solar radiation .

2. Building data:

NS = number of surfaces contributing to the zones energy balance.

NS_e = " " exterior surfaces (walls and roof).

A_i = area of exterior surface i.

Nw: number of windows *Aw_i: area of window i*

ψ_{se} se = 0,1..NSe exterior surface azimuth angle.

αs_{se} se = 0,1..Nse solar absorptance of exterior surfaces.

Window type: *U-value or thermal resistance, double glazing and kL value (extinction coefficient x thickness)*

A_{door}: external door area *R_{door}: external door R-value*

Wall construction: *Wall layer properties. For the interior layer, properties for transient analysis are required.*

h_i *inside combined surface heat transfer (film) coefficient for surface i*

Case study for Two zone model :

*The model is two zone direct gain passive solar house consists of a basement , ground and Ist floors.The ground and first level zones are heated with floor heating.Figure 4.2 (Chapter 4) Each floor has an area equal to 100sq.m (10*10m), the internal height is equal to 3m in each floor.*

$Hh := 3 \cdot m$ $Lh := 10 \cdot m$ $Wh := 10 \cdot m$

Surfaces contributing to energy balance: $NS := 11$

$i := 1, 2 .. NS$ *1-8 walls, 9-ceiling, 10,11-floors* $se := 1 .. 9$ *exterior surfaces*

$Nw := 8$ $iw := 1, 2 .. Nw$ *(eight windows , one window on each wall)*

Calculating the window and door areas:

$Aw_1 := 5 \cdot m^2$ $Aw_2 := 3 \cdot m^2$ $Aw_3 := Aw_2$ $Aw_4 := Aw_2$

$Aw_5 := Aw_1$ $Aw_6 := Aw_2$ $Aw_7 := Aw_2$ $Aw_8 := Aw_2$

$Ad_1 := 1.8 \cdot m^2$ $Ad_2 := 0$ $Ad_3 := 0$ $Ad_4 := 0$ $Ad_5 := 0$

$Ad_7 := 0$ $Ad_8 := 0$ $Ad_6 := 0$

Wall net areas: $A_1 := Lh \cdot Hh - Aw_1 - Ad_1$ $A_2 := Wh \cdot Hh - Aw_2$

$A_3 := Lh \cdot Hh - Aw_3$ $A_4 := Wh \cdot Hh - Aw_4$ $A_5 := Hh \cdot Lh - Aw_5$

$A_6 := Wh \cdot Hh - Aw_6$ $A_7 := Lh \cdot Hh - Aw_7$ $A_8 := Wh \cdot Hh - Aw_8$

$A_9 := Lh \cdot Wh$ $A_{10} := Wh \cdot Lh$ $A_{11} := A_{10}$

$Hi := 3 \cdot m$ *..internal height* $Vol_g := A_{11} \cdot Hi$ $Vol_1 := A_{10} \cdot Hi$

Thermal resistance for windows and doors:

$degC \equiv 1$ $Rd := 2 \cdot \frac{m^2 \cdot degC}{watt}$ *..door thermal resistance*

$R_w := 0.34 \cdot \frac{m^2 \cdot degC}{watt}$ *window resistance (double-glazed)*

Wall / window azimuth angles:

$\psi_1 := 0 \cdot deg$ *south facing* $\psi_2 := -90 \cdot deg$ *east facing* $\psi_3 := 180 \cdot deg$ *north facing*

$\psi_4 := 90 \cdot deg$ *west facing*

$\psi_5 := 0 \cdot deg$ $\psi_6 := -90 \cdot deg$ $\psi_7 := 180 \cdot deg$ $\psi_8 := 90 \cdot deg$

Wall absorptances: $\alpha s_i := 0.9$

Interior film coefficients:

$h_1 := 8.3 \cdot \frac{watt}{m^2 \cdot degC}$ $h_2 := h_1$ $h_3 := h_1$ $h_4 := h_1$ *..film coefficients*

$h_5 := h_1$ $h_6 := h_1$ $h_7 := h_1$ $h_8 := h_1$

$h_9 := 9.0 \cdot \frac{watt}{m^2 \cdot degC}$ $h_{10} := 9.3 \cdot \frac{watt}{m^2 \cdot degC}$ $h_{11} := h_{10}$

THERMAL RESISTANCE CALCULATION:

A- VERTICAL WALLS (Assuming all walls have the same construction):

1. gypsum board $L_l := 0.013 \cdot m$ $\rho_l := 800 \cdot \frac{kg}{m^3}$ *thickness, density.*

$k_l := 0.16 \cdot \frac{watt}{m \cdot degC}$ $c_l := 750 \cdot \frac{joule}{kg \cdot degC}$ *conductivity spec. heat*

2. insulation $R_{ins} := 5 \cdot m^2 \cdot \frac{degC}{watt}$

3. siding + sheathing $R_{sid} := 0.37 \cdot m^2 \cdot \frac{degC}{watt}$

4. exterior film $h_o := 22 \cdot \frac{watt}{m^2 \cdot degC}$ *(section 5.3 in MathCad (Athienitis))*

15% of area is framing $f_f := 0.15$ *..fraction of area which is framing*

2 by 4 wood stud with R-value: $R_f := 0.77 \cdot m^2 \cdot \frac{degC}{watt}$

$$R_l := \frac{1}{\frac{1 - f_f}{\left(\frac{L_l}{k_l} + R_{ins} + R_{sid} + \frac{1}{h_o} + \frac{1}{h_l}\right)} + \frac{f_f}{\left(\frac{L_l}{k_l} + R_f + R_{sid} + \frac{1}{h_o} + \frac{1}{h_l}\right)}}$$

$$R_1 = 3.854\,\frac{degC\cdot m^2}{watt} \qquad u_1 := \frac{1}{R_1 - \frac{L_1}{k_1} - \frac{1}{h_1}}$$

Assuming that all exterior walls are of the same construction: $ii := 2,3..8$

$L_{ii} := L_1 \quad R_{ii} := R_1 \quad u_{ii} := u_1 \quad k_{ii} := k_1 \quad \rho_{ii} := \rho_1 \quad c_{ii} := c_1$

B- ROOF-CEILING THERMAL RESISTANCE:

CEILING: *1. gypsum board* $L_9 := L_1 \quad k_9 := k_1 \quad c_9 := c_1 \quad \rho_9 := \rho_1$

2. insulation $R_{insc} := 5\cdot m^2\cdot\frac{degC}{watt}$

3. air-film (attic) $h_a := 12\cdot\frac{watt}{m^2\cdot degC}$

$$R_c := \frac{1}{\frac{1-f_f}{\left(\frac{L_9}{k_9} + R_{insc} + \frac{1}{h_a} + \frac{1}{h_9}\right)} + \frac{f_f}{\left(\frac{L_9}{k_9} + R_f + \frac{1}{h_a} + \frac{1}{h_9}\right)}} \qquad R_c = 3.283\,\frac{degC\cdot m^2}{watt}$$

ROOF: *1. exterior air film* $h_o := 20\cdot\frac{watt}{m^2\cdot degC}$

2. shingle backer board $R_b := 0.19\cdot m^2\cdot\frac{degC}{watt}$

3. wood shingles $R_{sh} := 0.17 \cdot m^2 \cdot \frac{degC}{watt}$

$$R_r := \frac{1}{\frac{1 - f_f}{\left(R_b + R_{sh} + \frac{1}{h_o} + \frac{1}{h_a}\right)} + \frac{f_f}{\left(R_f + R_b + R_{sh} + \frac{1}{h_o} + \frac{1}{h_a}\right)}} \qquad R_r = 0.543\,m^2 \cdot \frac{degC}{watt}$$

Assuming a 30 degree slope for the roof, we calculate the ceiling-roof combined resistance per unit ceiling area as follows:

$$A_r := \frac{A_9}{\cos(30 \cdot deg)} \qquad R_9 := \left(\frac{R_c}{A_9} + \frac{R_r}{A_r}\right) \cdot A_9$$

$$R_9 = 3.754\,m^2 \cdot \frac{degC}{watt} \qquad u_9 := \frac{1}{R_9 - \frac{L_9}{k_9} - \frac{1}{h_9}}$$

C- FLOOR THERMAL RESISTANCE FOR BOTH FLOORS:

SURFACE 10 (FLOOR FOR FIRST FLOOR)

1. *Concrete blocks 15cm thick)* $L_{10} := 0.15 \cdot m$ $k_{10} := 1.7 \cdot \frac{watt}{m \cdot degC}$ $\rho_{10} := 2200 \cdot \frac{kg}{m^3}$

2. *Insulation & plywood* $R_{ins} := 5 \cdot m^2 \cdot \frac{degC}{watt}$ $c_{10} := 800 \cdot \frac{joule}{kg \cdot degC}$

3. *Air film (horizontal heat flow upward)* $h_o := 9.3 \cdot \frac{watt}{m^2 \cdot degC}$

$$R_{10} := R_{ins} + \frac{L_{10}}{k_{10}} + \frac{1}{h_o} + \frac{1}{h_{10}} \qquad R_{10} = 5.303\,\frac{m^2 \cdot degC}{watt}$$

$$u_{10} := \frac{1}{R_{10} - \frac{L_{10}}{k_{10}} - \frac{1}{h_{10}}}$$

SURFACE 11 (FLOOR FOR THE GROUND FLOOR):

ASSUMING THE FLOOR CONSTRUCTION IS THE SAME IN BOTH FLOORS.

$L_{11} := L_{10}$ $\quad k_{11} := k_{10}$ $\quad \rho_{11} := \rho_{10}$ $\quad c_{11} := c_{10}$

$R_{11} := R_{10}$ $\quad R_{11} = 5.303\,m^2 \cdot \frac{degC}{watt}$ $\quad u_{11} := u_{10}$

CALCULATION OF WALL ADMITTANCES:

The self-admittance and the transfer admittance will be calculated for each wall, considering the thermal capacity of the room interior layer. Note that the steady-state value of the admittance is equal to the wall conductance. Admittances will be calculated to the interior surface and to the room air point. The analysis will be performed for the mean term and three harmonics of the weather inputs and heat sources.

Admittances:

$$Ys_{0,i} := \frac{A_i}{R_i - \frac{1}{h_i}} \qquad Yt_{0,i} := Ys_{0,i}$$

Steady state admittance to interior surface is equal to wall U-value (excluding interior film); first subscript indicates frequency, second subscript indicates surface number.

$$Y_{0,i} := \frac{A_i}{R_i} \qquad Yta_{0,i} := Y_{0,i}$$

..admittances from outside to room air (steady state)

$n := 1, 2 .. 3$ $\quad j := \sqrt{-1}$ $\quad \gamma_{n,i} := \sqrt{j \cdot \frac{2 \cdot \pi \cdot n}{\frac{k_i}{\rho_i \cdot c_i} \cdot 86400 \cdot sec}}$

$Ui_i := A_i \cdot h_i$ $\quad Uo_i := h_o \cdot A_i$ *..interior and exterior surface conductances*

$Uw_{iw} := \frac{Aw_{iw}}{R_w} + \frac{Ad_{iw}}{Rd}$ *..conductance of double-glazed windows and doors;*

$Ys_{n,i} := A_i \cdot \frac{u_i + k_i \cdot \gamma_{n,i} \cdot \tanh(\gamma_{n,i} \cdot L_i)}{\left(\frac{u_i}{k_i \cdot \gamma_{n,i}} \cdot \tanh(\gamma_{n,i} \cdot L_i)\right) + 1}$ $\quad Yt_{n,i} := \frac{A_i}{\frac{\cosh(\gamma_{n,i} \cdot L_i)}{u_i} + \frac{\sinh(\gamma_{n,i} \cdot L_i)}{k_i \cdot \gamma_{n,i}}}$

$Y_{n,i} := \frac{Ys_{n,i} \cdot Ui_i}{Ys_{n,i} + Ui_i}$ $\quad Yta_{n,i} := Yt_{n,i} \cdot \frac{Ui_i}{Ys_{n,i} + Ui_i}$ *Wall admittances from outside to inside air.*

$n := 0, 1 .. 3$ $\quad xi := 1, 2 .. 4$ $\quad vi := 5, 6 .. 8$ $\quad vii := 5, 6 .. 9$

ZONE ADMITTANCE FOR THE GROUND FLOOR Yg (from room temperature node):

$$Yg_n := \sum_{xi} Uw_{xi} + \sum_{xi} Y_{n,xi} + Y_{n,10} + Y_{n,11}$$

ZONE ADMITTANCE FOR THE FIRST FLOOR Y1 (from room temperature node):

$$Y1_n := \sum_{vi} Uw_{vi} + \sum_{vi} Y_{n,vi} + Y_{n,9} + Y_{n,10}$$

$$Y1 = \begin{pmatrix} 114.176 \\ 730.805 + 361.563j \\ 828.461 + 376.541j \\ 891.056 + 444.198j \end{pmatrix} \text{watt} \qquad Yg = \begin{pmatrix} 106.824 \\ 1.328 \times 10^3 + 563.461j \\ 1.487 \times 10^3 + 439.285j \\ 1.556 \times 10^3 + 430.904j \end{pmatrix} \text{watt}$$

Outside Temperature

The outside temperature for a day is modeled by a Fourier series based on NTo+1 values that are an input to the array below. If more detail is required, NTo may be increased. Then, the the Fourier series may be used to generate intermediate values as required by the time step of a finite difference model.

$NTo := 7$ $\quad it := 0, 1 .. NTo$ $\quad$ *...time index* $\quad t_{it} := it \cdot 3 \cdot hr$ $\quad$ *..time*

$n := 0, 1 .. 3$ $\quad$ *...harmonics* $\quad w_n := 2 \cdot \pi \cdot \frac{n}{24 \cdot hr}$ $\quad j := \sqrt{-1}$

$To_{it} :=$

−22
−25
−24
−20
−18
−15
−18
−20

$$Ton_n := \left(\sum_{it} To_{it} \cdot \frac{\exp\left(-j \cdot w_n \cdot t_{it}\right)}{NTo + 1} \right) \cdot degC$$ *...Fourier harmonic coefficients*

$$Ton = \begin{pmatrix} -20.25 \\ -1.384 + 1.634j \\ 0.25 \\ 0.384 + 0.134j \end{pmatrix}$$

$Ton_0 = -20.25\,degC$ $\quad$ *mean daily temperature*

Solar Radiation Calculation:

Solar radiation transmitted through the windows will be modeled as absorbed 70% at the floor surface, and the remainder by the other surfaces in proportion to their areas. First,the technique of section 7.3 [MathCad program (Athienitis)] used to determine solar radiation absorbed by exterior surfaces and the quantities transmitted through windows.

Location data(Montreal): $L := 45\cdot deg$ *..latitude* $\beta := 90\cdot deg$ *..tilt angle*

$n_d := 15$ *..day number (Jan,15)* $\rho_g := 0.2$ *..ground reflectance*

First perform solar geometry calculations

Declination angle $\delta := 23.45\cdot deg\cdot\sin\left(360\cdot\frac{284 + n_d}{365}\cdot deg\right)$ $\delta = -21.269\,deg$

Sunset time $t_s := \left(\operatorname{acos}\left(-\tan(L)\cdot\tan(\delta)\right)\right)\cdot\frac{hr}{15\cdot deg}$ $t_s = 4.473\,hr$

Time array: $it := 0, 1 .. 23$ $t_{it} := (it - 11.99)\cdot hr$ *..solar time for solar radiation calculations*

$ha_{it} := 15\cdot\frac{deg}{hr}\cdot t_{it}$ *..hour angle (0 at solar noon)* $ha_s := t_s\cdot 15\cdot\frac{deg}{hr}$ *..sunset hour angle*

Solar altitude: $\alpha_{it} := \operatorname{asin}\left(\cos(L)\cdot\cos(\delta)\cdot\cos\left(ha_{it}\right) + \sin(L)\cdot\sin(\delta)\right)\cdot\left(\left|t_{it}\right| < \left|t_s\right|\right)$

Solar azimuth: $\phi_{it} := \operatorname{acos}\left(\frac{\sin(\alpha_{it})\cdot\sin(L) - \sin(\delta)}{\cos(\alpha_{it})\cdot\cos(L)}\right)\cdot\frac{ha_{it}}{\left|ha_{it}\right|}$

Angle of incidence: $\cos\theta_{it,iw} := \cos(\alpha_{it})\cdot\cos\left(\left|\phi_{it} - \psi_{iw}\right|\right)\cdot\sin(\beta) + \sin(\alpha_{it})\cdot\cos(\beta)$

$$\theta_{it,iw} := \operatorname{acos}\left(\frac{\cos\theta_{it,iw} + \left|\cos\theta_{it,iw}\right|}{2}\right)$$

Calculate transmittance of atmosphere and glazing:

For average design day, the hourly clearness indeces will be used:

Daily clearness index for January: $K_T := 0.45$

Calculation of hourly total, beam and diffuse clearness indices

*The **hourly clearness index** may be found by the correlation (Colares-Rabl):*

$w_e := \frac{2\cdot\pi}{86400}\cdot\frac{rad}{sec}$ *... earth's spin rate*

$A_K := 0.409 + 0.5016\cdot\sin\left(ha_s - 1.047\cdot rad\right)$

$B_K := 0.6609 - 0.4767\cdot\sin\left(ha_s - 1.047\cdot rad\right)$

$k_{t_{it}} := \text{if}\left[\left[\left[A_K + B_K\cdot\cos\left[w_e\cdot(it - 12)\cdot hr\right]\right]\cdot K_T\right] > 0, \left[A_K + B_K\cdot\cos\left[w_e\cdot(it - 12)\cdot hr\right]\right]\cdot K_T, 0\right]$

*The **hourly diffuse clearness index** is found from the Orgill-Hollands correlation:*

$k_{d_{it}} := \text{if}\left[k_{t_{it}} < 0.35, \left[\left(1 - 0.249\cdot k_{t_{it}}\right)\cdot k_{t_{it}}\right], \text{if}\left[0.35 < k_{t_{it}} < 0.75, \left[\left(1.557 - 1.84\cdot k_{t_{it}}\right)\cdot k_{t_{it}}\right], 0.177\right]\right]$

*Then the **hourly beam clearness index** is equal to:*

$k_{b_{it}} := k_{t_{it}} - k_{d_{it}}$

Determine now the glazing properties as a function of time interval j:

Glass properties: $kL := 0.1$ *..extinction coeff.*glazing thickness*

$$n_g := 1.53 \qquad \text{..refractive index}$$

Angle of refraction and component reflectivity:

$$\theta'_{it,iw} := \operatorname{asin}\left(\frac{\sin(\theta_{it,iw})}{n_g}\right) \qquad r_{it,iw} := \frac{1}{2}\cdot\left[\left(\frac{\sin(\theta_{it,iw}-\theta'_{it,iw})}{\sin(\theta_{it,iw}+\theta'_{it,iw})}\right)^2+\left(\frac{\tan(\theta_{it,iw}-\theta'_{it,iw})}{\tan(\theta_{it,iw}+\theta'_{it,iw})}\right)^2\right]$$

Beam transmittance, τ, reflectance, ρo, and absorptance, α, of glazing:

$$a_{it,iw} := \exp\left[-\frac{kL}{\sqrt{1-\left(\frac{\sin(\theta_{it,iw})}{n_g}\right)^2}}\right] \qquad \tau_{it,iw} := \frac{\left(1-r_{it,iw}\right)^2\cdot a_{it,iw}}{1-\left(r_{it,iw}\right)^2\cdot\left(a_{it,iw}\right)^2}$$

$$\rho o_{it,iw} := r_{it,iw} + \frac{r_{it,iw}\cdot\left(1-r_{it,iw}\right)^2\cdot\left(a_{it,iw}\right)^2}{1-\left(r_{it,iw}\right)^2\cdot\left(a_{it,iw}\right)^2} \qquad \alpha_{s_{it,iw}} := 1-\rho o_{it,iw}-\tau_{it,iw}$$

For double glazed windows: $$\tau_{e_{it,iw}} := \frac{\left(\tau_{it,iw}\right)^2}{1-\left(\rho o_{it,iw}\right)^2}$$

$$\alpha_{i_{it,iw}} := \alpha_{s_{it,iw}}\cdot\frac{\tau_{it,iw}}{1-\left(\rho o_{it,iw}\right)^2} \qquad \alpha_{o_{it,iw}} := \alpha_{s_{it,iw}} + \alpha_{s_{it,iw}}\cdot\frac{\tau_{it,iw}\cdot\rho o_{it,iw}}{1-\left(\rho o_{it,iw}\right)^2}$$

$$\alpha_{xi_{it,xi}} := \alpha_{s_{it,xi}}\cdot\frac{\tau_{it,xi}}{1-\left(\rho o_{it,xi}\right)^2} \qquad \alpha_{o_{it,xi}} := \alpha_{s_{it,xi}} + \alpha_{s_{it,xi}}\cdot\frac{\tau_{it,xi}\cdot\rho o_{it,xi}}{1-\left(\rho o_{it,xi}\right)^2}$$

$$\alpha vi_{it,vi} := \alpha s_{it,vi} \cdot \frac{\tau_{it,vi}}{1 - (\rho o_{it,vi})^2} \qquad \alpha o_{it,vi} := \alpha s_{it,vi} + \alpha s_{it,vi} \cdot \frac{\tau_{it,vi} \cdot \rho o_{it,vi}}{1 - (\rho o_{it,vi})^2}$$

Determine the solar radiation incident on exterior walls and transmitted by windows

Extraterrestrial normal solar radiation:

$$I_{on} := 1353 \cdot \frac{watt}{m^2} \cdot \left(1 + 0.033 \cdot \cos\left(360 \cdot \frac{n_d}{365} \cdot deg\right)\right)$$

Determine beam solar radiation:

$$I_{b_{it,iw}} := \left(I_{on} \cdot k_{b_{it}} \cdot \cos(\theta_{it,iw})\right)$$ *..incident beam radiation*

$$G_{b_{it,iw}} := I_{b_{it,iw}} \cdot \tau_{e_{it,iw}}$$ *..transmitted beam radiation*

$\tau_{ed_{iw}} := \tau_{e_{10,1}}$ *..approximate value for diffuse transmittance (equal for all windows)* $\theta_{10,1} = 34.103\ deg$

$$I_{ds_{it}} := I_{on} \cdot \sin(\alpha_{it}) \cdot (k_{d_{it}}) \cdot \frac{1 + \cos(\beta)}{2}$$ *..incident instantaneous sky diffuse radiation*

$$I_{dg_{it}} := \left[I_{on} \cdot \sin(\alpha_{it}) \cdot (k_{d_{it}} + k_{b_{it}})\right] \cdot \rho_g \cdot \frac{1 - \cos(\beta)}{2}$$ *..ground reflected*

$$G_{d_{it,iw}} := \tau_{ed_{iw}} \cdot (I_{ds_{it}} + I_{dg_{it}})$$ *.. transmitted diffuse irradiation (instantaneous)*

$$G_{b_{it,iw}} := I_{b_{it,iw}} \cdot \tau_{e_{it,iw}}$$ *..beam transmitted solar radiation.*

Total instantaneous solar irradiation incident on exterior surfaces:

$$I_{it,iw} := Ib_{it,iw} + Ids_{it} + Idg_{it}$$ *..on vertical walls*

$$I_{it,9} := I_{on} \cdot \sin(\alpha_{it}) \cdot \left(kd_{it} + kb_{it}\right)$$ *..on roof*

Total instantaneous solar radiation transmitted by windows:

$$G_{it,iw} := Gb_{it,iw} + Gd_{it,iw}$$

$$Gao_{it,iw} := \alpha o_{it,iw} \cdot Ib_{it,iw} + \alpha o_{10,iw} \cdot \left(Ids_{it} + Idg_{it}\right)$$ *..radiation absorbed in outer glazings*

$$Gai_{it,iw} := \alpha i_{it,iw} \cdot Ib_{it,iw} + \alpha i_{10,iw} \cdot \left(Ids_{it} + Idg_{it}\right)$$ *..radiation absorbed in inner glazings*

Incident solar irradiation flux (watts/m²)

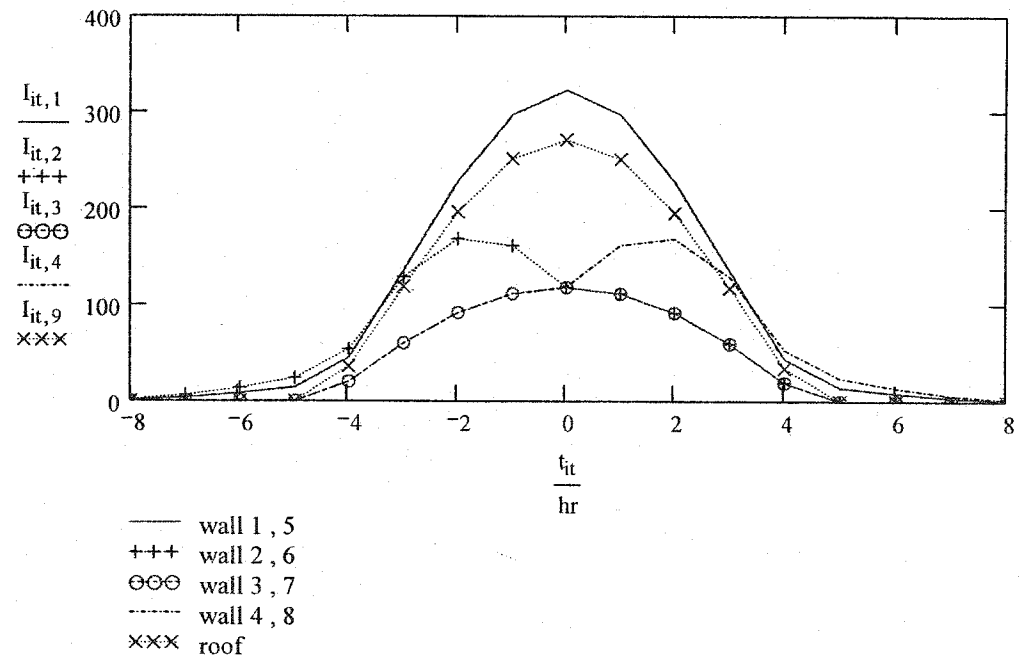

Transmitted solar radiation flux

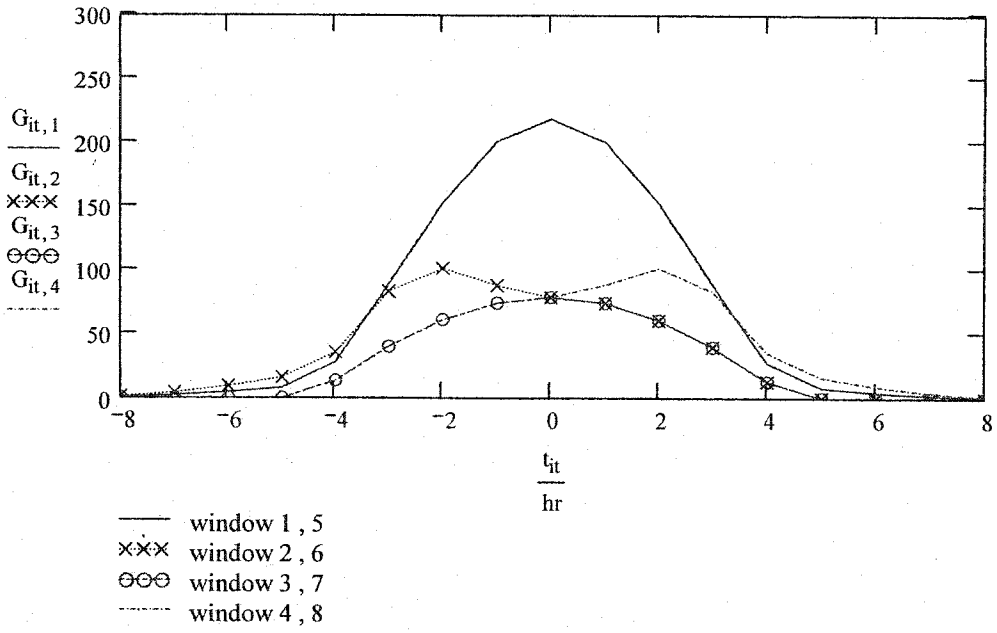

Before performing Fourier series calculations change the time origin from solar noon back to midnight:

$$t_{it} := t_{it} + 11.99 \cdot hr$$

Solar component of sol-air temperature for exterior surfaces:

$Ts_{it,iw} := I_{it,iw} \cdot \frac{\alpha s_{iw}}{h_{iw}}$ *For the Vertical Walls*

$Ts_{it,9} := I_{it,9} \cdot \frac{\alpha s_9}{h_9}$ *For the Roof*

Represent with Fourier series:

$n := 0, 1 .. 3$

$$Tsn_{n,se} := \left(\sum_{it} Ts_{it,se} \cdot \frac{\exp\left(-j \cdot w_n \cdot t_{it}\right)}{24} \right)$$

Equivalent or sol-air temperatures:

$$Teq_{n,se} := Ton_n + Tsn_{n,se}$$

Total instantaneous solar radiation transmitted through all windows for the Gound Floor :

$$Gtg_{it} := \sum_{xi} G_{it,xi} \cdot Aw_{xi}$$

Total instantaneous solar radiation transmitted through all windows for the First Floor :

$$Gt1_{it} := \left(\sum_{vi} G_{it,vi} \cdot Aw_{vi} \right)$$

Solar radiation absorbed by room surfaces for G.F:

$$S_{it,xi} := 0.3 \cdot Gtg_{it} \cdot \frac{A_{xi}}{\sum_{xi} A_{xi}}$$

Floor for G.F:

$$S_{it,11} := 0.7 \cdot Gtg_{it}$$

Solar radiation absorbed by room surfaces for 1st.F:

$$S_{it,vii} := 0.3 \cdot Gt1_{it} \cdot \frac{A_{vii}}{\sum_{vii} A_{vii}}$$

Floor for 1st.F:

$$S_{it,10} := 0.7 \cdot Gt1_{it}$$

Represent with Fourier series:

$$Sn_{n,i} := \left(\sum_{it} S_{it,i} \cdot \frac{\exp\left(-j \cdot w_n \cdot t_{it}\right)}{24} \right)$$

Solar radiation absorbed in glazings and released to room air for the G.F:

$$Qgg_{it} := \sum_{xi} \left[\frac{1}{R_w \cdot h_o} \cdot \left(\alpha o_{it,xi} \cdot I_{it,xi} \right) + \frac{1}{R_w} \cdot \left(R_w - \frac{1}{h_{xi}} \right) \cdot \left(\alpha xi_{it,xi} \cdot I_{it,xi} \right) \right] \cdot Aw_{xi}$$

$$Qggn_n := \left(\sum_{it} Qgg_{it} \cdot \frac{\exp\left(-j \cdot w_n \cdot t_{it}\right)}{24} \right) \qquad Qggn_0 = 45.436 \text{ watt}$$

Solar radiation absorbed in glazings and released to room air for the 1st.F:

$$Qg1_{it} := \sum_{vi} \left[\frac{1}{R_w \cdot h_o} \cdot \left(\alpha o_{it,vi} \cdot I_{it,vi} \right) + \frac{1}{R_w} \cdot \left(R_w - \frac{1}{h_{vi}} \right) \cdot \left(\alpha vi_{it,vi} \cdot I_{it,vi} \right) \right] \cdot Aw_{vi}$$

$$Qg1n_n := \left(\sum_{it} Qg1_{it} \cdot \frac{\exp\left(-j \cdot w_n \cdot t_{it}\right)}{24} \right) \qquad Qg1n_0 = 45.436 \text{ watt}$$

FINITE DIFFERENCE MODEL

The general form of the explicit finite difference formulation corresponding to node i and time interval p, is:

$$T(i,p+1) = \left(\frac{\Delta t}{C_i}\right)\cdot\left(q_i + \sum_j \frac{T(j,p) - T(i,p)}{R(i,j)}\right) + T(i,p)$$

where C is capacitance, j represents all nodes connected to node i, and q is a heat source such as auxiliary heating or solar radiation.

Critical time step: $\Delta t_{critical} = \min\left(\frac{C_i}{\sum_j \frac{1}{R_{i,j}}}\right)$ *for all nodes i. (the selected time step should be lower to ensure numerical stability)*

The thermal network is shown in figure 4. (Chapter 4).The floor is discretized into two layers (one thermal capacitance and two resistances for each layer).

$Ad_1 := 1.8\cdot m^2$ $Ad_2 := 0$ $Ad_3 := 0$ $Ad_4 := 0$ *Door areas*

Thermal capacitances and resistances:

$L_{11} := 0.15\cdot m$ $k_{11} := 1.7\cdot\frac{watt}{m\cdot degC}$ $L_{10} := L_{11}$ $k_{10} := k_{11}$

$L_1 := 0.013\cdot m$ $\rho_1 := 800\cdot\frac{kg}{m^3}$ $c_1 := 750\cdot\frac{joule}{kg\cdot degC}$ $k_1 := 0.16\cdot\frac{watt}{m\cdot degC}$

$L_{ii} := L_1$ $k_{ii} := k_1$ $\rho_{ii} := \rho_1$ $c_{ii} := c_1$ $L_9 := L_1$ $k_9 := k_1$

$\rho_9 := \rho_1$ $c_9 := c_1$

Calculating the thermal capacitances for all layers :

$C_{floor} := c_{11}\cdot\rho_{11}\cdot A_{11}\cdot L_{11}$ $C_4 := \frac{C_{floor}}{2}$ $C_3 := C_4$ *..thermal capacitances*

$C_8 := C_4$ $C_9 := C_4$ $C_4 = 1.32 \times 10^{7}\,kg\,m^{2}\,sec^{-2}$

The thermal capacitance of interior layer of unheated surfaces (Vertical Wall in the G.F)

$$C_5 := \sum_{xi} A_{xi} \cdot L_{xi} \cdot c_{xi} \cdot \rho_{xi} \qquad C_5 = 8.128 \times 10^{5}\,kg\,m^{2}\,sec^{-2}$$

The thermal capacitance of interior layer of unheated surfaces for the 1st.F :

$$C_{13} := \sum_{vii} A_{vii} \cdot L_{vii} \cdot c_{vii} \cdot \rho_{vii} \qquad C_{13} = 1.607 \times 10^{6}\,kg\,m^{2}\,sec^{-2}$$

Calculating the thermal resistances :

1-The thermal resistance between the basement and the 1/4 of the floor in the G.F :

$$R_{4o} := \frac{1}{u_{11} \cdot A_{11}} + \frac{L_{11}}{4 \cdot k_{11} \cdot A_{11}} \qquad R_{4o} = 0.051\,\frac{degC}{watt}$$

2- The thermal resistance for the half of the Floor in the G.F :

$$R_{34} := \frac{L_{11}}{2 \cdot k_{11} \cdot A_{11}} \qquad R_{34} = 4.412 \times 10^{-4}\,\frac{degC}{watt}$$

3- The thermal resistance for the second half of the Floor in the G.F :

$$R_{23} := \frac{R_{34}}{2} \qquad R_{23} = 2.206 \times 10^{-4}\,\frac{degC}{watt}$$

4 - The thermal resistance by convection between the room air temp.in the G.F and the floor surface for the G.F :

$$R_{12} := \frac{1}{A_{11} \cdot h_{11}} \qquad R_{12} = 1.075 \times 10^{-3} \frac{degC}{watt}$$

5 - The thermal resistance by radiation between the floor surface for the G.F and the walls for G.F

$$h_{11r} := 4 \cdot \frac{watt}{m^2 \cdot degC}$$ *..radiation heat transfer coefficient between floor and unheated surfaces*

$$R_{26} := \frac{1}{h_{11r} \cdot A_{11}} \qquad R_{26} = 2.5 \times 10^{-3} \frac{degC}{watt}$$

6- The thermal resistance of half of the innermost layer of the unheated surfaces in the G.F :

$$R_{56} := \frac{1}{\sum_{xi} \frac{k_{xi} \cdot A_{xi} \cdot 2}{L_{xi}}} \qquad R_{56} = 3.899 \times 10^{-4} \frac{degC}{watt}$$

7- The thermal resistance by convection between the room air temp. in the G.F and the unheated surfaces :

$$R_{16} := \frac{1}{\sum_{xi} A_{xi} \cdot h_{xi}} \qquad R_{16} = 1.156 \times 10^{-3} \frac{degC}{watt}$$

8- the thermal resistance between the interior layer for the unheated surfaces and the outside :

$$R_{5o} := R_{56} + \frac{1}{\sum_{xi} \frac{A_{xi}}{R_{xi}}} \qquad R_{5o} = 0.037 \frac{degC}{watt}$$

9 -The thermal resistance between the room air temp. for the G.F and the outside

$$R_{1o} := \frac{1}{\sum_{xi}\left(\frac{Aw_{xi}}{R_w} + \frac{Ad_{xi}}{Rd}\right)} \qquad R_{1o} = 0.024\,\frac{degC}{watt}$$

10- The Thermal Resistance by radiation between the Floor for G.F and the Ceiling for the G.F

$$R_{27} := \frac{1}{h_{11r} \cdot A_{11}} \qquad R_{27} = 2.5 \times 10^{-3}\,\frac{degC}{watt}$$

11- The thermal resistance by convection between the G.F room air Temp. and the ceiling for the G.F .

$$R_{17} := \frac{1}{A_{10} \cdot h_{10}} \qquad R_{17} = 1.075 \times 10^{-3}\,\frac{degC}{watt}$$

12-The thermal resistance between the ceiling in the G.F and the 1/4 of the floor in the 1st.F :

$$R_{78} := \left(\frac{1}{u_{10} \cdot A_{10}} + \frac{L_{10}}{4 \cdot k_{10} \cdot A_{10}}\right) \qquad R_{78} = 0.051\,\frac{degC}{watt}$$

13- The thermal resistance for the half of the Floor in the 1st.F :

$$R_{89} := \frac{L_{10}}{2 \cdot k_{10} \cdot A_{10}} \qquad R_{89} = 4.412 \times 10^{-4}\,\frac{degC}{watt}$$

14- The thermal resistance for the second half of the Floor in the 1st.F :

$$R_{910} := \frac{R_{89}}{2} \qquad R_{910} = 2.206 \times 10^{-4}\,\frac{degC}{watt}$$

15- The Thermal Resistance by radiation between the Floor for 1st.F and the unheated surfaces the 1st.F .

$$R_{1012} := \frac{1}{h_{11r} \cdot A_{10}} \qquad R_{1012} = 2.5 \times 10^{-3} \frac{\text{degC}}{\text{watt}}$$

16- The thermal resistance by convection between the 1st.F room air Temp. and the floor for the 1st.F .

$$R_{1011} := \frac{1}{A_{10} \cdot h_{10}} \qquad R_{1011} = 1.075 \times 10^{-3} \frac{\text{degC}}{\text{watt}}$$

17 - The thermal resistance by convection between the 1st.F room air Temp. and the unheated surfaces for the 1st.F .

$$R_{1112} := \frac{1}{\sum_{vii} A_{vii} \cdot h_{vii}} \qquad R_{1112} = 5.619 \times 10^{-4} \frac{\text{degC}}{\text{watt}}$$

18- The thermal resistance of half of the innermost layer of the unheated surfaces in the 1st.F :

$$R_{1213} := \frac{1}{\sum_{vii} \frac{k_{vii} \cdot A_{vii} \cdot 2}{L_{vii}}} \qquad R_{1213} = 1.972 \times 10^{-4} \frac{\text{degC}}{\text{watt}}$$

19 -The thermal resistance between the interior layer for the unheated surfaces in the 1st.F and the outside :

$$R_{13o} := R_{1213} + \frac{1}{\sum_{vii} \frac{A_{vii}}{R_{vii}}} \qquad R_{13o} = 0.019 \frac{\text{degC}}{\text{watt}}$$

20 -The thermal resistance between the room air temp. for the 1st.F and the outside

$$R_{11o} := \frac{1}{\sum_{vi} \frac{Aw_{vi}}{R_w}} \qquad R_{11o} = 0.024 \frac{degC}{watt}$$

21 - The thermal resistance by radiation between the ceiling and other surfaces in the G.F:

$$R_{67} := \frac{1}{h_{11r} \cdot A_{11}} \qquad R_{67} = 2.5 \times 10^{-3} \frac{degC}{watt}$$

Stability test to select time step:

$$TS := \left(\frac{C_3}{\frac{1}{R_{23}} + \frac{1}{R_{34}}} \quad \frac{C_4}{\frac{1}{R_{4o}} + \frac{1}{R_{34}}} \quad \frac{C_5}{\frac{1}{R_{56}} + \frac{1}{R_{5o}}} \quad \frac{C_8}{\frac{1}{R_{78}} + \frac{1}{R_{89}}} \quad \frac{C_9}{\frac{1}{R_{89}} + \frac{1}{R_{910}}} \quad \frac{C_{13}}{\frac{1}{R_{1213}} + \frac{1}{R_{13o}}} \right)$$

The time step Dt should be lower than the minimum of the six values in the vector TS

$\Delta t_{critical} := \min(TS)$ $\qquad \Delta t_{critical} = 313.562\,sec$ $\qquad \Delta t := 300 \cdot sec$

The simulation will be performed for two days (periodic). Thus, weather data have to be generated for NT times as follows:

$NT := 86400 \cdot \frac{sec}{\Delta t} \cdot 2$ $\qquad NT = 576$ $\qquad$ *...number of time steps for two days*

$p := 0, 1 .. NT$ $\qquad t_p := p \cdot \Delta t$ $\qquad$ *..times at which simulation is to be performed.* $\qquad n1 := 1, 2 .. 3$

$$To_p := Ton_0 + 2 \cdot \sum_{n1} Re\left[\left(Ton_{n1}\right) \cdot \exp\left(j \cdot w_{n1} \cdot t_p\right)\right]$$

Ambient temperature

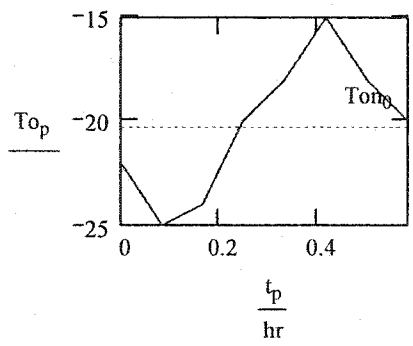

Control strategy :

The control strategy used is to lower the set point for the ground floor at night to avoid possible overheating, while it is to lower the set point for the first floor during the daytime and increase it at night.The control profile is shown in the figure below.

$setb := 4 \qquad setb1 := 3$

$$Tspg_p := 22 - - - setb \cdot \left(mod\left(\frac{t_p}{hr}, 24 \right) < 6 \right) - - - setb \cdot \left(mod\left(\frac{t_p}{hr}, 24 \right) > 21 \right)$$ *Ground floor set point*

$$Tsp1_p := 19 - - setb1 \cdot \left(mod\left(\frac{t_p}{hr}, 24 \right) < 7 \right) - - setb1 \cdot \left(mod\left(\frac{t_p}{hr}, 24 \right) > 14 \right)$$ *First floor set point*

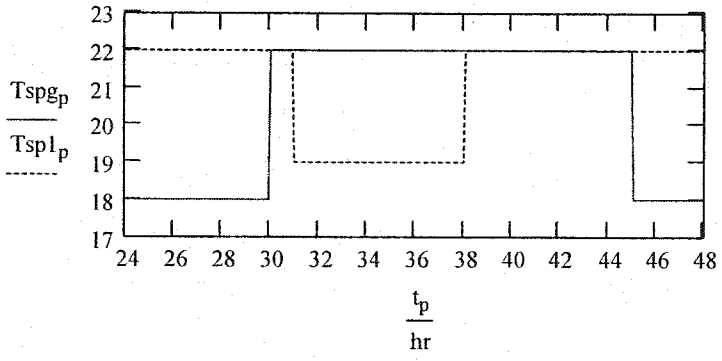

Solar radiation absorbed in the interior surfaces:

Solar radiation absorbed by the Vertical Walls in G.F

$$Sgt_p := \sum_{xi} \left[Sn_{0,xi} + 2 \cdot \sum_{n1} Re\left[\left(Sn_{n1,xi} \right) \cdot \exp\left(j \cdot w_{n1} \cdot t_p \right) \right] \right]$$

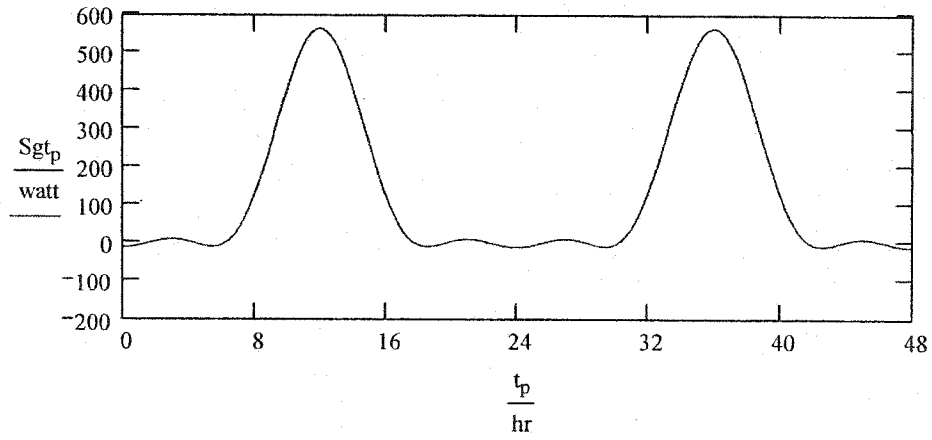

Solar radiation absorbed by the floor in G.F

$$St_{p,11} := Sn_{0,11} + 2\cdot\left[\sum_{n1} Re\left[\left(Sn_{n1,11}\right)\cdot\exp\left(j\cdot w_{n1}\cdot t_p\right)\right]\right]$$

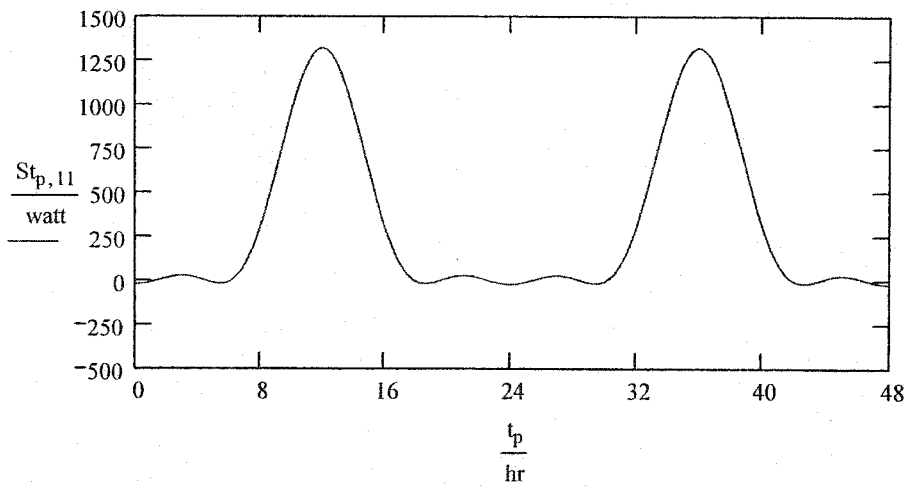

Solar radiation absorbed by the unheated surfaces in the 1st.F :

$$S1t_p := \sum_{vii}\left[Sn_{0,vii} + 2\cdot\sum_{n1} Re\left[\left(Sn_{n1,vii}\right)\cdot\exp\left(j\cdot w_{n1}\cdot t_p\right)\right]\right]$$

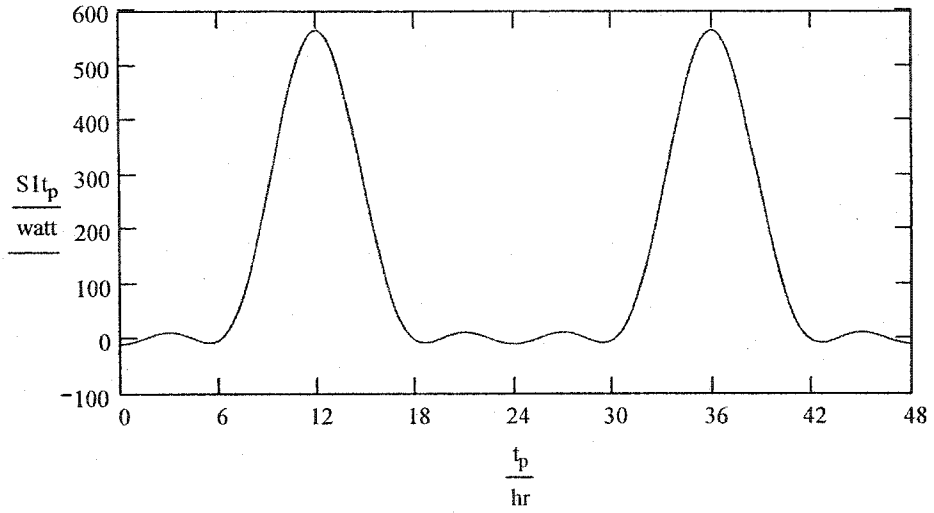

Solar radiation absorbed by the floor in the 1st.F :

$$St_{p,10} := Sn_{0,10} + 2\cdot\sum_{n1} Re\left[\left(Sn_{n1,10}\right)\cdot\exp\left(j\cdot w_{n1}\cdot t_p\right)\right]$$

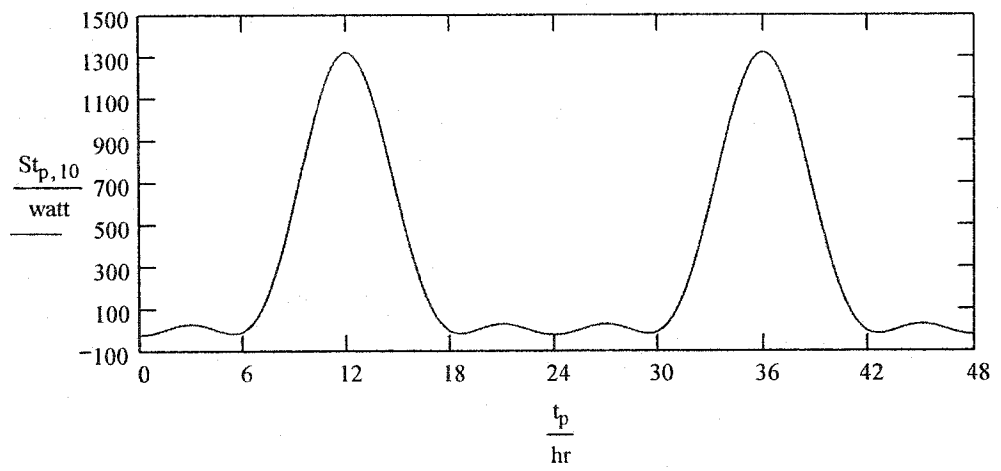

$Tb_p := 16\cdot degC$ *Assuming the basement temperature is constant:*

Initial conditions must first be assumed. Also, the size of the heating system q_{max} has to be decided together with the proportional control constant Kp.

$q_{maxg} := \left|Yg_0\right| \cdot 42 \cdot degC \cdot 1.5$ $q_{maxg} = 6.73 \times 10^3\ watt$ *For the G.F*

$q_{max1} := \left|Y1_0\right| \cdot 47 \cdot degC \cdot 1.5$ $q_{max1} = 8.049 \times 10^3\ watt$ *For the 1st.F*

$qaux1_0 := 0 \cdot watt$ $qauxg_0 := 0 \cdot watt$

$K1_p := 6155 \cdot \frac{watt}{degC}$ $Kg_p := 5355 \cdot \frac{watt}{degC}$ *..proportional control constant (assumed equal to $q_{max}/2$)*

Initial estimates of temperatures:

$$\begin{pmatrix} T_{1,0} \\ T_{2,0} \\ T_{3,0} \\ T_{4,0} \\ T_{5,0} \\ T_{6,0} \\ T_{7,0} \\ T_{8,0} \\ T_{9,0} \\ T_{10,0} \\ T_{11,0} \\ T_{12,0} \\ T_{13,0} \end{pmatrix} := \begin{pmatrix} 21 \\ 24 \\ 26 \\ 29 \\ 17 \\ 18 \\ 23 \\ 26 \\ 29 \\ 26 \\ 23 \\ 20 \\ 19 \end{pmatrix} \cdot degC$$

$\rho_{air} := 1.2 \cdot \frac{kg}{m^3}$ $c_{pair} := 1000 \cdot \frac{joule}{kg \cdot degC}$

Air Flow inside the house:

Velocity for air flow inside the house was calculated using CFD method, and the average velocity was found equal to 0.04m/sec.the mass flow rate is calculated as follows:

$\upsilon := 0.04 \frac{m}{sec}$ *Air velocity*

$A_m := 2m^2$ *Opening area betweent he two floors*

$q_{up_p} := \rho_{air} \cdot A_m \cdot \upsilon$

$q_{up_0} = 0.096 \frac{kg}{sec}$ *Mass flow rate up*

$q_{down_p} := \rho_{air} \cdot A_m \cdot \upsilon$

$q_{down_0} = 0.096 \frac{kg}{sec}$ *Mass flow down*

Coupled air flow - thermal :

The two thermal networks for ground & first floor was coupled by thermal resistance by convection which represents the air flow between the two floors and calculated as follows:

$$R_{11\_1} := \frac{1}{q_{down_0} \cdot c_{pair}}$$

$R_{11\_1} = 0.01 \frac{degC}{watt}$

Thermal resistance due to the mass flow down.

$$R_{1\_11} := \frac{1}{q_{up_0} \cdot c_{pair}}$$

$R_{1\_11} = 0.01 \frac{degC}{watt}$

Thermal resistance due to the mass flow up

$$\begin{pmatrix} T_{1,p+1} \\ T_{2,p+1} \\ T_{3,p+1} \\ T_{4,p+1} \\ T_{5,p+1} \\ T_{6,p+1} \\ T_{7,p+1} \\ T_{8,p+1} \\ T_{9,p+1} \\ T_{10,p+1} \\ T_{11,p+1} \\ T_{12,p+1} \\ T_{13,p+1} \\ q_{p+1} \\ R_{q_{p+1}} \\ R_{1\_0_{p+1}} \\ R_{11\_0_{p+1}} \end{pmatrix} := \begin{bmatrix} \dfrac{\dfrac{T_{2,p}}{R_{12}} + \dfrac{To_p}{R_{1\_0_p}} + \dfrac{T_{6,p}}{R_{16}} + \dfrac{T_{7,p}}{R_{17}} + \dfrac{T_{11,p}}{R_{q_p}}}{\dfrac{1}{R_{12}} + \dfrac{1}{R_{16}} + \dfrac{1}{R_{17}} + \dfrac{1}{R_{1\_0_p}} + \dfrac{1}{R_{q_p}}} \\ \dfrac{\dfrac{T_{3,p}}{R_{23}} + \dfrac{T_{6,p}}{R_{26}} + \dfrac{T_{1,p}}{R_{12}} + \dfrac{T_{7,p}}{R_{27}} + St_{p,11}}{\dfrac{1}{R_{23}} + \dfrac{1}{R_{26}} + \dfrac{1}{R_{12}} + \dfrac{1}{R_{27}}} \\ \dfrac{\Delta t}{C_3}\cdot\left(\dfrac{T_{4,p} - T_{3,p}}{R_{34}} + \dfrac{T_{2,p} - T_{3,p}}{R_{23}}\right) + T_{3,p} \\ \dfrac{\Delta t}{C_4}\cdot\left(\dfrac{Tb_p - T_{4,p}}{R_{4o}} + \dfrac{T_{3,p} - T_{4,p}}{R_{34}}\right) + T_{4,p} \\ \dfrac{\Delta t}{C_5}\cdot\left(\dfrac{T_{6,p} - T_{5,p}}{R_{56}} + \dfrac{To_p - T_{5,p}}{R_{5o}}\right) + T_{5,p} \\ \dfrac{\dfrac{T_{2,p}}{R_{26}} + \dfrac{T_{5,p}}{R_{56}} + \dfrac{T_{1,p}}{R_{16}} + \dfrac{T_{7,p}}{R_{67}} + Sgt_p}{\left(\dfrac{1}{R_{56}} + \dfrac{1}{R_{26}} + \dfrac{1}{R_{16}} + \dfrac{1}{R_{67}}\right)} \\ \dfrac{\dfrac{T_{2,p}}{R_{27}} + \dfrac{T_{1,p}}{R_{17}} + \dfrac{T_{8,p}}{R_{78}} + \dfrac{T_{6,p}}{R_{67}}}{\dfrac{1}{R_{27}} + \dfrac{1}{R_{17}} + \dfrac{1}{R_{78}} + \dfrac{1}{R_{67}}} \\ \dfrac{\Delta t}{C_8}\cdot\left(\dfrac{T_{7,p} - T_{8,p}}{R_{78}} + \dfrac{T_{9,p} - T_{8,p}}{R_{89}}\right) + T_{8,p} \\ \dfrac{\Delta t}{C_9}\cdot\left(\dfrac{T_{8,p} - T_{9,p}}{R_{89}} + \dfrac{T_{10,p} - T_{9,p}}{R_{910}}\right) + T_{9,p} \\ \dfrac{\dfrac{T_{9,p}}{R_{910}} + \dfrac{T_{12,p}}{R_{1012}} + \dfrac{T_{11,p}}{R_{1112}} + St_{p,10}}{\left(\dfrac{1}{R_{910}} + \dfrac{1}{R_{1012}} + \dfrac{1}{R_{1112}}\right)} \\ \dfrac{\dfrac{T_{10,p}}{R_{1011}} + \dfrac{T_{12,p}}{R_{1112}} + \dfrac{T_{1,p}}{R_{q_p}} + \dfrac{To_p}{R_{11\_0_p}}}{\dfrac{1}{R_{1011}} + \dfrac{1}{R_{1112}} + \dfrac{1}{R_{11\_0_p}} + \dfrac{1}{R_{q_p}}} \\ \dfrac{\dfrac{T_{10,p}}{R_{1012}} + \dfrac{T_{13,p}}{R_{1213}} + \dfrac{T_{11,p}}{R_{1112}} + Slt_p}{\dfrac{1}{R_{1012}} + \dfrac{1}{R_{1213}} + \dfrac{1}{R_{1112}}} \\ \dfrac{\Delta t}{C_{13}}\cdot\left(\dfrac{T_{12,p} - T_{13,p}}{R_{1213}} + \dfrac{To_p - T_{13,p}}{R_{13o}}\right) + T_{13,p} \\ if\left[\left(mod\left(\dfrac{t_p}{hr},24\right) > 10\right)\cdot\left(mod\left(\dfrac{t_p}{hr},24\right) < 18\right), \dfrac{1}{R_{1o}\cdot c_{pair}}, \rho_{air}\cdot Cd\cdot A_p\cdot\sqrt{\left(\dfrac{\left|T_{1,p} - To_p\right|}{To_p + 273}\cdot g\cdot hb\right) + \left(\dfrac{\left|T_{11,p} - To_p\right|}{To_p + 273}\cdot g\cdot ht\right)}\right] \\ if\left[\left(mod\left(\dfrac{t_p}{hr},24\right) > 10\right)\cdot\left(mod\left(\dfrac{t_p}{hr},24\right) < 18\right), \dfrac{1}{\rho_{air}\cdot 2\cdot m^2\cdot 0.04\cdot\dfrac{m}{sec}\cdot c_{pair}}, \dfrac{1}{q_p\cdot c_{pair}}\right] \\ if\left[\left(mod\left(\dfrac{t_p}{hr},24\right) > 10\right)\cdot\left(mod\left(\dfrac{t_p}{hr},24\right) < 18\right), \dfrac{1}{\sum_{xi}\left(\dfrac{Aw_{xi}}{R_w} + \dfrac{Ad_{xi}}{Rd}\right) + U_{inf}}, \dfrac{R_{1o}\cdot R_{q_p}}{R_{1o} + R_{q_p}}\right] \\ if\left[\left(mod\left(\dfrac{t_p}{hr},24\right) > 10\right)\cdot\left(mod\left(\dfrac{t_p}{hr},24\right) < 18\right), \dfrac{1}{\sum_{vi}\left(\dfrac{Aw_{vi}}{R_w}\right) + U_{inf}}, \dfrac{R_{11o}\cdot R_{q_p}}{R_{11o} + R_{q_p}}\right] \end{bmatrix}$$

Results : *Results for second day (first day is affected by assumed initial conditions)*

The figure below shows the most important temperatures which are the room air temperature for ground floor T1 and the room air temperature for the first floor T11.

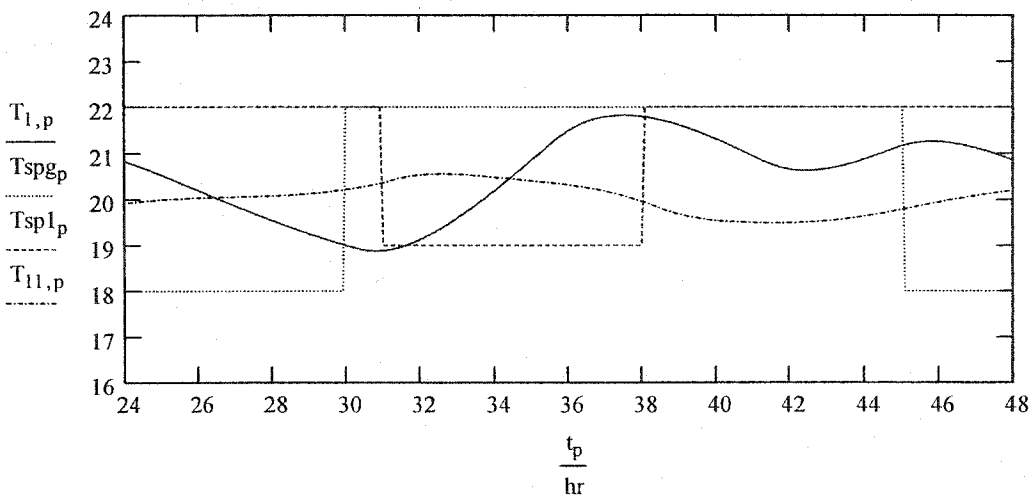

T1 : is the room air temperatuer for the ground floor
T11 : is the room air temperatuer for the first floor
Tspg : the set point for the ground floor
Tsp1 : the set point for the first floor

Heating profile for the ground floor :

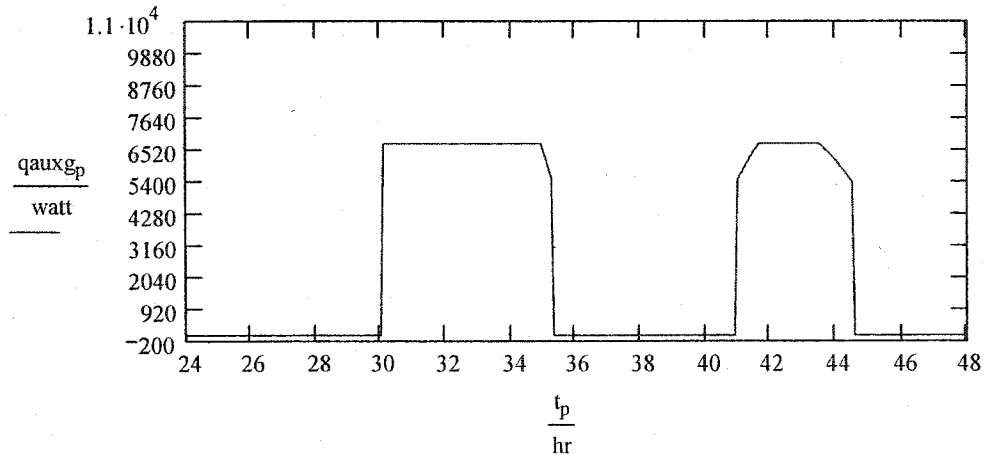

Heating profile for the first floor:

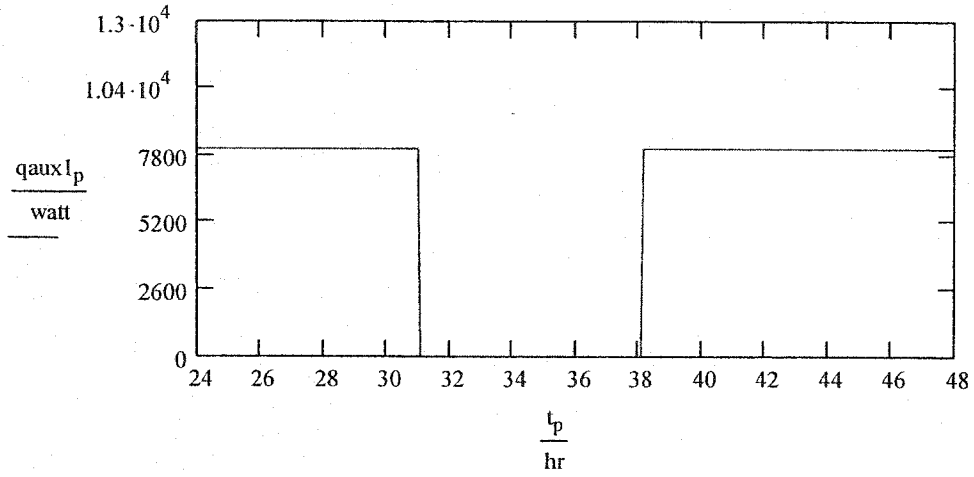

$$MJ := 10^6 \cdot joule$$

Heating energy consumption by numerical integration for second day:

$$v := \frac{NT}{2}, \frac{NT}{2} + 1 .. NT - 1$$

$$Qhg := \sum_v \frac{qauxg_v + |qauxg_v| + (qauxg_{v+1}) + |qauxg_{v+1}|}{4} \cdot (t_{v+1} - t_v)$$ *For the ground floor*

$$Qhg = 2.09 \times 10^8 \, joule$$

$$Qh1 := \sum_v \frac{qaux1_v + |qaux1_v| + (qaux1_{v+1}) + |qaux1_{v+1}|}{4} \cdot (t_{v+1} - t_v)$$ *For the first floor*

$$Qh1 = 4.902 \times 10^8 \, joule$$

TWO ZONE MODEL
(Summer)

The model for Summer is two zone direct gain naturally ventilated house. the house is shown in figure 4.2 Chapter 4 .

House Dimmensions, Window areas, door areas, net wall areas, Wall / window azimuth angles, Wall absorptances, and Interior film coefficients are the same as winter shown in appendix A.

Calculation of infiltration conductance:

$degC \equiv 1$

$ach := 0.1$ *ach= air changes /hour*

$Vol_g := 300 \cdot m^3$

$c_{pair} \equiv 1000 \cdot \frac{joule}{kg \cdot degC}$ $\rho_{air} \equiv 1.2 \cdot \frac{kg}{m^3}$ *..specific heat and density of air*

$U_{inf} := c_{pair} \cdot \rho_{air} \cdot \frac{ach \cdot Vol_g}{3600.sec}$ $U_{inf} = 10\,watt$

Thermal resistances for the walls, floors and ceiling are the same in winter (the calculation for it is shown in Appindix A).

Outside Temperature

The outside temperature for a day is modeled by a Fourier series based on NTo+1 values that are an input to the array below. If more detail is required, NTo may be increased. Then, the the Fourier series may be used to generate intermediate values as required by the time step of a finite difference model.

$NTo := 7$ $it := 0, 1 .. NTo$ *...time index* $t_{it} := it \cdot 3 \cdot hr$ *..time*

$n := 0, 1 .. 3$ *...harmonics* $w_n := 2 \cdot \pi \cdot \frac{n}{24 \cdot hr}$ $j := \sqrt{-1}$

$To_{it} :=$

19
16
19
22
27
30
26
22

$$Ton_n := \left(\sum_{it} To_{it} \cdot \frac{\exp\left(-j \cdot w_n \cdot t_{it}\right)}{NTo + 1} \right) \cdot degC$$ *...Fourier harmonic coefficients*

$$Ton = \begin{pmatrix} 22.625 \\ -2.237 + 2.112j \\ 0.125 - 0.25j \\ 0.237 + 0.362j \end{pmatrix}$$

$Ton_0 = 22.625\,degC$ *mean daily temperature*

Solar Radiation Calculation Using Hottel's Clear Sky Model:

Solar radiation transmitted through the windows will be modeled as absorbed 70% at the floor surface, and the remainder by the other surfaces in proportion to their areas.

Location data: $L := 45 \cdot deg$ *..latitude* $\beta := 90 \cdot deg$ *..tilt angle*

$n_d := 196$ *..day number (July 15)* $\rho_g := 0.2$ *..ground reflectance*

First perform solar geometry calculations

Declination angle $\delta := 23.45 \cdot deg \cdot \sin\left(360 \cdot \frac{284 + n_d}{365} \cdot deg\right)$ $\delta = 21.517\,deg$

Sunset time $t_s := \left(\operatorname{acos}\left(-\tan(L) \cdot \tan(\delta)\right)\right) \cdot \frac{hr}{15 \cdot deg}$ $t_s = 7.548\,hr$

Time array: $it := 0, 1 .. 23$ $t_{it} := (it - 11.99) \cdot hr$ *..solar time for solar radiation calculations*

$ha_{it} := 15 \cdot \frac{deg}{hr} \cdot t_{it}$ *..hour angle (0 at solar noon)* $ha_s := t_s \cdot 15 \cdot \frac{deg}{hr}$ *..sunset hour angle*

Solar altitude: $\alpha_{it} := \operatorname{asin}\left(\cos(L) \cdot \cos(\delta) \cdot \cos\left(ha_{it}\right) + \sin(L) \cdot \sin(\delta)\right) \cdot \left(\left|t_{it}\right| < \left|t_s\right|\right)$

Solar azimuth: $\phi_{it} := \operatorname{acos}\left(\frac{\sin(\alpha_{it}) \cdot \sin(L) - \sin(\delta)}{\cos(\alpha_{it}) \cdot \cos(L)}\right) \cdot \frac{ha_{it}}{\left|ha_{it}\right|}$

Angle of incidence: $\cos\theta_{it,iw} := \cos(\alpha_{it}) \cdot \cos\left(\left|\phi_{it} - \psi_{iw}\right|\right) \cdot \sin(\beta) + \sin(\alpha_{it}) \cdot \cos(\beta)$

$$\theta_{it,iw} := \operatorname{acos}\left(\frac{\cos\theta_{it,iw} + \left|\cos\theta_{it,iw}\right|}{2}\right)$$

Calculate transmittance of atmosphere and glazing (Hottel's clear sky model):

Beam atmospheric transmittance calculations: $Al := 0.5$ *altitude (km)*

$$a_0 := 0.97 \cdot \left[0.4237 - 0.00821 \cdot (6 - Al)^2 \right] \qquad a_1 := 0.99 \cdot \left[0.5055 + [0.00595 \cdot (6.5 - Al)]^2 \right]$$

$$k := 1.02 \cdot \left[0.2711 + [0.01858 \cdot (2.5 - Al)]^2 \right]$$

$$\tau b_{it} := if\left[\left(|t_{it}| < |t_s| \right), a_0 + a_1 \cdot \exp\left(\frac{-k}{\sin(\alpha_{it})} \right), 0 \right]$$

Determine now the glazing properties as a function of time interval j:

Glass properties:

$kL := 0.1$ *..extinction coeff.*glazing thickness*

$n_g := 1.53$ *..refractive index*

Angle of refraction and component reflectivity:

$$\theta'_{it,iw} := \operatorname{asin}\left(\frac{\sin(\theta_{it,iw})}{n_g} \right) \qquad r_{it,iw} := \frac{1}{2} \cdot \left[\left(\frac{\sin(\theta_{it,iw} - \theta'_{it,iw})}{\sin(\theta_{it,iw} + \theta'_{it,iw})} \right)^2 + \left(\frac{\tan(\theta_{it,iw} - \theta'_{it,iw})}{\tan(\theta_{it,iw} + \theta'_{it,iw})} \right)^2 \right]$$

Beam transmittance, τ, reflectance, ρo, and absorptance, α, of glazing:

$$a_{it,iw} := \exp\left[\frac{-kL}{\sqrt{1 - \left(\frac{\sin(\theta_{it,iw})}{n_g} \right)^2}} \right] \qquad \tau_{it,iw} := \frac{\left(1 - r_{it,iw}\right)^2 \cdot a_{it,iw}}{1 - \left(r_{it,iw}\right)^2 \cdot \left(a_{it,iw}\right)^2}$$

$$\rho o_{it,iw} := r_{it,iw} + \frac{r_{it,iw}\cdot\left(1 - r_{it,iw}\right)^2\cdot\left(a_{it,iw}\right)^2}{1 - \left(r_{it,iw}\right)^2\cdot\left(a_{it,iw}\right)^2} \qquad \alpha s_{it,iw} := 1 - \rho o_{it,iw} - \tau_{it,iw}$$

For double glazed windows:

$$\tau e_{it,iw} := \frac{\left(\tau_{it,iw}\right)^2}{1 - \left(\rho o_{it,iw}\right)^2}$$

$$\alpha i_{it,iw} := \alpha s_{it,iw}\cdot\frac{\tau_{it,iw}}{1 - \left(\rho o_{it,iw}\right)^2} \qquad \alpha o_{it,iw} := \alpha s_{it,iw} + \alpha s_{it,iw}\cdot\frac{\tau_{it,iw}\cdot\rho o_{it,iw}}{1 - \left(\rho o_{it,iw}\right)^2}$$

$$\alpha xi_{it,xi} := \alpha s_{it,xi}\cdot\frac{\tau_{it,xi}}{1 - \left(\rho o_{it,xi}\right)^2} \qquad \alpha o_{it,xi} := \alpha s_{it,xi} + \alpha s_{it,xi}\cdot\frac{\tau_{it,xi}\cdot\rho o_{it,xi}}{1 - \left(\rho o_{it,xi}\right)^2}$$

$$\alpha vi_{it,vi} := \alpha s_{it,vi}\cdot\frac{\tau_{it,vi}}{1 - \left(\rho o_{it,vi}\right)^2} \qquad \alpha o_{it,vi} := \alpha s_{it,vi} + \alpha s_{it,vi}\cdot\frac{\tau_{it,vi}\cdot\rho o_{it,vi}}{1 - \left(\rho o_{it,vi}\right)^2}$$

Determine the solar radiation incident on exterior walls and transmitted by windows

Extraterrestrial normal solar radiation:

$$I_{on} := 1353\cdot\frac{watt}{m^2}\cdot\left(1 + 0.033\cdot\cos\left(360\cdot\frac{n_d}{365}\cdot deg\right)\right)$$

Determine beam solar radiation:

$$Ib_{it,iw} := \left(I_{on}\cdot\tau b_{it}\cdot\cos\left(\theta_{it,iw}\right)\right)$$ *..incident beam radiation*

$$Gb_{it,iw} := Ib_{it,iw} \cdot \tau e_{it,iw}$$ *..transmitted beam radiation*

$$\tau ed_{iw} := \tau e_{10,1}$$ *..approximate value for diffuse transmittance (equal for all windows)*

$\theta_{10,1} = 71.869\,\text{deg}$

$$Ids_{it} := Ion \cdot \sin(\alpha_{it}) \cdot \left(0.2710 - 0.2939 \cdot \tau b_{it}\right) \cdot \frac{1 + \cos(\beta)}{2}$$ *..incident instantaneous sky diffuse radiation*

$$Idg_{it} := \left[Ion \cdot \sin(\alpha_{it}) \cdot \left(0.2710 - 0.2939 \cdot \tau b_{it} + \tau b_{it}\right)\right] \cdot \rho g \cdot \frac{1 - \cos(\beta)}{2}$$ *..ground reflected*

$$Gd_{it,iw} := \tau ed_{iw} \cdot \left(Ids_{it} + Idg_{it}\right)$$ *.. transmitted diffuse irradiation (instantaneous)*

$$Gb_{it,iw} := Ib_{it,iw} \cdot \tau e_{it,iw}$$ *..beam transmitted solar radiation.*

Total instantaneous solar irradiation incident on exterior surfaces:

$$I_{it,iw} := Ib_{it,iw} + Ids_{it} + Idg_{it}$$ *..on vertical walls*

$$I_{it,9} := Ion \cdot \sin(\alpha_{it}) \cdot \left(0.2710 - 0.2939 \cdot \tau b_{it} + \tau b_{it}\right)$$ *..on roof*

Total instantaneous solar radiation transmitted by windows:

$$G_{it,iw} := Gb_{it,iw} + Gd_{it,iw}$$

$$Gao_{it,iw} := \alpha o_{it,iw} \cdot Ib_{it,iw} + \alpha o_{10,iw} \cdot \left(Ids_{it} + Idg_{it}\right)$$ *..radiation absorbed in outer glazings*

$$Gai_{it,iw} := \alpha i_{it,iw} \cdot Ib_{it,iw} + \alpha i_{10,iw} \cdot \left(Ids_{it} + Idg_{it}\right)$$

..radiation absorbed in inner glazings

Incident solar irradiation flux (watts/m²)

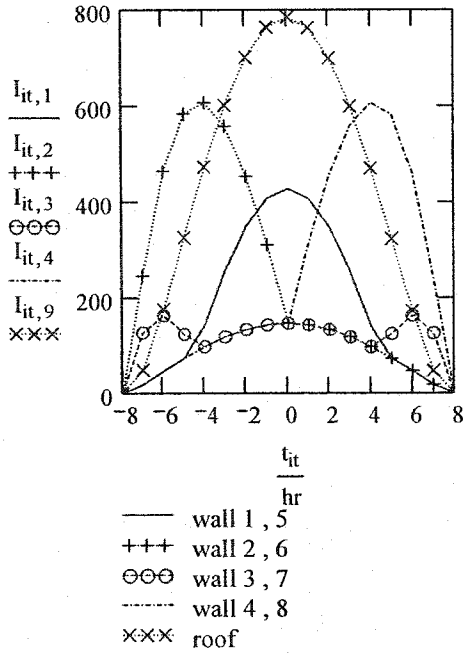

Transmitted solar radiation flux

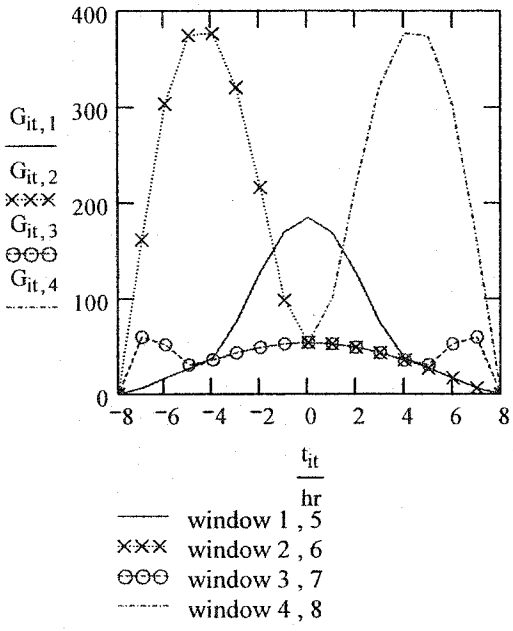

Before performing Fourier series calculations change the time origin from solar noon back to midnight:

$$t_{it} := t_{it} + 11.99 \cdot hr$$

Solar component of sol-air temperature for exterior surfaces:

$$Ts_{it,iw} := I_{it,iw} \cdot \frac{\alpha s_{iw}}{h_{iw}}$$ *For the Vertical Walls*

$$Ts_{it,9} := I_{it,9} \cdot \frac{\alpha s_9}{h_9}$$ *For the Roof*

Represent with Fourier series:

$$n := 0, 1 .. 3$$

$$Tsn_{n,se} := \left(\sum_{it} Ts_{it,se} \cdot \frac{\exp\left(-j \cdot w_n \cdot t_{it}\right)}{24} \right)$$

Equivalent or sol-air temperatures:

$$Teq_{n,se} := Ton_n + Tsn_{n,se}$$

Total instantaneous solar radiation transmitted through all windows for the Gound Floor :

$$Gtg_{it} := \sum_{xi} G_{it,xi} \cdot Aw_{xi}$$

Total instantaneous solar radiation transmitted through all windows for the First Floor :

$$Gtl_{it} := \left(\sum_{vi} G_{it,vi} \cdot Aw_{vi} \right)$$

Solar radiation absorbed by room surfaces for G.F:

$$S_{it,xi} := 0.3 \cdot Gtg_{it} \cdot \frac{A_{xi}}{\sum_{xi} A_{xi}}$$

Floor for G.F: $S_{it,11} := 0.7 \cdot Gtg_{it}$

Solar radiation absorbed by room surfaces for 1st.F:

$$S_{it,vii} := 0.3 \cdot Gtl_{it} \cdot \frac{A_{vii}}{\sum_{vii} A_{vii}}$$

Floor for 1st.F: $S_{it,10} := 0.7 \cdot Gtl_{it}$

Represent with Fourier series:

$$Sn_{n,i} := \left(\sum_{it} S_{it,i} \cdot \frac{\exp\left(-j \cdot w_n \cdot t_{it}\right)}{24} \right)$$

Solar radiation absorbed in glazings and released to room air for the G.F:

$$Qgg_{it} := \sum_{xi} \left[\frac{1}{R_W \cdot h_o} \cdot \left(\alpha o_{it,xi} \cdot I_{it,xi} \right) + \frac{1}{R_W} \cdot \left(R_W - \frac{1}{h_{xi}} \right) \cdot \left(\alpha xi_{it,xi} \cdot I_{it,xi} \right) \right] \cdot Aw_{xi}$$

$$Qggn_n := \left(\sum_{it} Qgg_{it} \cdot \frac{\exp\left(-j \cdot w_n \cdot t_{it}\right)}{24} \right) \qquad Qggn_0 = 130.463 \text{ watt}$$

Solar radiation absorbed in glazings and released to room air for the 1st.F:

$$Qg1_{it} := \sum_{vi} \left[\frac{1}{R_w \cdot h_o} \cdot \left(\alpha o_{it,vi} \cdot I_{it,vi} \right) + \frac{1}{R_w} \cdot \left(R_w - \frac{1}{h_{vi}} \right) \cdot \left(\alpha vi_{it,vi} \cdot I_{it,vi} \right) \right] \cdot Aw_{vi}$$

$$Qg1n_n := \left(\sum_{it} Qg1_{it} \cdot \frac{\exp\left(-j \cdot w_n \cdot t_{it}\right)}{24} \right) \qquad Qg1n_0 = 130.463 \text{ watt}$$

Basement temperature assumed to be constant: $T_b := 20 \cdot degC$

The Thermal Netwrok of the house is the same as winter thermal netwrok but without auxiliary heat (figure 4.3, Chapter 4).

The thermal capacitances and thermal resistances is the same as winter case. The calculation is shown in Appindix A.
The difference is R1o and R11o.

9 -The thermal resistance between the room air temp. for the G.F and the outside

$$R_{1o} := \frac{1}{\left[\sum_{xi} \left(\frac{\frac{1}{2} Aw_{xi}}{R_w} + \frac{Ad_{xi}}{Rd} \right) + U_{inf} \right]} \qquad R_{1o} = 0.032 \frac{degC}{watt}$$

20 -The thermal resistance between the room air temp. for the 1st.F and the outside

$$R_{11o} := \frac{1}{\sum_{vi} \frac{\frac{1}{2} Aw_{vi}}{R_w} + U_{inf}} \qquad R_{11o} = 0.033 \frac{degC}{watt}$$

Time step selecetd is equal to 300 sec. The calculation for time step is the same as in Appindex A.

$\Delta t := 300 \cdot sec$

The simulation will be performed for two days (periodic). Thus, weather data have to be generated for NT times as follows:

$NT := 86400 \cdot \frac{sec}{\Delta t} \cdot 2$ $NT = 576$ *...number of time steps for two days*

$p := 0, 1 .. NT$ $t_p := p \cdot \Delta t$ *..times at which simulation is to be performed.* $n1 := 1, 2 .. 3$

$To_p := Ton_0 + 2 \cdot \sum_{n1} Re\left[\left(Ton_{n1}\right) \cdot \exp\left(j \cdot w_{n1} \cdot t_p\right)\right]$ $Ton_0 = 22.625\ degC$

SOLAR RADIATION ABSORBED BY INTERIOR SURFACES:

1- Solar radiation for the Vertical Walls in G.F

$$Sgt_p := \sum_{xi}\left[Sn_{0,xi} + 2\cdot\sum_{n1} Re\left[\left(Sn_{n1,xi}\right)\cdot\exp\left(j\cdot w_{n1}\cdot t_p\right)\right]\right]$$

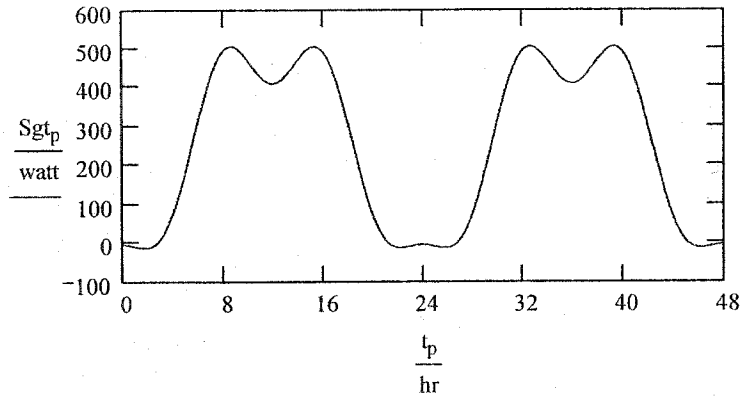

2- Solar radiation for the floor in G.F

$$St_{p,11} := Sn_{0,11} + 2\cdot\left[\sum_{n1} Re\left[\left(Sn_{n1,11}\right)\cdot\exp\left(j\cdot w_{n1}\cdot t_p\right)\right]\right]$$

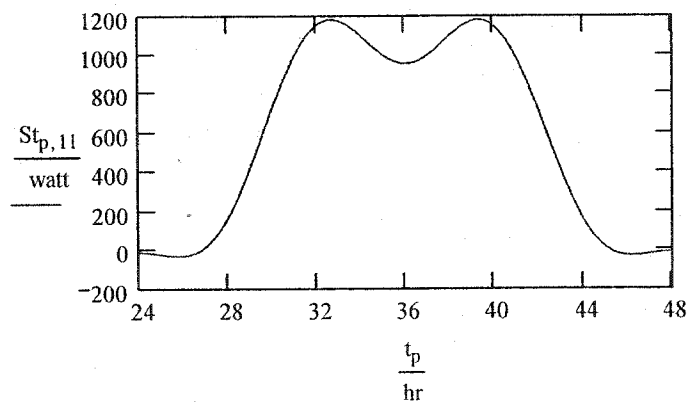

3- Solar radiation absorbed by the unheated surfaces in the 1st.F :

$$Slt_p := \sum_{vii}\left[Sn_{0,vii} + 2\cdot\sum_{n1} Re\left[\left(Sn_{n1,vii}\right)\cdot\exp\left(j\cdot w_{n1}\cdot t_p\right)\right]\right]$$

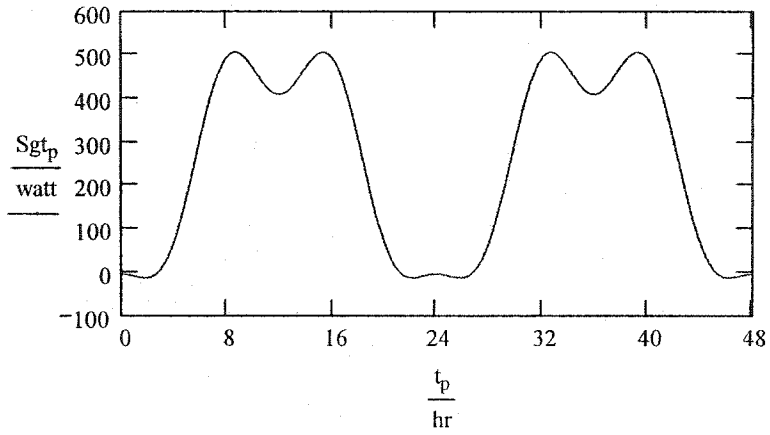

4- Solar radiation absorbed by the floor in the 1st.F :

$$St_{p,10} := Sn_{0,10} + 2\cdot\sum_{n1} Re\left[\left(Sn_{n1,10}\right)\cdot\exp\left(j\cdot w_{n1}\cdot t_p\right)\right]$$

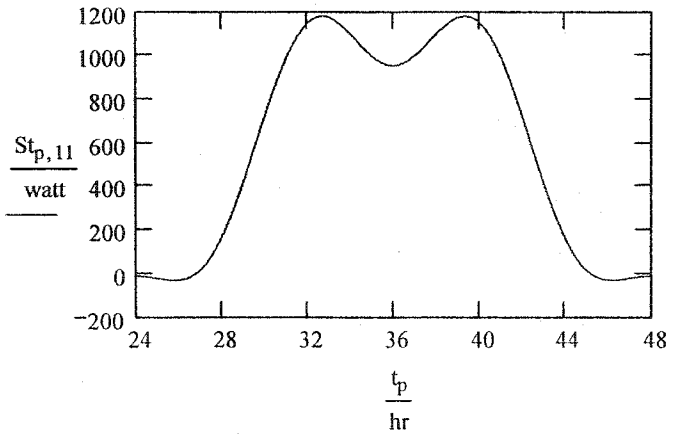

Initial estimates of temperatures:

$$\begin{pmatrix} T_{1,0} \\ T_{2,0} \\ T_{3,0} \\ T_{4,0} \\ T_{5,0} \\ T_{6,0} \\ T_{7,0} \\ T_{8,0} \\ T_{9,0} \\ T_{10,0} \\ T_{11,0} \\ T_{12,0} \\ T_{13,0} \end{pmatrix} := \begin{pmatrix} 20 \\ 21 \\ 23 \\ 24 \\ 19 \\ 20 \\ 21 \\ 24 \\ 23 \\ 22 \\ 21 \\ 21 \\ 22 \end{pmatrix} \cdot \text{degC}$$

Calculation the mass flow rate:

$Cd := 0.65$ *Discharge Coeff.* $g := 9.81 \cdot \frac{m}{sec^2}$ *Gravity acceleration*

$hb := 1 \cdot m$ $ht := 1 \cdot m$ $Am := 2 \cdot m^2$ *opening area between the two floors.*

$$Ab_p := if\left[\left(mod\left(\frac{t_p}{hr}, 24\right) > 10\right) \cdot \left(mod\left(\frac{t_p}{hr}, 24\right) < 18\right), 0.0001 \cdot m^2, \frac{\sum_{xi} Aw_{xi}}{2}\right]$$ *bottom opening area*

$At_p := Ab_p$ *top opening area*

$$Atmb_p := \frac{\sqrt{(Ab_p)^2 \cdot (At_p)^2 + (At_p)^2 \cdot Am^2 + (Ab_p)^2 \cdot Am^2}}{m^2}$$

$$A_p := \frac{(2 \cdot Am \cdot At_p \cdot Ab_p)}{Atmb_p \cdot m^2}$$ *effective area*

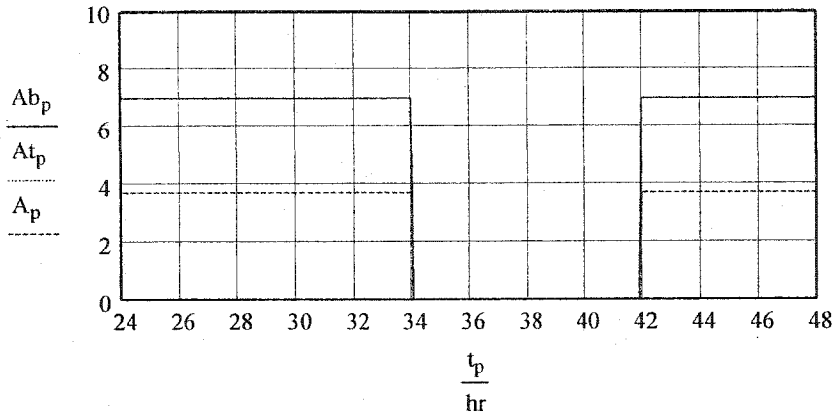

The air enters from the ground floor and exits from the first floor. The mass flow rate is equal to:

$$q_0 := \rho_{air} \cdot Cd \cdot A_0 \cdot \sqrt{\left(\frac{\left|T_{1,0} - To_0\right|}{To_0 + 273} \cdot g \cdot hb\right) + \left(\frac{\left|T_{11,0} - To_0\right|}{To_0 + 273} \cdot g \cdot ht\right)} \qquad q_0 = 0.956 \frac{kg}{sec}$$

$$cpair := 1000 \cdot \frac{joule}{kg \cdot degC}$$

The air flow is coupled with the thermal netwrok by 3 resistances which are calculated as follows:

$$R_{q_0} := \frac{1}{q_0 \cdot cpair} \qquad R_{q_0} = 1.046 \times 10^{-3} \frac{degC}{watt}$$

Between the two floors.

$$R_{1\_0_0} := \frac{R_{1o} \cdot R_{q_0}}{R_{1o} + R_{q_0}}$$

Thermal resistance between the room air temperature in the ground floor and the outside.

$$R_{11\_0_0} := \frac{R_{11o} \cdot R_{q_0}}{R_{11o} + R_{q_0}}$$

Thermal resistance between the room air temperature in the first floor and the outside.

$$
\begin{pmatrix}
qauxg_{p+1} \\
qaux1_{p+1} \\
T_{1,p+1} \\
T_{2,p+1} \\
T_{3,p+1} \\
T_{4,p+1} \\
T_{5,p+1} \\
T_{6,p+1} \\
T_{7,p+1} \\
T_{8,p+1} \\
T_{9,p+1} \\
T_{10,p+1} \\
T_{11,p+1} \\
T_{12,p+1} \\
T_{13,p+1}
\end{pmatrix}
:=
\begin{bmatrix}
\left[if\left[Kg_p \cdot \left(Tspg_p - T_{1,p} \right) > q\_maxg, q\_maxg, Kg_p \cdot \left(Tspg_p - T_{1,p} \right) \right] \right] \cdot \left[\left(Tspg_p - T_{1,p} \right) > 1.0 \right] \\
\left[if\left[K1_p \cdot \left(Tsp1_p - T_{11,p} \right) > q\_max1, q\_max1, K1_p \cdot \left(Tsp1_p - T_{11,p} \right) \right] \right] \cdot \left[\left(Tsp1_p - T_{11,p} \right) > 1.0 \right] \\
\dfrac{\dfrac{T_{2,p}}{R_{12}} + \dfrac{To_p}{R_{1o}} + \dfrac{T_{6,p}}{R_{16}} + \dfrac{T_{7,p}}{R_{17}} + \dfrac{T_{11,p}}{R_{11\_1}}}{\dfrac{1}{R_{12}} + \dfrac{1}{R_{1o}} + \dfrac{1}{R_{16}} + \dfrac{1}{R_{17}} + \dfrac{1}{R_{11\_1}}} \\
\dfrac{\dfrac{T_{3,p}}{R_{23}} + \dfrac{T_{6,p}}{R_{26}} + \dfrac{T_{1,p}}{R_{12}} + \dfrac{T_{7,p}}{R_{27}} + St_{p,11}}{\dfrac{1}{R_{23}} + \dfrac{1}{R_{26}} + \dfrac{1}{R_{12}} + \dfrac{1}{R_{27}}} \\
\dfrac{\Delta t}{C_3} \cdot \left(\dfrac{T_{4,p} - T_{3,p}}{R_{34}} + \dfrac{T_{2,p} - T_{3,p}}{R_{23}} \right) + T_{3,p} \\
\dfrac{\Delta t}{C_4} \cdot \left(\dfrac{Tb_p - T_{4,p}}{R_{4o}} + \dfrac{T_{3,p} - T_{4,p}}{R_{34}} + qauxg_p \right) + T_{4,p} \\
\dfrac{\Delta t}{C_5} \cdot \left(\dfrac{T_{6,p} - T_{5,p}}{R_{56}} + \dfrac{To_p - T_{5,p}}{R_{5o}} \right) + T_{5,p} \\
\dfrac{\dfrac{T_{2,p}}{R_{26}} + \dfrac{T_{5,p}}{R_{56}} + \dfrac{T_{1,p}}{R_{16}} + \dfrac{T_{7,p}}{R_{67}} + Sgt_p}{\dfrac{1}{R_{56}} + \dfrac{1}{R_{26}} + \dfrac{1}{R_{16}} + \dfrac{1}{R_{67}}} \\
\dfrac{\dfrac{T_{2,p}}{R_{27}} + \dfrac{T_{1,p}}{R_{17}} + \dfrac{T_{8,p}}{R_{78}} + \dfrac{T_{6,p}}{R_{67}}}{\left(\dfrac{1}{R_{27}} + \dfrac{1}{R_{17}} + \dfrac{1}{R_{78}} + \dfrac{1}{R_{67}} \right)} \\
\dfrac{\Delta t}{C_8} \cdot \left(\dfrac{T_{7,p} - T_{8,p}}{R_{78}} + \dfrac{T_{9,p} - T_{8,p}}{R_{89}} + qaux1_p \right) + T_{8,p} \\
\dfrac{\Delta t}{C_9} \cdot \left(\dfrac{T_{8,p} - T_{9,p}}{R_{89}} + \dfrac{T_{10,p} - T_{9,p}}{R_{910}} \right) + T_{9,p} \\
\dfrac{\dfrac{T_{9,p}}{R_{910}} + \dfrac{T_{12,p}}{R_{1012}} + \dfrac{T_{11,p}}{R_{1112}} + St_{p,10}}{\dfrac{1}{R_{910}} + \dfrac{1}{R_{1012}} + \dfrac{1}{R_{1112}}} \\
\dfrac{\dfrac{T_{10,p}}{R_{1011}} + \dfrac{To_p}{R_{11o}} + \dfrac{T_{12,p}}{R_{1112}} + \dfrac{T_{1,p}}{R_{1\_11}}}{\dfrac{1}{R_{1011}} + \dfrac{1}{R_{11o}} + \dfrac{1}{R_{1112}} + \dfrac{1}{R_{1\_11}}} \\
\dfrac{\dfrac{T_{10,p}}{R_{1012}} + \dfrac{T_{13,p}}{R_{1213}} + \dfrac{T_{11,p}}{R_{1112}} + Slt_p}{\left(\dfrac{1}{R_{1012}} + \dfrac{1}{R_{1213}} + \dfrac{1}{R_{1112}} \right)} \\
\dfrac{\Delta t}{C_{13}} \cdot \left(\dfrac{T_{12,p} - T_{13,p}}{R_{1213}} + \dfrac{To_p - T_{13,p}}{R_{13o}} \right) + T_{13,p}
\end{bmatrix}
$$

Results for second day (first day is affected by assumed initial conditions):

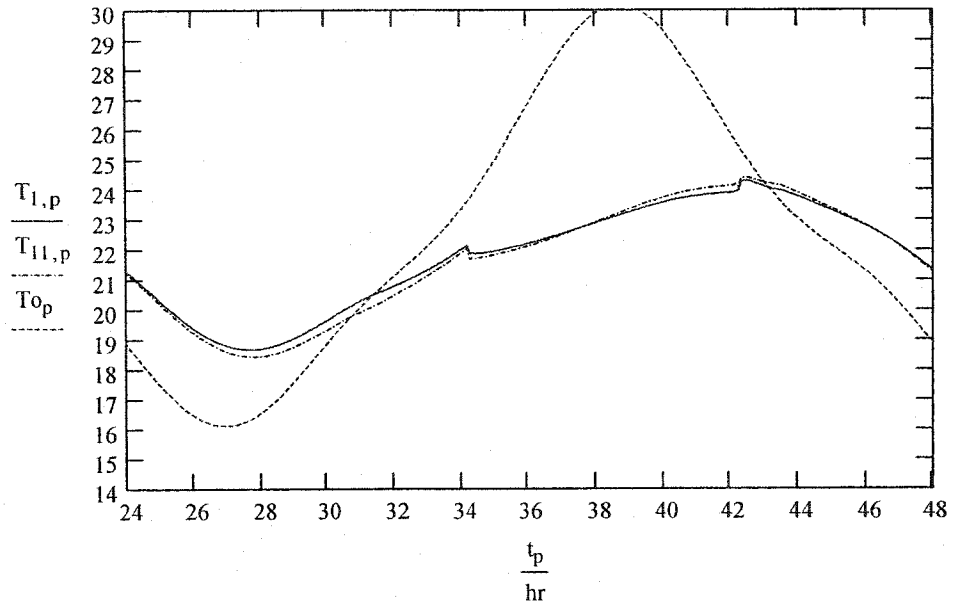

Note: T1 is room air temperature for the ground floor. and T11 is the room air temperature for the first floor.